REACTIVE POLYMERS
FOR
LIFE SCIENCES

by

Tuğba Genç

B.S., Chemistry, Yıldız Technical University, 2008

Submitted to the Institute for Graduate Studies in
Science and Engineering in partial fulfillment of
the requirements for the degree of
Master of Science

Graduate Program in Chemistry

Boğaziçi University

2010

REACTIVE POLYMERS
FOR
LIFE SCIENCES

APPROVED BY:

Assist. Prof. Rana Sanyal ……....
(Thesis Supervisor)

Assist. Prof. Amitav Sanyal ……

Prof. Yusuf Z. Menceloğlu ……

DATE OF APPROVAL: 22.09.2010

Aileme

ACKNOWLEDGEMENTS

This dissertation would not have been possible without the guidance and the help of several individuals who in one way or another contributed and extended their valuable assistance during my master's study.

I would like to express my most sincere gratitude to my thesis supervisor Assist. Prof. Rana Sanyal for her endless attention and scientific guidance throughout this study. I appreciate her support and patience over the last two years.

I wish to extend my thanks to my committee members Assist. Prof. Amitav Sanyal and Prof. Yusuf Z. Menceloğlu for their careful and constructive review of the final manuscript. I am indebted to Prof. Yusuf Z. Menceloğlu also for consenting me to utilize the opportunity of being a part of his group, his reliance and interest for this study.

I would like to thank to Burcu Selen Çağlayan, Ayla Türkekul, Bilge Gedik Uluocak for their help running NMR and SEM analysis.

I gratefully acknowledge Eren Şimşek for his willingness to share his precious time with me, toleration, hilarious friendship and enriching my mind.

I would like to express my great appreciation to my former and present labmates, particularly my hoodmate Gönül Demirci, for their cheerful company. I also thank to Gizem Dübek for her help in synthesis and making me guffaw ever so often. My special thanks go to E. Ece Manavoğlu, Sezin Yiğit and Nergiz Cengiz for embellishing my life and introducing me to a magnificent heart. I would like to thank all my friends and all the members of the faculty in the Chemistry Department.

Finally, I owe my deepest gratitude to my whole family and Hamdi Ciğerim for their endless love, support and encouragement throughout these years.

This research has been supported by TÜBİTAK (107T623).

LIST OF SYMBOLS/ ABBREVIATIONS

J	Coupling constant
υ	Frequency

AHMA	6-azidohexyl methacrylate
ATRP	Atom transfer radical polymerization
$CDCl_3$	Deuterated chloroform
CH_2Cl_2	Dichloromethane
DC	Direct-current
D_2O	Deuterated water
rDA	Retro Diels-Alder
EtOAc	Ethyl Acetate
FMA	Furfuryl methacrylate
FuM-MA	Furan protected maleimide monomer
HFuM-MA	Hydrogenated furan protecte maleimide monomer
GPC	Gel Permeation Chromotography
MeOH	Methanol
MMA	Methylmetacrylate
NHSMA	N-methacryloxysuccinimide
NMR	Nuclear Magnetic Resonance
PBS	Phosphate Buffered Saline
PEG	Poly(ethylene glycol)
PEGMA	Poly(ethylene glycol) methacrylate
PEGMEMA	Poly(ethylene glycol) monomethyl ether methacrylate
PMDETA	N,N,N',N',N''-pentamethyldiethylenetriamine
SEC	Size-Exclusion Chromatography
TEA	Triethylamine
THF	Tetrahydrofuran
TLC	Thin Layer Chromatography
UV	Ultraviolet

ABSTRACT

REACTIVE POLYMERS FOR LIFE SCIENCES

Synthesis of polymers with reactive side chains has attracted considerable attention since these polymers are widely utilized in bioengineering applications such as controlled drug delivery, wound dressing and tissue engineering. First part of this study introduces the synthesis of polymers decorated with succinimide and azide units as 'reactive' functional groups for polymer – drug conjugation. First part of this thesis expands on the polymerization, functionalization and biodegradation studies of the abovementioned polymers. Since the synthesis of such reactive polymers with narrow molecular weight distributions is desirable for many applications, Atom Transfer Radical Polymerization (ATRP) has been employed to obtain such polymers. Poly (ethylene glycol) (PEG) based polymers are known to be non-immunogenic, biocompatible and biodegradable, therefore they are promising candidates for formulation of polymer-drug conjugates. As one part of this study, water soluble PEG methacrylate based copolymers that contain amine and alkyne reactive side chains have been synthesized using ATRP. Finally, amine functionality has been proven and *in vitro* biodegradability behaviors depending on molecular weight, pH and composition effects were investigated.

Recently, nanofibrous scaffolds are of great interest due to their unique properties and wide range of application areas. Such increased interest also necessitates synthesis of novel polymeric materials to widen the scope of intended applications of nanostructures. With this motivation, in the second part of this study, several amine, thiol or dual reactive polymers were synthesized with multifarious compositional arrangements. Electrospinning, which is a former yet still the only technique for nanofiber production, attracts attention, lately. We utilized this technique to obtain both thiol and amine reactive nanofibers and nanoparticles. The successful formation of reactive nanostructures was investigated by surface characterization techniques.

ÖZET

YAŞAMBİLİM İÇİN REAKTİF POLİMERLER

Kontrollü ilaç salınımı, yara örtüleme ve doku mühendisliği gibi biyomühendislik uygulamalarında çokça kullanım alanı bulduğundan, yan dallarında reaktif grup bulunduran polimerlerin sentezi, büyük önem kazanmıştır. Bu çalışmanın ilk bölümü, polimer – ilaç konjugasyonlarında kullanılmak üzere, reaktif grup olarak süksinimid ve azid grupları bağlanmış polimerlerin sentezini içerir. Bu tezin ilk bölümü yukarıda bahsedilen polimerlerin polimerizasyonu, fonksiyonelleştirilmesi ve biyobozunurluk çalışmalarını açıklamaktadır. Bu tip reaktif polimerlerlerin moleküler ağırlık dağılımları dar olacak şekilde sentezlenmesi arzu edildiği için Atom Transfer Serbest Radikal Polimerleşme (ATRP) yöntemi kullanılmıştır. Polietilen glikol (PEG) bazlı polimerler immun sistemini uyarmayan, biyouyumlu ve biyobozunur olarak bilinirler, ve polimere bağlı ilaç formülasyonları için umut vaad eden adaylardır. Bu çalışmanın bir kısmı, yan dallarında amin ve alkin reaktif gruplar bulunduran PEG metakrilat bazlı suda çözünebilen kopolimerlerin ATRP yöntemi kullanılarak sentezlenmesini içermektedir. Son olarak, amin fonksiyonelliği kanıtlanmış ve moleküler ağırlık, pH ve kompozisyon parametreleri doğrultusunda canlı dışında biyobozunurluk davranışları incelenmiştir.

Bu günlerde, geniş çaplı uygulama alanları bulması ve benzersiz özelliklerinden ötürü nano iplik yapılara duyulan ilgi oldukça artmıştır. Bu artan ilgi, amaçlanan kullanım alanlarının kapsamını genişletmek amacıyla yeni reaktif polimerik malzemelerin sentezlenmesini gerekli kılmıştır. Bu sebeple, bu çalışmanın ikinci yarısında, amin, tiol ve her iki reaktif grubu da barındıran çeşitli içerik düzenlemelerine sahip birçok polimer sentezlenmiştir. Eski fakat hala nano iplik oluşumunda kullanılan tek teknik olan elektroeğirme yöntemi son zamanlarda ilgi çekmektedir. Biz de hem tiol hem de amin reaktif nano yapıları elde etmek amacıyla bu tekniği kullanmış bulunmaktayız. Başarıyla oluşturulan nano yapıların incelenmesi yüzey karakterizasyonu ile tamamlanmıştır.

TABLE OF CONTENTS

LIST OF FIGURES

LIST OF TABLES

1. INTRODUCTION

1.1. Reactive Polymeric Supports for Drug Delivery Approaches

Drug delivery is a rapidly developing and evolving discipline underpinned by the principles and development in related fields from classic chemistry to modern biotechnology [1]. Performances of drug delivery systems are continuously improved with the purpose to maximize therapeutic activity and to minimize undesirable side-effects. For being effective, the administrated drug must be released at a constant predetermined rate that maintains the drug level in the therapeutic zone. The ideal release profile is schematized in Figure 1.1. [2].

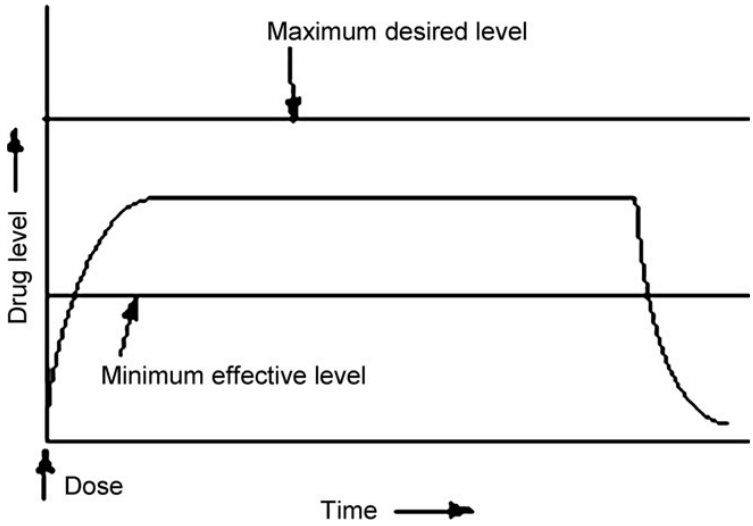

Figure 1.1. Drug level in the blood with a controlled delivery dosing

Among the drug delivery approaches, polymer conjugation is emerging for its applicability to either low molecular weight drugs or proteins. A water soluble polymer can confer several properties to the linked molecules: i) increased half-life due to reduced kidney clearance, ii) protection against degrading enzymes or reduced uptake by reticulo-endothelial system (RES), thanks to the polymer steric hindrance, iii) augmentation of water solubility, particularly relevant for some anticancer drugs with low solubility, iv) prevention of immunogenicity and v) selective tumour accumulation. This last property is

a consequence of the highly active angiogenesis in many solid tumours, resulting in an increased tumour vascularization and blood flow [3].

One strong incentive to use macromolecular carriers is their preferential accumulation in solid tumors. The accumulation of macromolecules in tumors is currently explained by the micro vascular hyper permeability of tumors to circulating macromolecules and the impaired lymphatic drainage of macromolecules in these tissues. This phenomenon, known as the ‘‘enhanced permeability and retention’’ (EPR) effect [4-7], is very beneficial because it results in the selective uptake of the polymer encapsulated drug by the tumor. In sharp contrast, healthy tissues are exposed and damaged by non-encapsulated drugs (Figure 1.2). This drawback can be reduced or overcome by polymer conjugation [8].

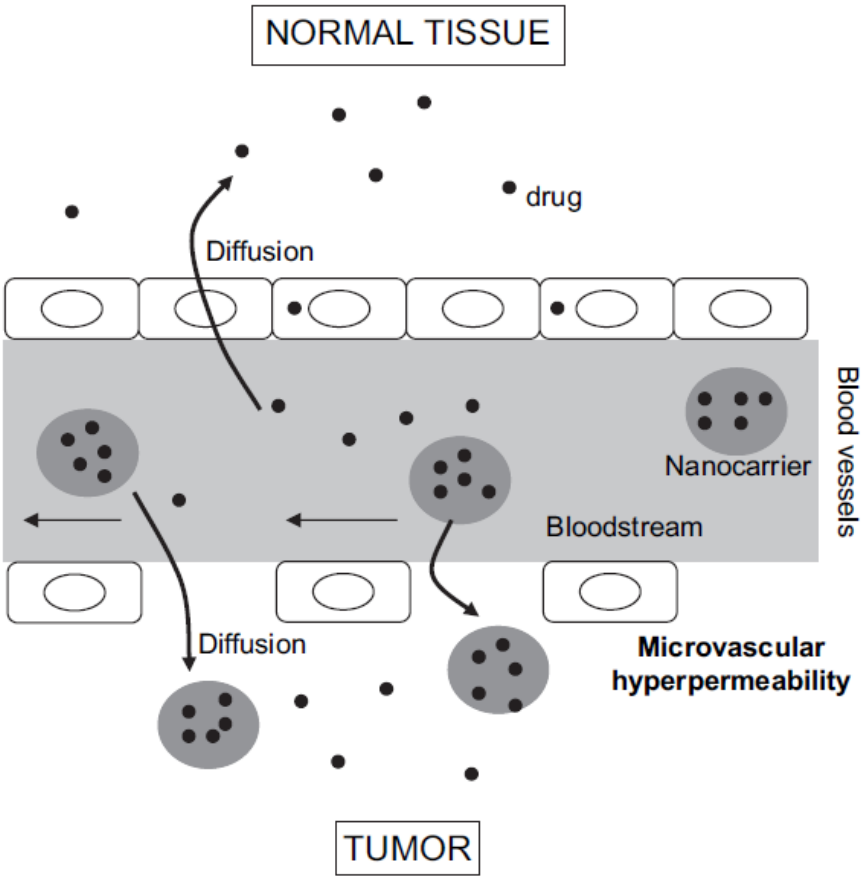

Figure 1.2. Anatomical differences between normal tissues and solid tumors

For a suitable conjugation to chemical and biopharmaceutical drugs, many polymers have been proposed as carriers and among these poly (ethylene glycol) (PEG) has gained particular importance [9, 10]. The great popularity of PEG-conjugates is driven by the unique combination of physicochemical and biological properties of the polymer. These include excellent solubility in aqueous and most organic solutions [11]. Among the important biological properties of PEG (of molecular weights over 2000) are favorable pharmacokinetics, tissue distribution, lack of toxicity and immunogenicity [12-14]. The experience accumulated over the last two decades has shown that the useful characteristics of PEG can usually be conveyed to its conjugates. The conjugates also receive protection against protease attack and, because of their larger size, have a reduced rate of kidney clearance [15-18].

Shunmugam, Tew and their co-workers reported that ATRP of the NHSMA monomer with a homogeneous CuBr/PMDETA catalyst system in nonpolar anisole has produced well-defined homopolymers and copolymers (Figure 1.3). These macromolecules with active ester moieties represent an extremely versatile platform for generating highly functional materials [19].

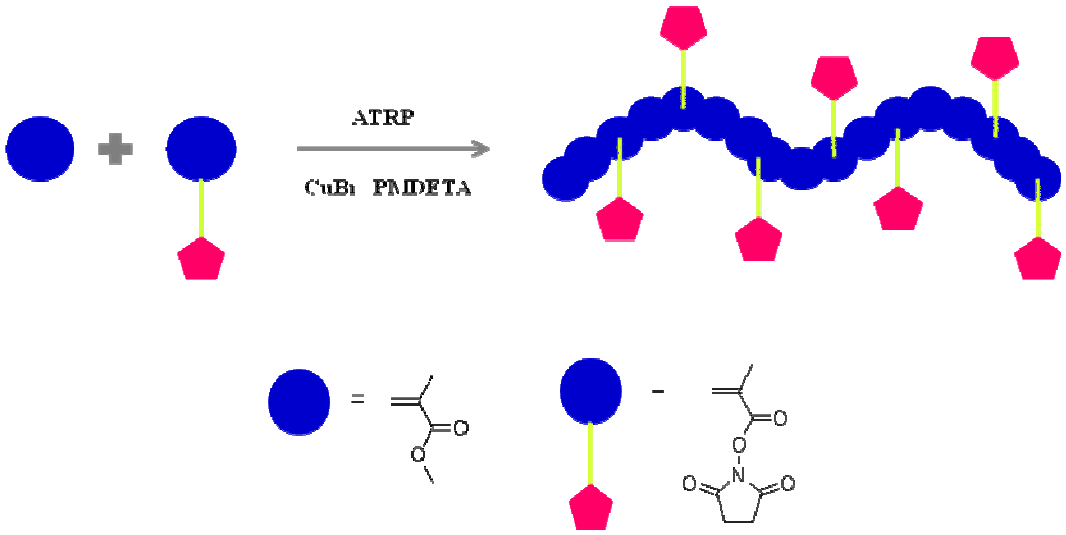

Figure 1.3. Synthesis of active ester polymers

1.1.1. Utility of Polymer-Drug Conjugates in Pharmacokinetics

PEG polymers are composed of repeating units of ethylene glycol, which can be produced as linear or branched chains, with functional groups at one or more termini to

enable a variety of conjugation possibilities. In all cases, the conjugated molecule benefits from the pharmaceutical properties of PEG, which include increased solubility, stability over a wide range of temperature and pH, and high mobility in solution [20].

The characteristic prolonged circulation time that PEG endows on proteins and peptides arises through two principal effects; a decrease in the rate of kidney clearance and an increase in protection from proteolytic degradation, both of which decrease the overall clearance of the drug. Since PEG polymers are highly hydrated, with two water molecules per ethylene glycol unit, their hydrodynamic radii are approximately 5- to 10-fold greater than would be predicted by their nominal molecular weight [19], underlying a dramatic increase in the effective molecular size of the PEG conjugate. At lower molecular weights of PEG, clearance occurs primarily by the kidneys; above a molecular weight of approximately 20 kDa renal filtration decreases in favor of excretion by the bile, and above approximately 50 kDa, hepatobiliary clearance dominates [21, 22].

In 2001, Dosio et al. obtained a PEGylated macromolecular pro-drug of paclitaxel that is active against tumor cells, more soluble and with enhanced in vivo characteristics (Figure 1.4) [23].

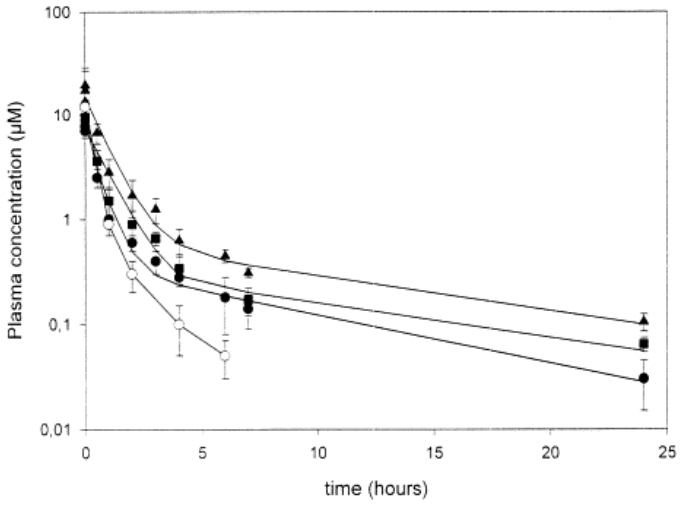

Figure 1.4. Representative plasma paclitaxel values obtained from mice injected i.v. with paclitaxel as such (outlined circles), HSA–paclitaxel (solid circles), 2 kDa PEG conjugate (squares) and 5 kDa conjugate (triangles). Concentrations were determined by radioactivity associated to paclitaxel [23]

1.1.2. Functionalization of Reactive Polymers

With the ever-increasing demand for prolix polymeric materials in order to be used for wide range of application, many researchers have started working on combinatorial approaches. Ever after, functional polymers remain great interest.

Brocchini and co-workers, Haddleton and co-workers, and others have applied the combinatorial approach toward developing water-soluble polymers for drug and gene delivery systems [24-30]. To expedite the library synthesis process, the former two groups employed the use of the activated homopolymeric precursor, polymethacryloxysuccinimide, to which primary amine-containing functional groups (NH2-FGs) can be covalently bound via amidation chemistry (Figure 1.5) [31].

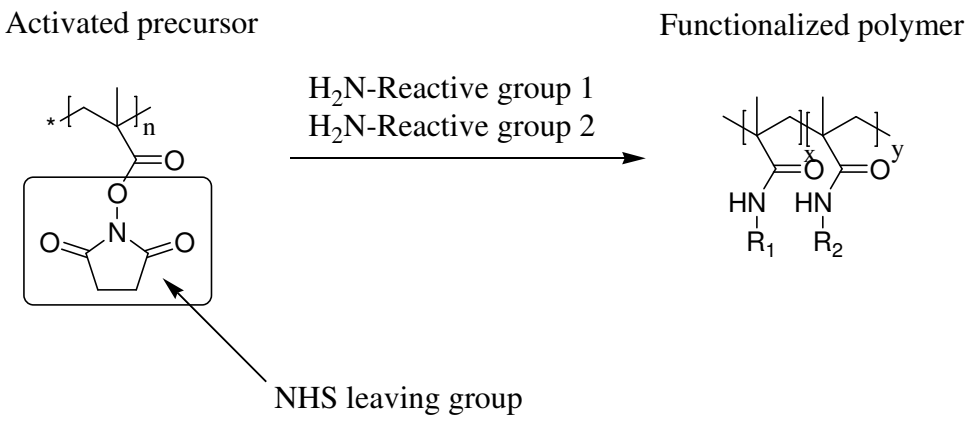

Figure 1.5. Functionalizing the *N*-Hydroxysuccinimide (NHS)-Activated Precursor

In 2005, a study that highlights the potential use of NHS leaving group for subsequent functionalization with various pendant chemistries (Figure 1.6) was reported by Shunmugam, Tew and their coworkers [19].

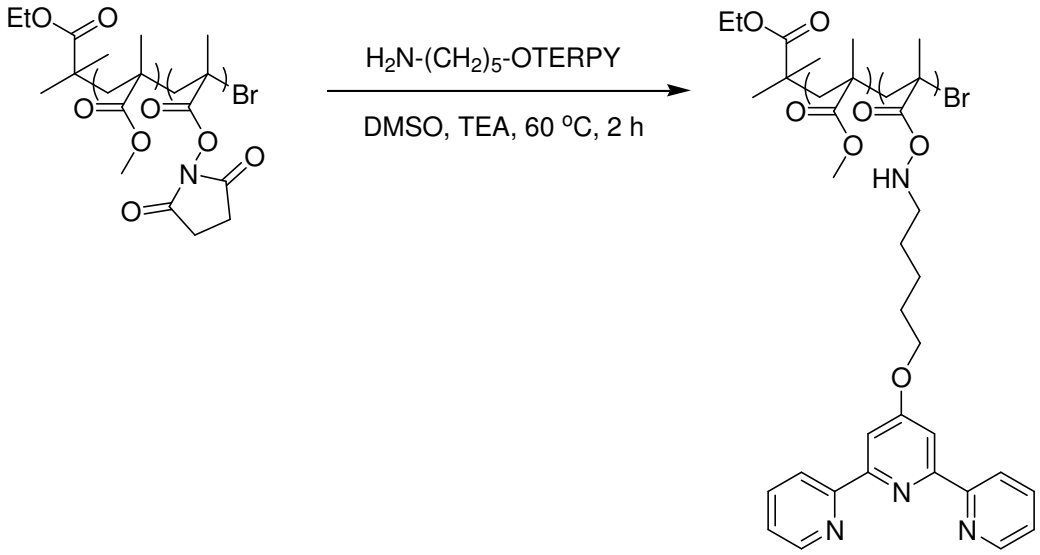

Figure 1.6. Synthetic conversion of the active esters in poly (NHSMA-r-MMA) copolymers to incorporate terpy pendant groups

Benicewicz and Li reported a post functionalization approach of combining surface initiated RAFT polymerization and click reactions to modify the surface of nanoparticles. In this study, a monomer with a pendant "clickable" moiety, 6-azidohexyl methacrylate (AHMA), was utilized to obtain functionalization [32].

The polymer chains with pendant azido groups can be side-functionalized with alkynes via the highly efficient click reaction (Figure 1.7). Throughout this research, the derived PAHMA grafted nanoparticles have a large number of reactive azido groups on the grafted PAHMA chains that are excellent precursors for attaching various functional alkynes.

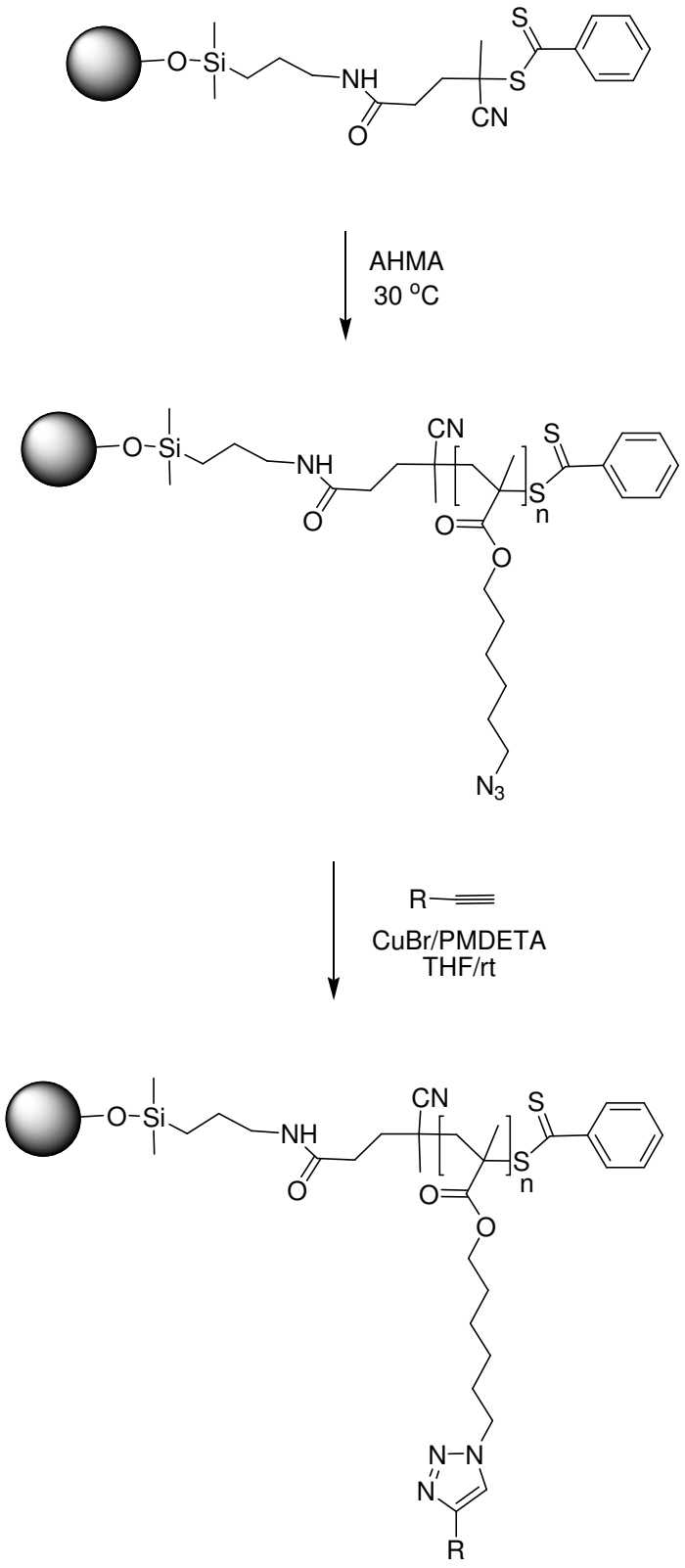

Figure 1.7. Functionalization of azido groups

1.1.3. Biodegradation Behaviors of Reactive Polymers

Interest in synthetic biodegradable polymers has grown tremendously during the past two decades. Synthetic biodegradable polymers are attractive candidate materials for short-term medical applications, like sutures, drug delivery devices, orthopedic fixation devices, wound dressings, temporary vascular grafts, stents, different types of tissue engineered grafts, etc. [33].

The development of implantable drug delivery systems is perhaps the most widely investigated application of biodegradable polymers proportional to their advantages. They do not require surgical removal after their intended application due to their transient nature and thus can circumvent some of the problems related to the long-term safety of non-degradable implanted devices.

Biodegradable polymers are those that degrade both in vitro and in vivo into products that are either normal metabolites or into products that could be completely eliminated from the body with or without further metabolic transformations. Biodegradation actually involves two complementary processes, degradation and erosion. Degradation refers to the bond cleavage during which polymer chains are cleaved to low molecular weight fractions and erosion refers to the physical phenomena such as dissolution and diffusion of these low molecular weight fractions from the polymer matrix [34]. There are mainly two ways of degradation: passive degradation via hydrolysis (Figure 1.8) or active degradation via enzymatic reactions.

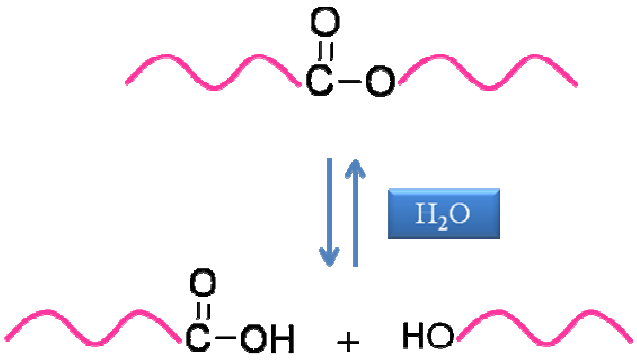

Figure 1.8. Hydrolytic degradation process of polyester

Shortly, the mechanism of elimination of the biodegradable polymers from the body involves the degradation of the polymer into water-soluble degradation products, which are carried away from the implantation site and eliminated.

Although many polymers have been examined preclinically, almost all conjugates reaching clinical evaluation have used PEG [35, 36] or copolymers. Even though, they are well tolerated in man, they share the disadvantage that the main chain is not biodegradable in vivo. Therefore, their utility is restricted to a molecular weight <40 000 g/mol, depending on structure, if renal elimination is to be ensured.

In 2007, Jun Pan and coworkers provided a method to graft PLA with low Mw PEG, approximately 600, to achieve good protein resistance and to introduce reactive groups for further functionalization. First, was maleic anhydride was grafted onto the side chain of PLA by free radical reaction. Second, amidation the anhydride and ester groups with diaminoPEG took place resulting in a polymer (Figure 1.9) with good hydrophilicity, pH dependent degradability (Figure 1.10), protein-resistance, cellular compatibility and reactivity, all of which may lead to potential applications in drug delivery [37].

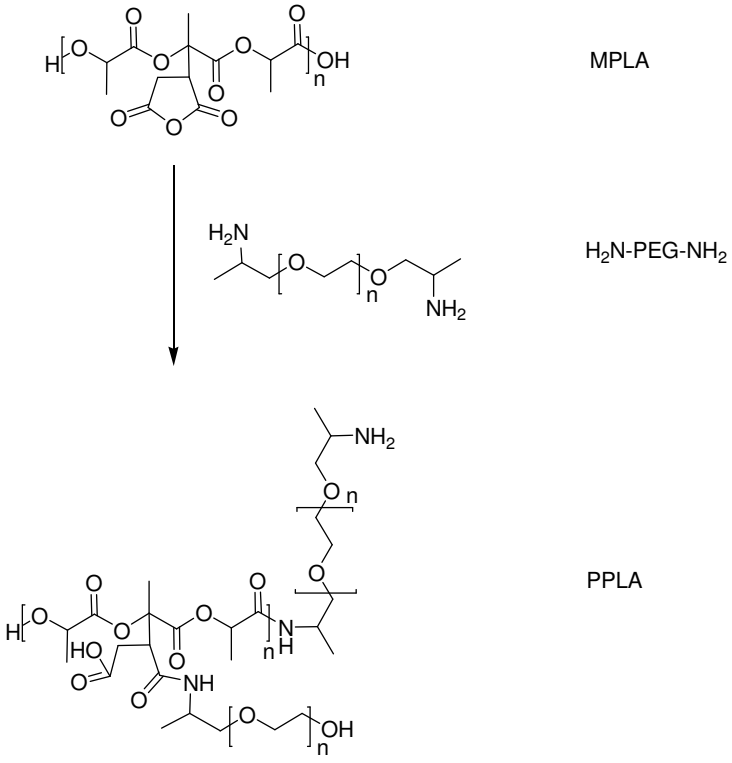

Figure 1.9. Synthesis of PEG grafted PLA polymer

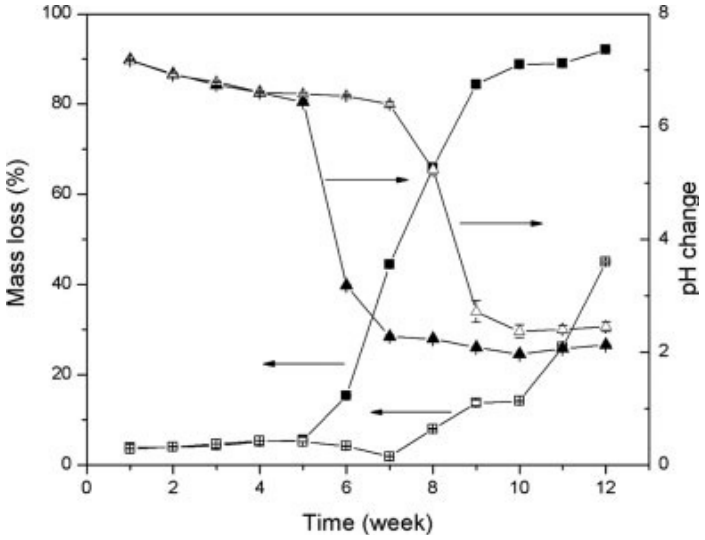

Figure 1.10. pH changes (▲) and mass losses (■) of PPLA (filled symbols) and MPLA (unfilled symbols) during degradation of 12 weeks in 0.1M PBS at 37 ˚C [37].

1.2. Reactive Fibrous Scaffolds

When the diameters of polymer fiber materials are shrunk from micrometers to submicrons or nanometer (Figure 1.11), there appear several amazing characteristics such as very large surface area to volume ratio, flexibility in surface functionalities, and superior mechanical properties such as stiffness and tensile strength compared to any other known form of the material. These outstanding properties make the polymer nanofibers to be optimal candidates for many important applications [38].

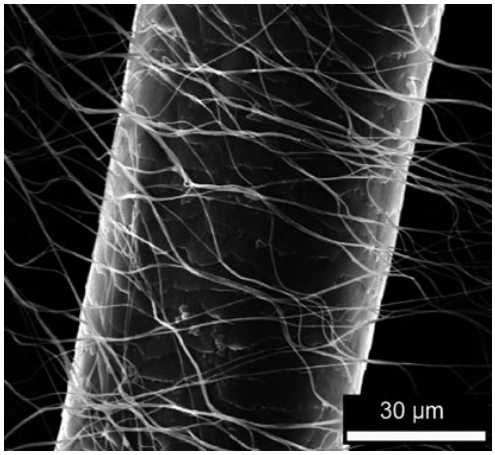

Figure 1.11. Scanning electron microscope (SEM) image of a human hair surrounded by electrospun fibers of poly (vinyl alcohol) [39]

Polymer nanofibers are utilized in various application areas as filtrations, affinity membranes and recovery of metal ions, tissue engineering scaffolds, wound dressing, controlled drug delivery approaches, catalyst and enzyme carriers, sensors, cosmetics, protective clothing and energy storage.

Tissue engineering, a gripping field in which nanofibers are utilized, makes use of scaffolds to provide support for cells to regenerate new extra cellular matrix which has been destroyed by disease, injury or congenital defects without stimulating any immune response.

Another application that is of great interest is drug delivery where either biodegradable or non-degradable materials can be used to control whether drug release occurs via diffusion alone or diffusion and scaffold degradation. Besides, due to the flexibility in material selection a number of drugs can be delivered including: antibiotics, anticancer drugs, proteins, and DNA.

One of the most widely investigated application field of nanofibers is wound dressing. Nanofibrous scaffolds with more homogeneity besides meeting other requirements like oxygen permeation and protection of wound from infection and dehydration for use as wound-dressing materials. These materials are used for the treatment of wounds or burns of a human skin, as well as designed for hemostatic devices with some unique characteristics. In cooperation with electric field, fine fibers of biodegradable polymers can be directly sprayed/spun onto the injured location of skin to form a fibrous mat dressing (Figure 1.12), leading wounds heal by encouraging the formation of normal skin growth and eliminate the formation of scar tissue that would occur in a traditional treatment.

Figure 1.12. Nanofibers for wound dressing (www.electrosols.com)

A number of processing techniques such as drawing, template synthesis, phase separation, self-assembly, electrospinning, etc. have been used to prepare polymer nanofibers in recent years [38]. However, due to the restrictions and drawbacks, the electrospinning process seems to be the only method which can be further developed for production of one-by-one continuous nanofibers from various polymers.

1.2.1. Electrospinning Technique

The combined use of two techniques namely electrospray and spinning is made use in a highly versatile technique called electrospinning (electro + spinning). A high electric field is applied to the droplet of a fluid which may be a melt or solution coming out from the tip of a die, which acts as one of the electrodes. This leads to the droplet deformation and finally to the ejection of a charged jet from the tip of the cone accelerating towards the counter electrode leading to the formation of continuous fibers [40].

Briefly, the basic electrospinning process uses a polymeric solution driven from a syringe into a needle by a syringe pump. Under a high electric field, a droplet at the nozzle

tip is deformed into a conical structure known as a Taylor cone. These charged jets undergo a deposition process, resulting in the formation of fine fibers. Under an increasing electric field, a critical voltage is attained where the repulsive electrostatic force overcomes the surface tension, allowing charged fluid jets to be ejected from the tip of the Taylor cone. The jets undergo a whipping motion and elongate continuously via electrostatic repulsion until they are deposited on a grounded collector [41].

A typical electrospinning setup consists of a capillary through which the liquid to be electrospun is forced; a high voltage source with positive or negative polarity, which injects charge into the liquid; and a grounded collector (Figure 1.13). A syringe pump, gravitational forces, or pressurized gas are typically used to force the liquid through a small-diameter capillary forming a pendant drop at the tip. An electrode from the high voltage source is then immersed in the liquid or can be directly attached to the capillary if a metal needle is used. The voltage source is then turned on and charge is injected into the polymer solution. Increasing the electric field strength causes the repulsive interactions between like charges in the liquid and the attractive forces between the oppositely charged liquid and collector to begin to exert tensile forces on the liquid, elongating the pendant drop at the tip of the capillary. As the electric field strength is increased further a point will be reached at which the electrostatic forces balance out the surface tension of the liquid leading to the development of the Taylor cone. If the applied voltage is increased beyond this point a fiber jet will be ejected from the apex of the cone and be accelerated toward the grounded collector [42].

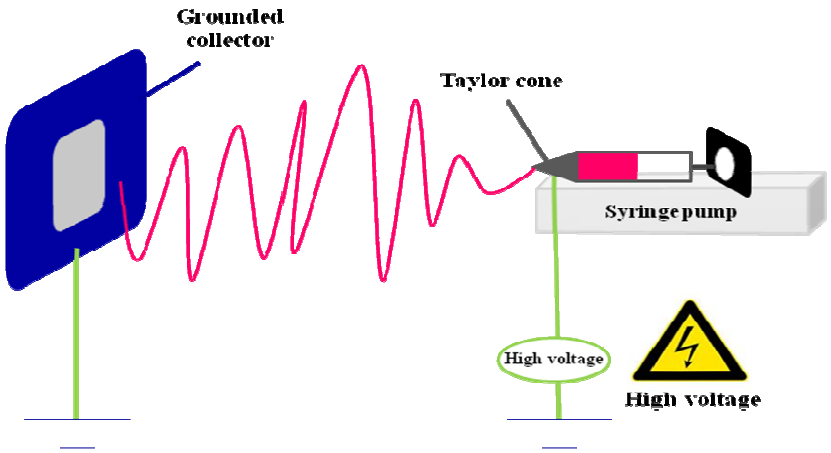

Figure 1.13. Schematic of electrospinning system

1.2.2. Processing Parameters

Despite the fact that electrospinning is a technique which is relatively easy to use, there are a number of processing parameters that can greatly affect fiber formation and structure. When these parameters are grouped in order of relative impact to the electrospinning process, the sequence would be: applied voltage, polymer flow rate, and capillary-collector distance. Nevertheless, all three parameters can influence the formation of bead defects.

The strength of the applied electric field controls formation of fibers from several microns in diameter to tens of nanometers. Thus, suboptimal field strength could lead to bead defects in the spun fibers or even failure in jet formation. Deitzel et al. examined a polyethylene oxide (PEO)/water system and found that increases in applied voltage altered the shape of the surface at which the Taylor cone and fiber jet were formed [43]. On the other hand, at lower applied voltages the Taylor cone formed at the tip of the pendent drop, whereas, when the applied voltage was increased the volume of the drop decreased until the Taylor cone was formed at the tip of the capillary, which was associated with an increase in bead defects seen among the electrospun fibers (Figure 1.14).

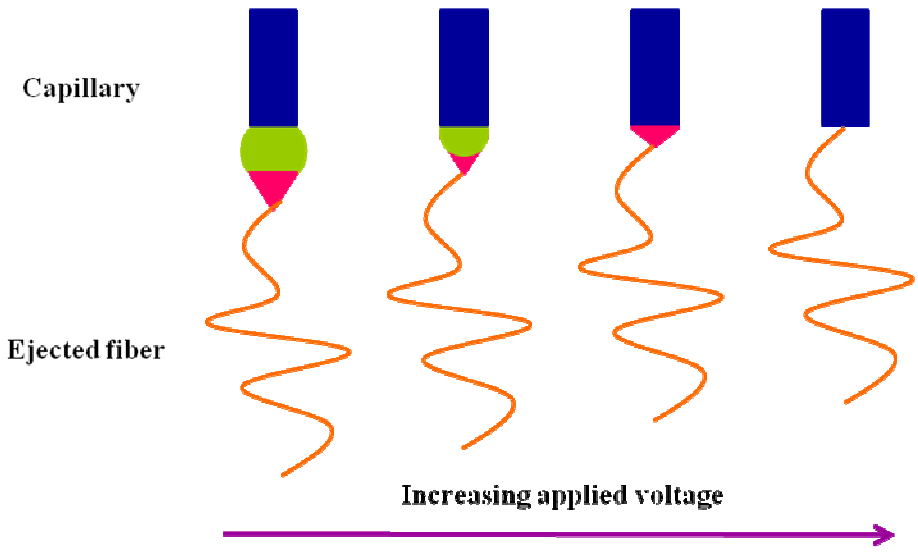

Figure 1.14. Effect of applied voltage on the formation of Tailor cone

Polymer flow rate is another effective parameter on fiber diameter, besides can influence fiber porosity as well as fiber shape. In 1969, Taylor realized that the cone shape at the tip of the capillary cannot be maintained if the flow of solution through the capillary is insufficient to replace the solution ejected as the fiber jet [44]. In 2002, Megelski et al. examined the effects of flow rate on the structure of electrospun fibers from a polystyrene/tetrahydrofuran (THF) solution [45]. They demonstrated that both fiber diameter and pore size increase with increasing flow rate. Additionally, at high flow rates significant amounts of bead defects were noticeable, due to the inability of fibers to dry completely before reaching the collector. Incomplete fiber drying also leads to the formation of ribbon like (or flattened) fibers as compared to fibers with a circular cross section.

Although playing a much smaller role, the distance between capillary tip and collector can also influence fiber size by 1-2 orders of magnitude, at the same time this distance can dictate whether the end result is electrospinning or electrospraying.

1.2.3. Solution Parameters

In addition to the processing parameters a number of solution parameters play an important role in fiber formation and structure. When these parameters are grouped in order of relative impact to the electrospinning process, the sequence would be: polymer concentration, solvent volatility and solvent conductivity.

The polymer concentration designates the spinnability of a solution, meaning that whether a fiber forms or not. In other words, the solution must have a high enough polymer concentration for chain entanglements to occur but the solution cannot be either too dilute or too concentrated. The importance of polymer concentration in electrospinning grows from the fact that it influences both the viscosity and the surface tension of the solution, both of which are very important parameters in the electrospinning process. If the solution is too dilute then the polymer fiber will break up into droplets before reaching the collector due to the effects of surface tension. On the other hand, if the solution is too concentrated then fibers cannot be formed due to the high viscosity, which makes it difficult to control the solution flow rate through the capillary. Therefore, an optimum range of polymer

concentrations exists in which fibers can be electrospun when all other parameters are held constant. Doshi and Reneker, electrospun fibers from PEG/water solutions containing various PEG concentrations and found that solutions with viscosity less than 800 centipoises broke up into droplets upon electrospinning while solutions with viscosity greater than 4000 centipoises were too thick to electrospin [46]. According to literature, it can be claimed that within the optimal range of polymer concentrations fiber diameter increases with increasing polymer concentration. Megelski et al. found that by increasing the concentration of polystyrene in THF the fiber diameter increased and the distribution of pore sizes became narrower [45]. Deitzel et al. found that fiber diameter of fibers electrospun from PEO/water solution were related to PEO concentration by a power law relationship [43].

Solvent choice is another critical parameter as to whether fibers are capable of forming, as well as influencing fiber porosity. In order for sufficient solvent evaporation to occur between the capillary tip and the collector a volatile solvent must be used. When the fiber jet travels through the atmosphere toward the collector a phase separation, which is a process that is mainly influenced by the volatility of the solvent, occurs before the solid polymer fibers are deposited. Megelski et al. examined the structural properties of polystyrene fibers electrospun from solutions containing various ratios of DMF and THF [44]. While solutions electrospun from 100% THF (more volatile) demonstrated a high density of pores, which increased the surface area of the fiber by as much as 20-40% depending on the fiber diameter, solutions electrospun from 100% DMF (less volatile) demonstrated almost a complete loss of microtexture with the formation of smooth fibers, concluding that pore size increased with decreased pore depth as the solvent volatility decreased.

Solution conductivity plays a little role. It is claimed that solutions with high conductivity will have a greater charge carrying capacity than solutions with low conductivity, as the fiber jet of highly conductive solutions will be subjected to a greater tensile force in the presence of an electric field than will a fiber jet from a solution with a low conductivity. As it was predicted, Baumgarten was able to show that the radius of the fiber jet is inversely related to the cube root of the solution conductivity [47]. Additionally, Hayati et al. were able to show that highly conductive solutions were extremely unstable in

the presence of strong electric fields, which led to a dramatic bending instability as well as a broad diameter distribution [48].

1.2.4. Smart Nanofibers

Functional nanofibers are of considerable interest due to their wide range of potential applications. Among those, nanofibers with smart surfaces responding to the environment and solvent resistant structures become outstanding. These smart nanofibers are promising especially for sensors, controlled drug delivery systems and bioengineering applications.

Fu and coworkers developed a simple method to elaborate solvent resistant nanofibers with thermal-sensitive surfaces by the combined technology of RAFT polymerization, ATRP, electrospinning, and “click chemistry” (Figure 1.15). After the chloromethylstvrene copolymer was synthesized and electrospun, it was functionalized with sodium azide obtaining reactive azide groups on the surface. Separately synthesized thermoresposive polymer beaing alkyne end group was covalently attached on the surface of electrospun nanofibers resulting in nanofibers with a thermal-sensitive surface [49].

In a latter study, Fu and coworkers demonstrated that a novel photo responsive controlled release system, in which prodrugs were loaded on the photo responsive and cross-linked nanofiber surface via host-guest interaction, could be constructed (Figure 1.16). The main difference of this smart system from the other controlled release systems, in which the drug was loaded inside the carrier and was susceptible to release delays in response to external stimuli, was providing a photo controlled fast “ON-OFF” release characteristic. With the availability of a wide variety of CD prodrugs, stimuli-responsive nanofiber systems with loaded CD prodrugs are expected to provide unique opportunities for the effective and controlled “ON-OFF” release of therapeutic agents [50].

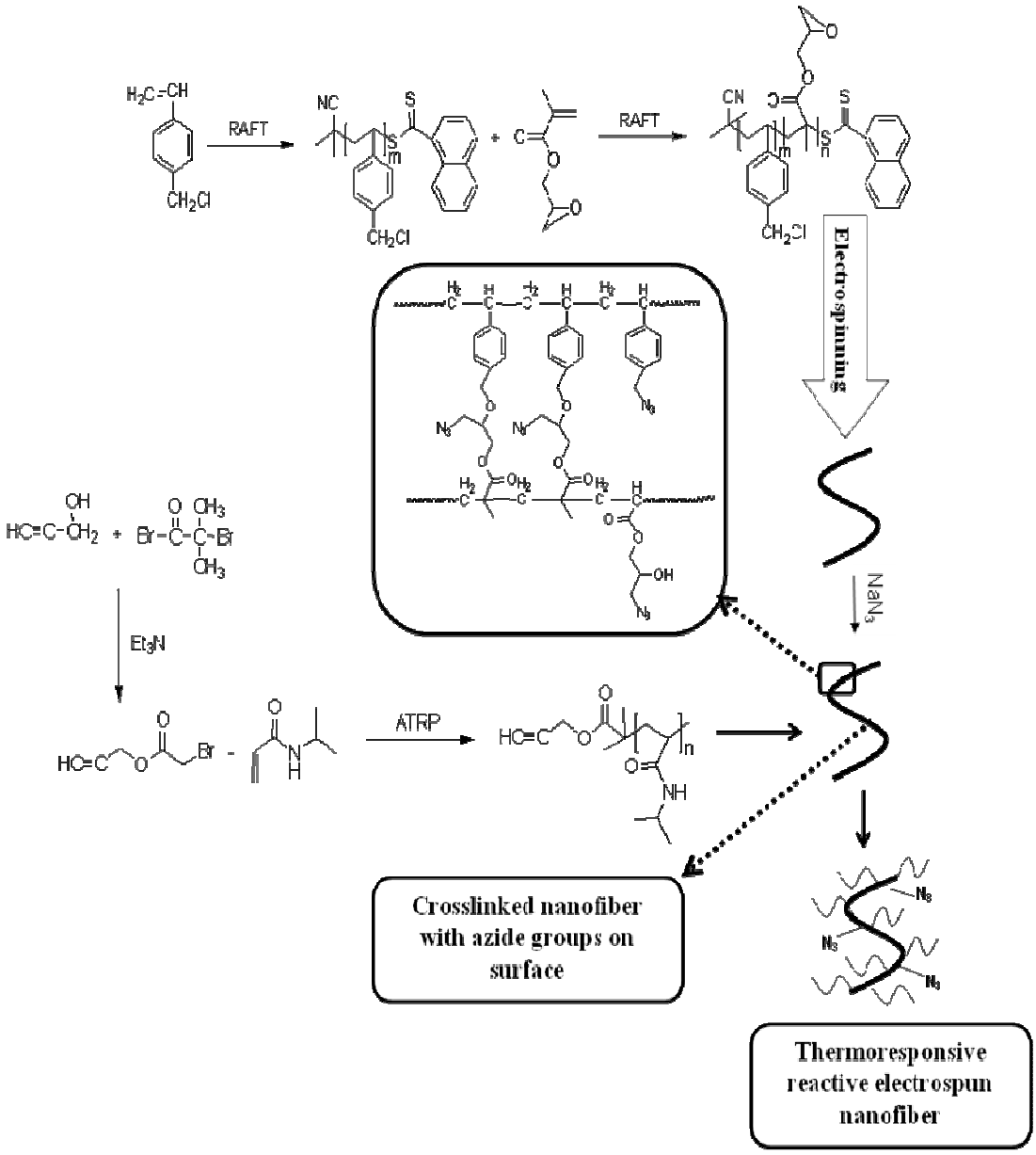

Figure 1.15. Constitution of Solvent-Resistant Nanofibers

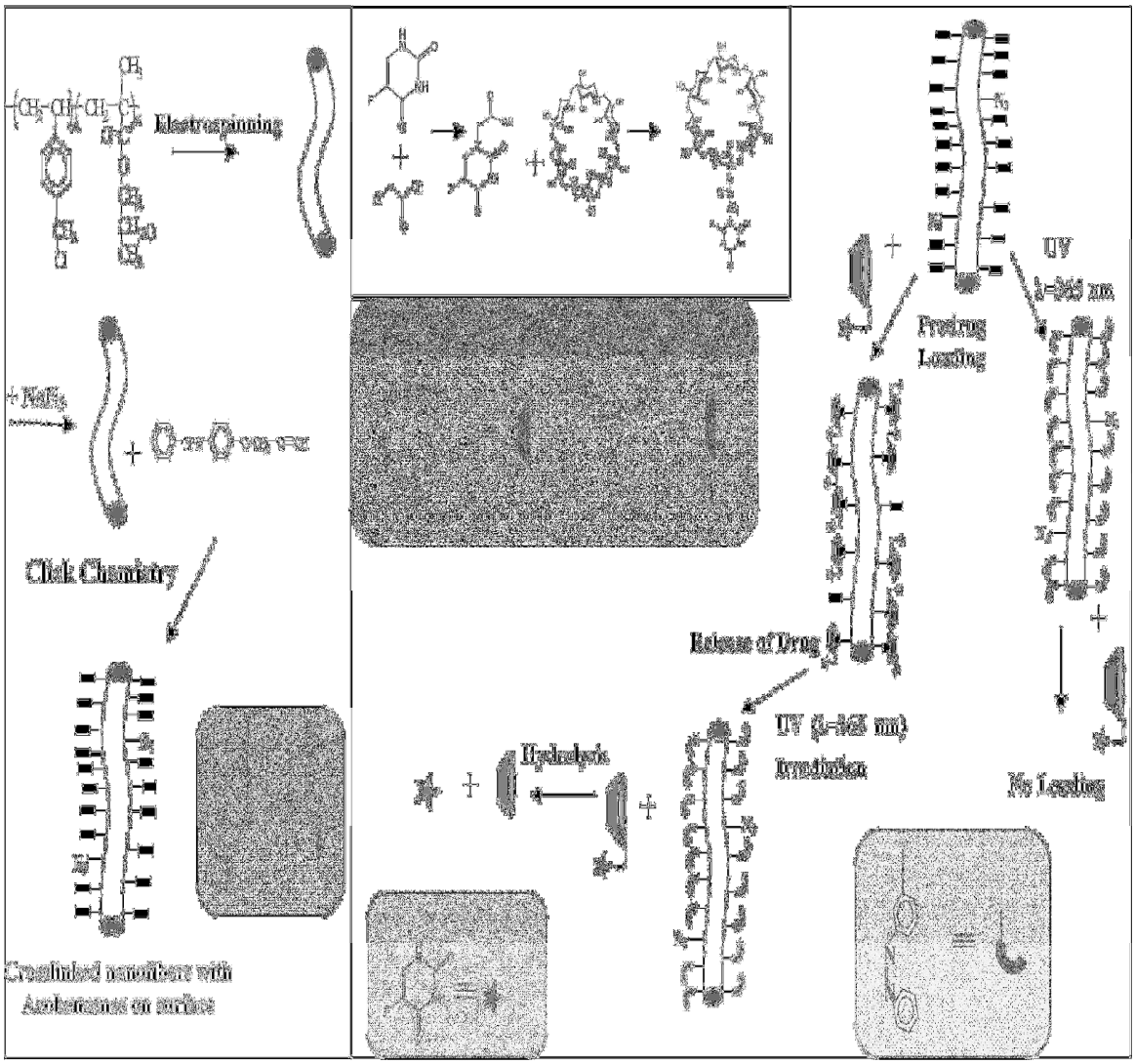

Figure 1.16. Preparation of stimuli responsive nanofiber system [50]

2. AIM OF THE STUDY

2.1. Reactive Polymeric Supports for Drug Delivery Approaches

Water soluble, biocompatible and biodegradable reactive polymeric supports are instrumental in design and development of novel drug delivery platforms. Drug delivery systems are needed to overcome the low solubility drawback of most of the drug molecules. Therefore, water solubility is one of the preferential demands for the polymers which are cogitated to be utilized in drug delivery. Amine and alkyne reactive groups broaden the range of drug molecules that might be attached onto the polymer. Biocompatibility is the basic desirable property for the polymers designed to be used in controlled drug delivery systems. Additionally, these polymeric supports are required to be biodegradable in order to allow elimination of the polymeric substances from the body and also to deliver the drug molecule to the desired site. Herein, water soluble poly (ethylene glycol) methacrylate based random copolymers containing amine or alkyne reactive groups have been synthesized using the Atom Transfer Radical Polymerization method. Reactivity towards amines is tested by functionalizing the reactive polymer with benzyl amine. Biodegradation behaviors of the reactive polymers are evaluated (Figure 2.1).

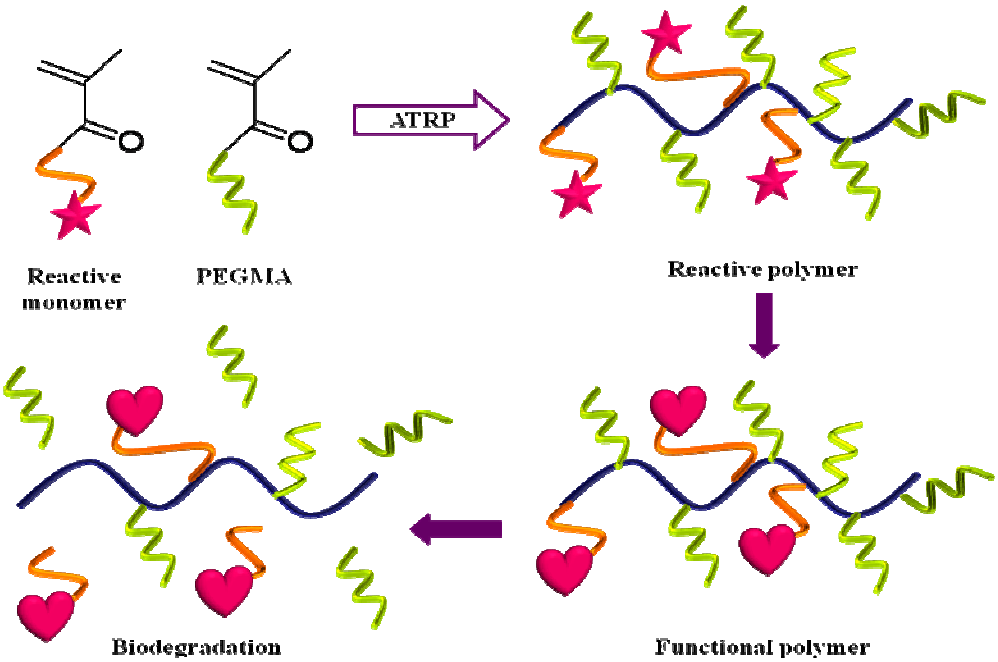

Figure 2.1. Process of reactive copolymer

2.2. Reactive Fibrous Scaffolds

Biocompatible and stable nanofibrous structures are of great interest which is an outstanding development especially in biomedical field. Combining both hydrophillic (for biocompatibility) and hydrophobic (for stability) monomers with various reactive monomers polymers with different properties can be obtained. Electrospinning, is the most convenient method to produce nano sized fibers. These nanofibers can be crosslinked to achieve stable structures that are also further functionalizable for wide range of applications. In this study, using different combinations of MMA, PEGMEMA, FMA, NHSMA, furan protected maleimide monomer and hydrogenated protected maleimide monomer, various polymers are obtained. Consequently, protected reactive groups on the polymers are activated. Subsequently, different concentrations of polymer solutions are evaluated for electrospinning in order to obtain smooth nanofibers acquiring amine, thiol or both reactive groups at the same time (Figure 2.2).

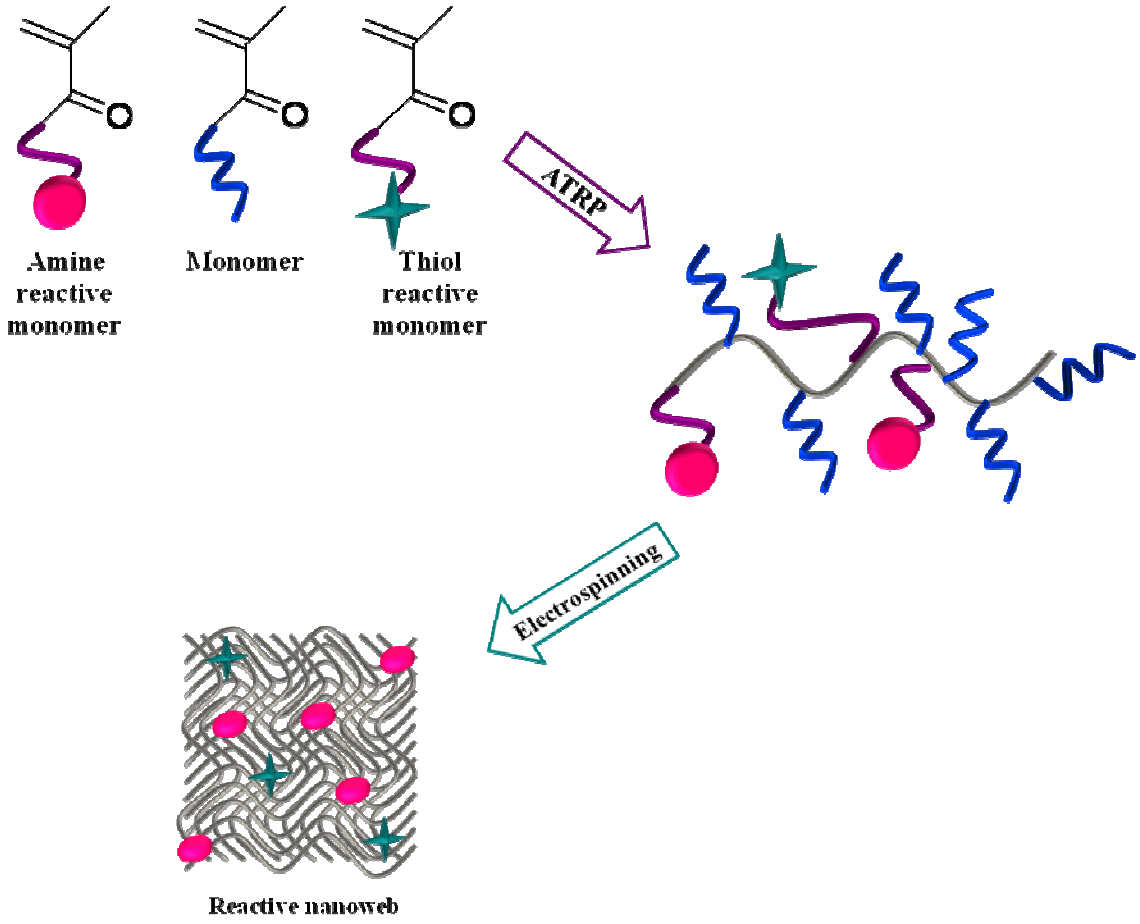

Figure 2.2. Elaboration of reactive nanowebs

3. RESULTS AND DISCUSSION

3.1. Reactive Polymers for Polymer – Drug Conjugates

Following the synthesis, amine reactive succinimide monomer (NHSMA, 3) and alkyne reactive azide monomer (AHMA, 7) are copolymerized with water soluble and biocompatible poly (ethylene glycol) methacrylate, compound 4, via atom transfer radical polymerization, namely ATRP, resulting in reactive copolymers enabling conjugations with drug molecules via different pathways (Figure 3.1).

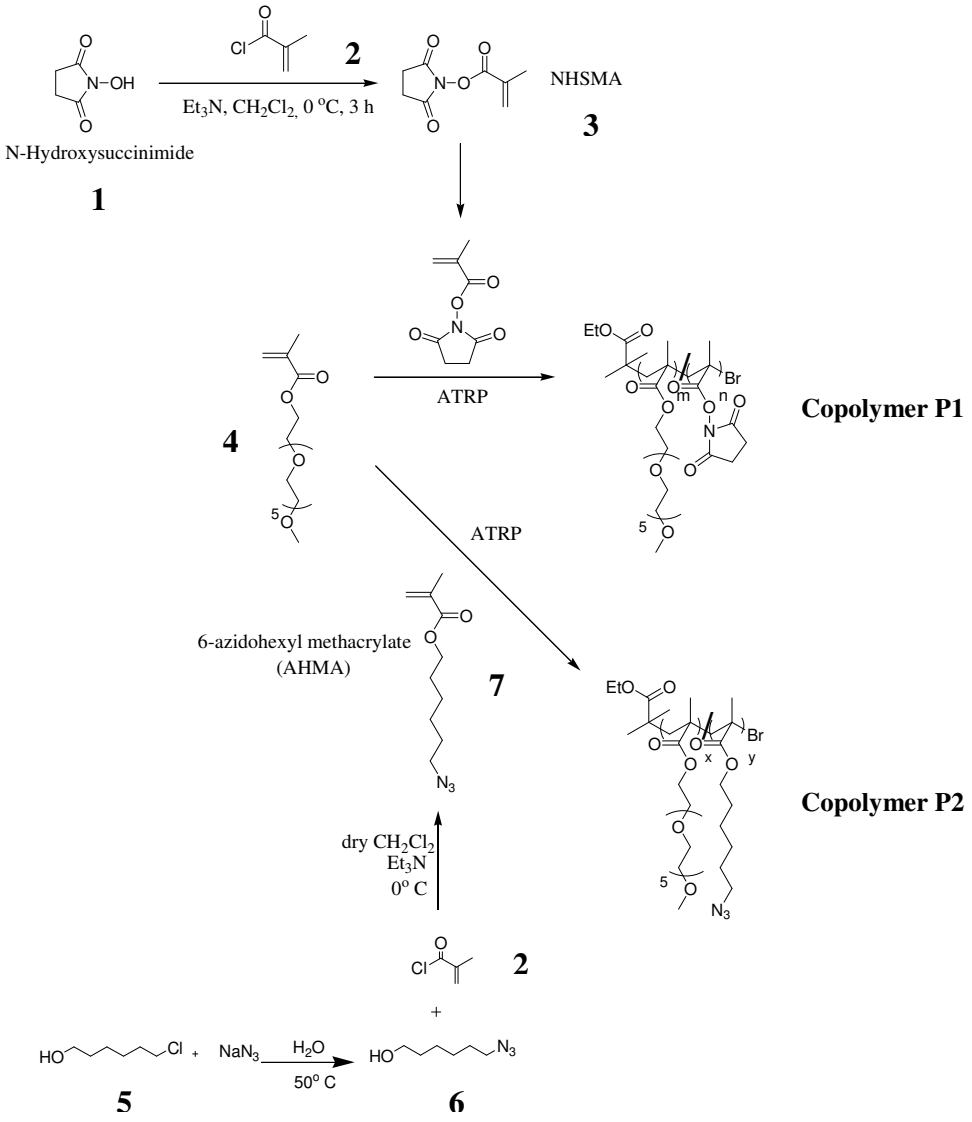

Figure 3.1. General scheme for reactive copolymer synthesis

It is crucial to use polymers with narrow polydisperties and known architecture for biological applications. To be able to have control over molecular weight distribution ATRP technique is used in polymerizations. ATRP is a controlled living polymerization method which is initiated by an alkyl halide (R-X) and catalyzed by a transition metal complex, such as CuX/bpy. In this study, Ethyl 2-bromoisobutyrate initiator is used as the alkyl halide initiator and CuBr/PMDETA as the catalyst system. Reaction time and solvent ratio is investigated for obtaining polymers with narrow polydispersities and desired molecular weights.

The aim is to obtain water soluble reactive copolymers, for this reason poly (ethylene glycol) monomethyl ether methacrylate is used as a comonomer. Poly (ethylene glycol) (PEG) is chosen since it is water soluble and at the same time biocompatible and antibiofouling - meaning that it prevents bioadhesion. PEG with a Mw than 50 000 can be excreted from the kidneys and thus, accumulation toxicity may not become a problem unless PEG with a Mw higher than the critical value is used in the polymerization process [52]. Antibiofouling property of the PEG stems from its protein resistivity due to steric repulsion between hydrated PEG chains and proteins.

In ATRP method, numerous combinations of solvent and temperature system can be used. In this study, reaction conditions and monomer ratios are investigated in order to optimize reactive copolymers' properties which are molecular weight, poly dispersity index, number of reactive groups on the polymer and hydrodynamic volume regarding to the branched structure.

Combinations and results of ATRP conditions can be followed in Table 3.1. In the case of decreasing the equivalence of catalyst system, average molecular weight increases (Entry 3 & 8 and 5 & 7). In addition, monomer ratio also influences the molecular weight. In other words, under the same conditions, when the ratio of PEGMEMA is increased the molecular weight of the copolymer increases (Entry 1 & 2 and 7 & 9). Solvent amount is another important parameter that has an effect on both molecular weight and PDI, meaning that in the case of larger solvent amount, copolymers having lower molecular weight and better PDI are obtained (Entry 3 & 4, 6 & 7 and 8 & 9).

Table 3.1. Synthesis of Copolymer P1

Entry	Conversion (%)	Mn	PDI	Catalyst system (PMDETA:CuBr:EBIB) (eq.)	Monomer ratio (PEGMEMA:NHSMA) (eq.)	Solvent (mL)
1	90	38000	1.29	0.25:0.125:0.125	100:0	1
2	78	28400	1.22	0.25:0.125:0.125	86:14	1
3	72	28100	1.51	1:0.5:0.5	80:20	1
4	33	17600	1.33	1:0.5:0.5	80:20	2
5	32	15200	1.25	1.5:0.75:0.75	86:14	2
6	73	14100	1.41	2:1:1	86:14	1
7	65	13700	1.31	2:1:1	86:14	2
8	83	17000	1.53	2:1:1	80:20	1
9	38	12600	1.34	2:1:1	80:20	2

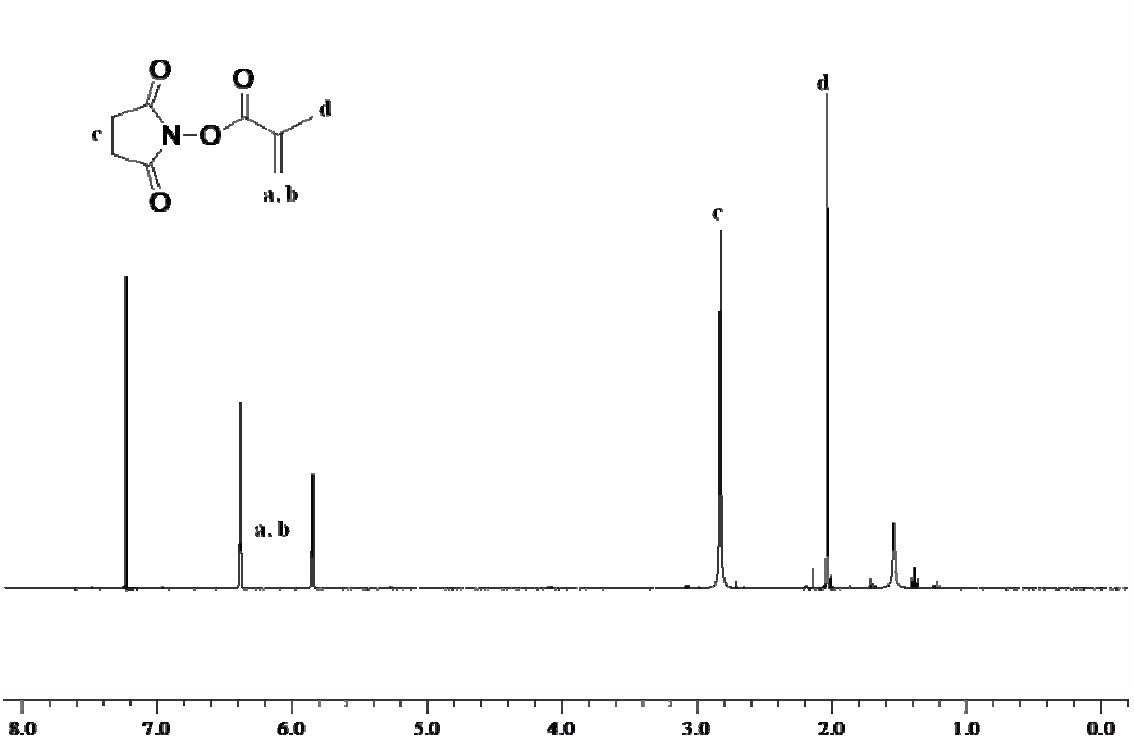

Figure 3.2. ^{1}H NMR of NHSMA

Polymerization (Figure 3.3) of compound 3 should result in disappearance of the proton resonances from the acrylate unit at 6.41 ppm (s, 1H, CH2=C) and 5.88 ppm (m, 1H, CH2=C) (Figure 3.2, peak a & b, respectively) to give Copolymer P1 since unreacted monomers were eliminated by precipitating the polymer solution in diethyl ether. The composition of the copolymers could be easily determined from the integration of the ^{1}H NMR spectra. The ratio of area under the peak at 2.80 ppm (peak c, Figure 3.4) corresponding to the ring protons of the succinimide monomer to the area under the methyl ether group of PEGMEMA at 3.34 ppm (peak b, Figure 3.4) was used for copolymer composition determinations.

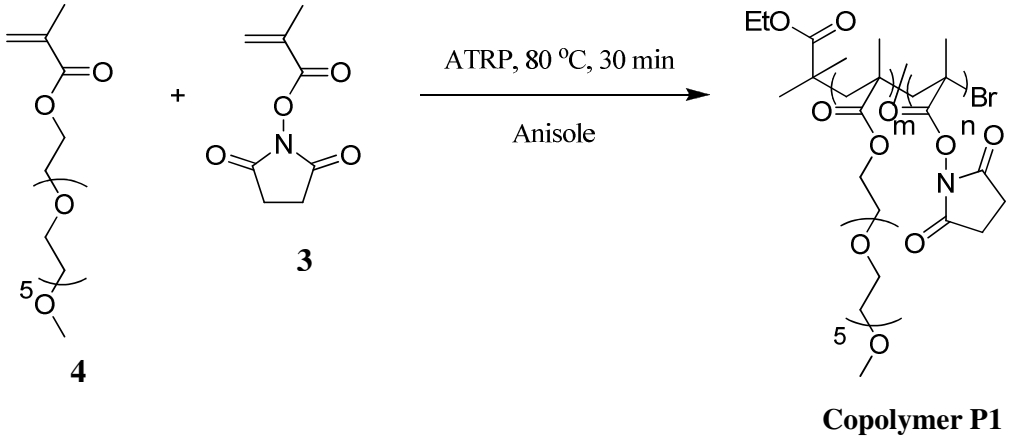

Figure 3.3. Synthesis of Copolymer P1

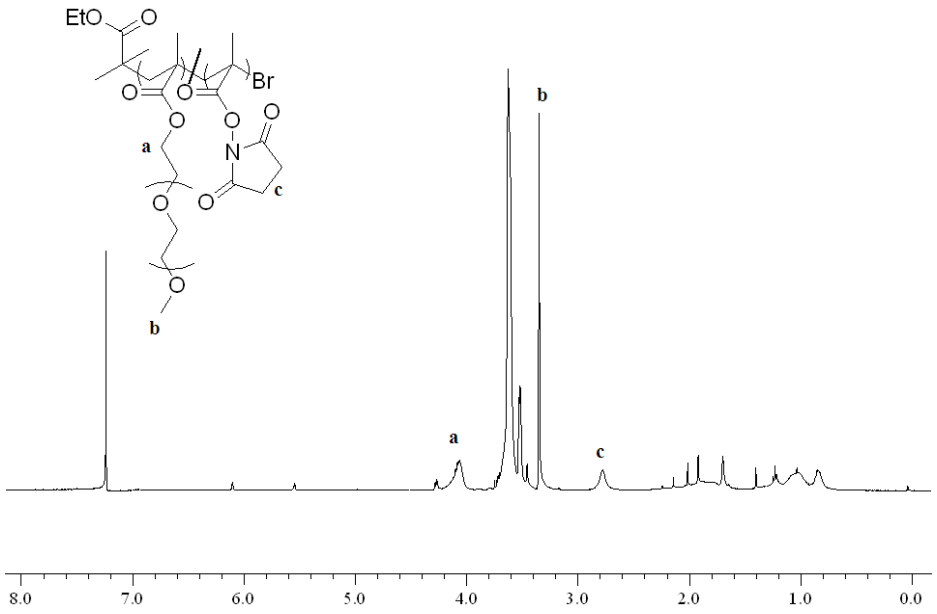

Figure 3.4. ^{1}H NMR of Copolymer P1

Polymerization (Figure 3.5) of compound 7 should result in appearance of a new peak from the azide unit at 3.24 ppm (t, 2H, J =7,6) (peak c, Figure 3.6) to give Copolymer P2. The composition of the copolymers could be easily determined from the integration of the ^{1}H NMR spectra. The ratio of area under the peak at 3.24 ppm (peak c, Figure 3.6) corresponding to the protons of the compound 7 to the area under the methyl ether group of PEGMEMA at 3.34 ppm (peak b, Figure 3.6) was used for copolymer composition determinations.

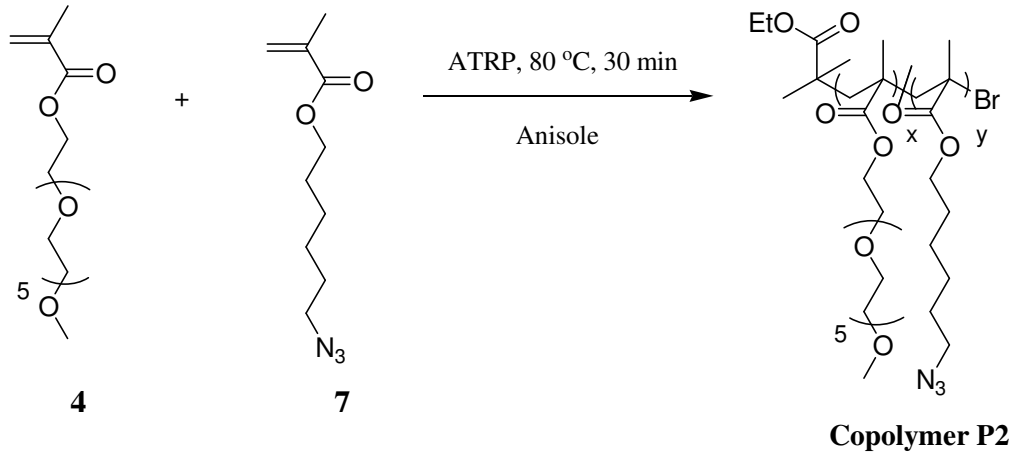

Figure 3.5. Synthesis of Copolymer P2

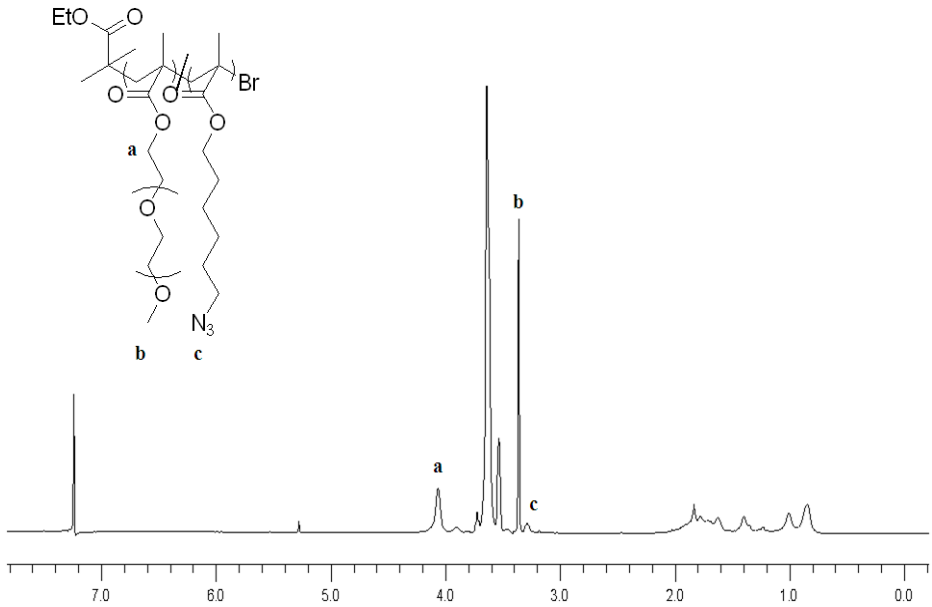

Figure 3.6. ^{1}H NMR of Copolymer P2

3.1.1. Functionalization of the NHS Copolymer

Previously synthesized Copolymer P1 is functionalized with benzyl amine in order to prove the reactivity of the polymer. Through this process different procedures were followed and finally reaction conditions were optimized and the polymer was functionalized with benzyl amine successfully (Figure 3.7). Regarding ^{1}H NMR analysis, appearance of a new peak between 7.19 - 7.39 ppm and 4.39 ppm (Figure 3.7, peak d & c, respectively), accompanied by disappearance of peak at 2.80 ppm (Figure 3.4, peak c) corresponding to the succinimide reactive group shows successful functionalization (Figure A.1).

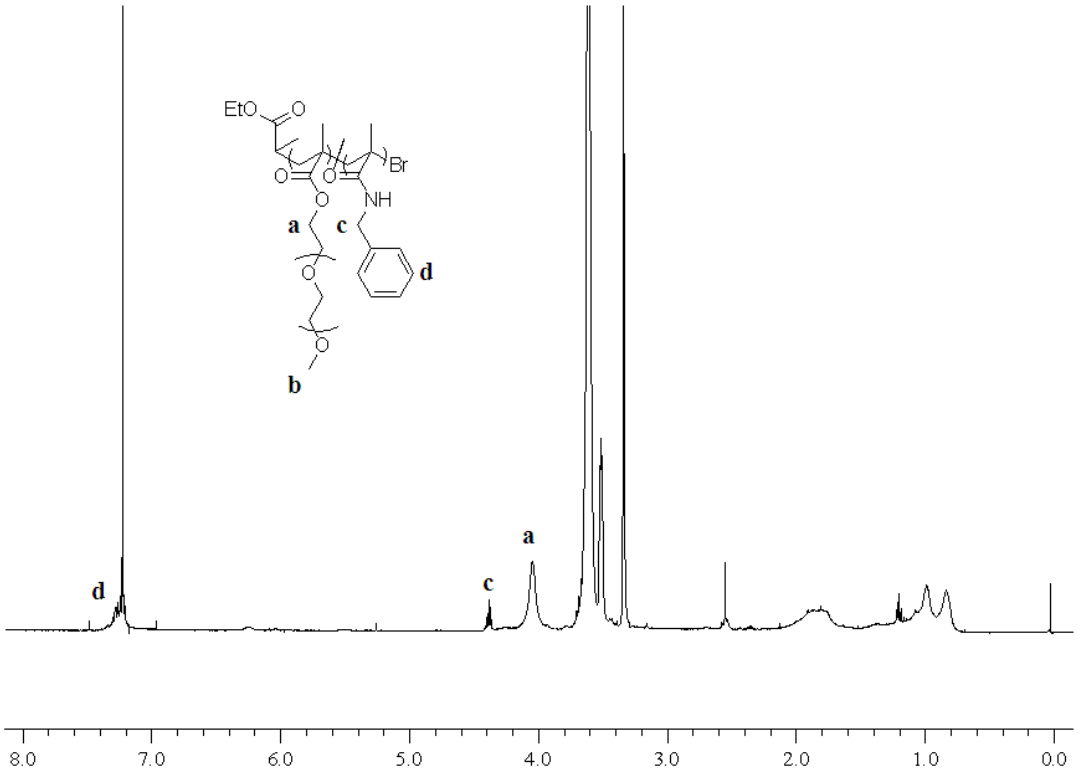

Figure 3.7. ^{1}H NMR of functionalized polymer

3.1.2. Biodegradation Behaviors of the Reactive Copolymers

Biodegradation behaviors of the both reactive copolymers are observed in vitro. For the in vitro experiments it is crucial to be at 37 °C as average healthy human body

temperature. Since approximately 70 % of human body is composed of water, *in vitro* experiments are generated in phosphate buffer solution, namely PBS. Acidity of the PBS is controlled with a pH-meter to obtain 2 different pH values taking into account that tumor cells differ from the healthy tissues in acidity, pH 5.5 and pH 7.4, respectively.

The copolymers that are synthesized in the first part of the research have side chains bearing easily hydrolyzable ester bonds. Therefore, during biodegradation, it is expected that the side chains would leave the backbone earlier. Additionally, a decrease in molecular weight is predicted proportional to the initial molecular weights and acidity of the moiety.

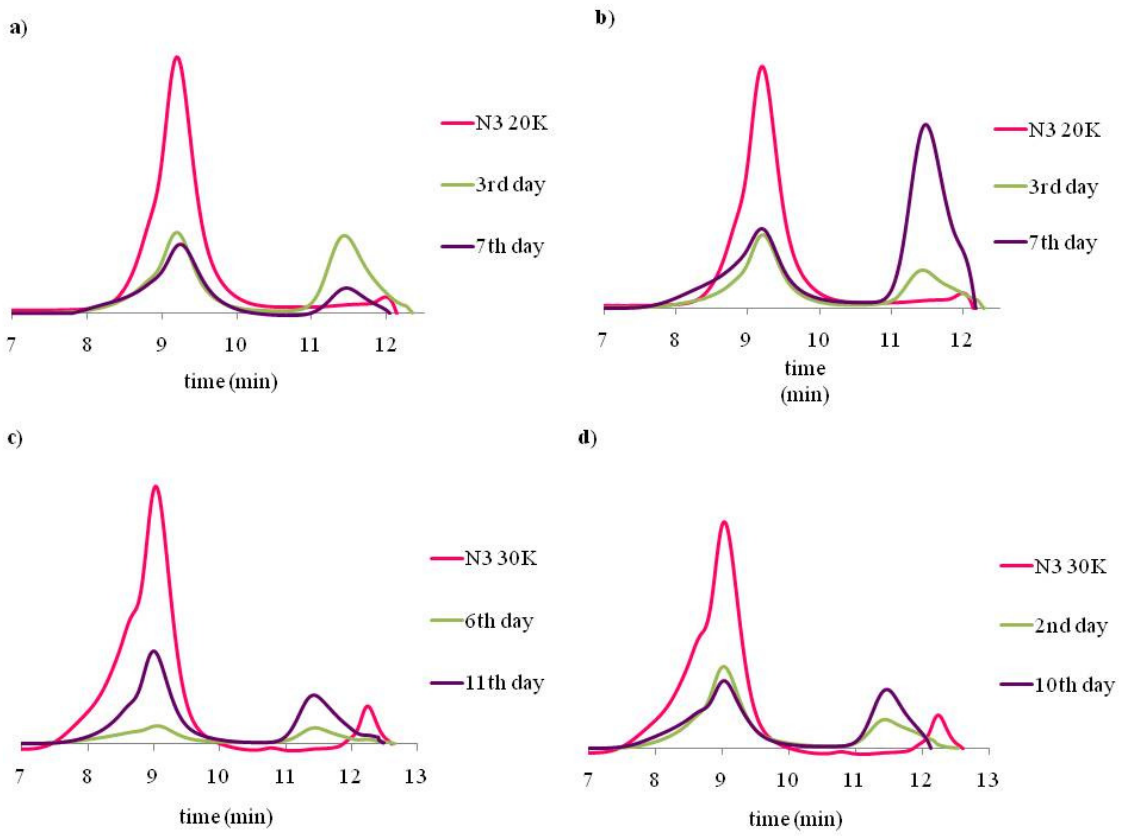

Figure 3.8. GPC traces of Copolymer P2

a) 20K, pH 7.4, b) 20K, pH 5.5, c) 30K, pH 7.4, d) 30K, pH 5.5

The molecular weight changes are determined with gel permeation chromatography, namely GPC. Due to the decrease in molecular weight, GPC traces shift

to left for all reactive copolymers in both pH conditions. In addition, a decrease in intensity of peaks belong to polymer backbone (8-10 min) and an increase in intensity of peaks belong to the side chains (11-12 min) are observed (Figure 3.8 and 3.9) which means degradation starts with side chain detachment.

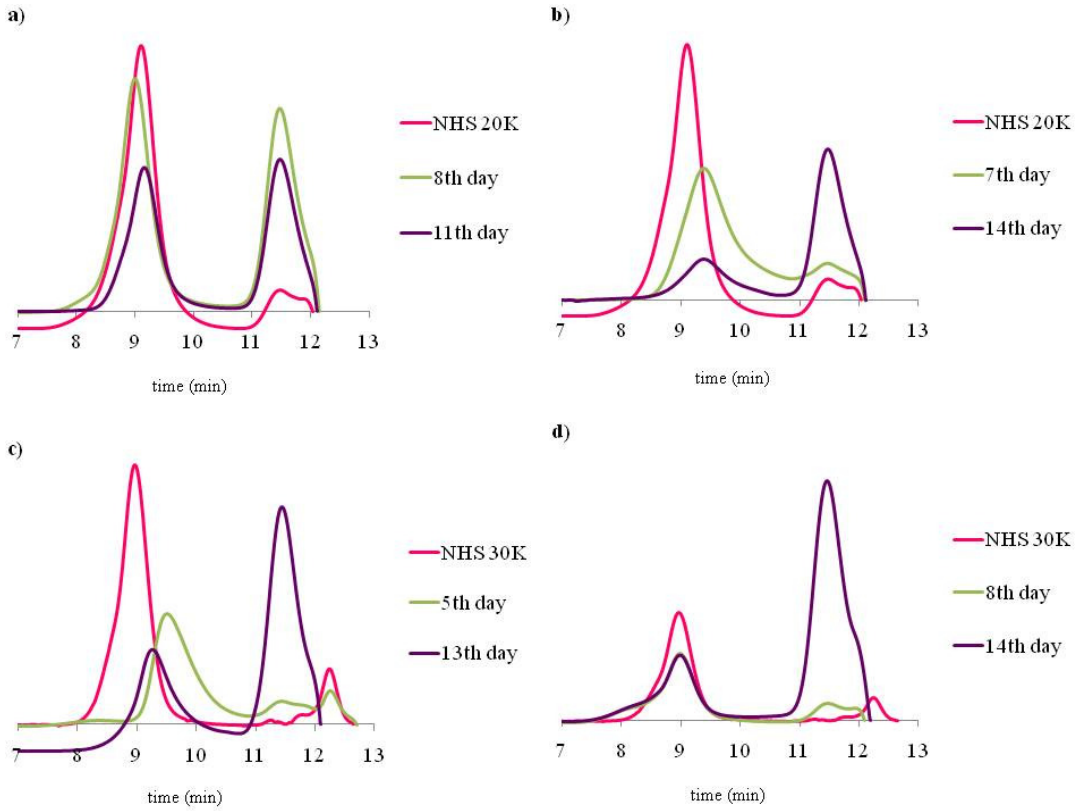

Figure 3.9. GPC traces of Copolymer P1
a) 20K, pH 7.4, b) 20K, pH 5.5, c) 30K, pH 7.4, d) 30K, pH 5.5

As expected, longer biodegradation time is required for reactive copolymers with higher initial molecular weights. In both acidic and neutral media, both polymers with 20K and 30K molecular weight show a parallel decreasing trend and 30K molecular weight polymers keep their advantage (Figure 3.10).

However, a significant difference is noted relative to the variant reactive groups in dissimilar pH conditions. Copolymer P2 degrades faster than Copolymer P1 at pH 5.5, whereas at pH 7.4 Copolymer P1 degrades faster while both polymers with higher average molecular weights degrade slower as expected (Figure 3.11).

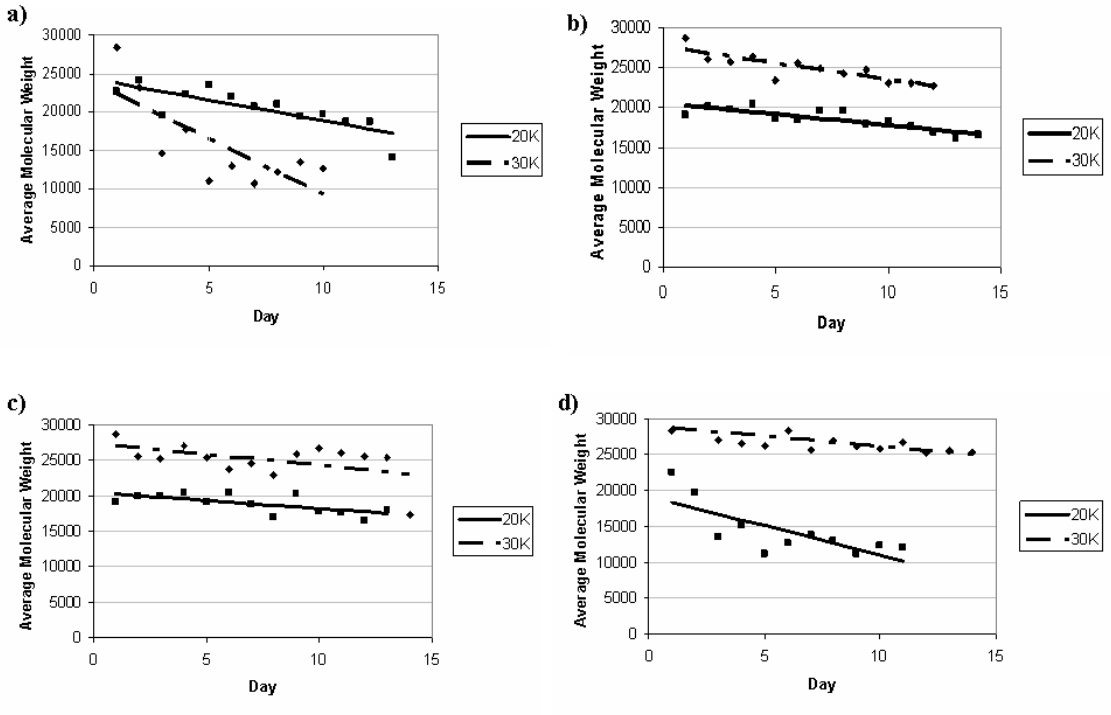

Figure 3.10. Molecular weight changes of copolymers with 20K vs. 30K initial average molecular weights a) Copolymer P1, pH 5.5, b) Copolymer P1, pH 7.4, c) Copolymer P2, pH 5.5, d) Copolymer P2, pH 7.4

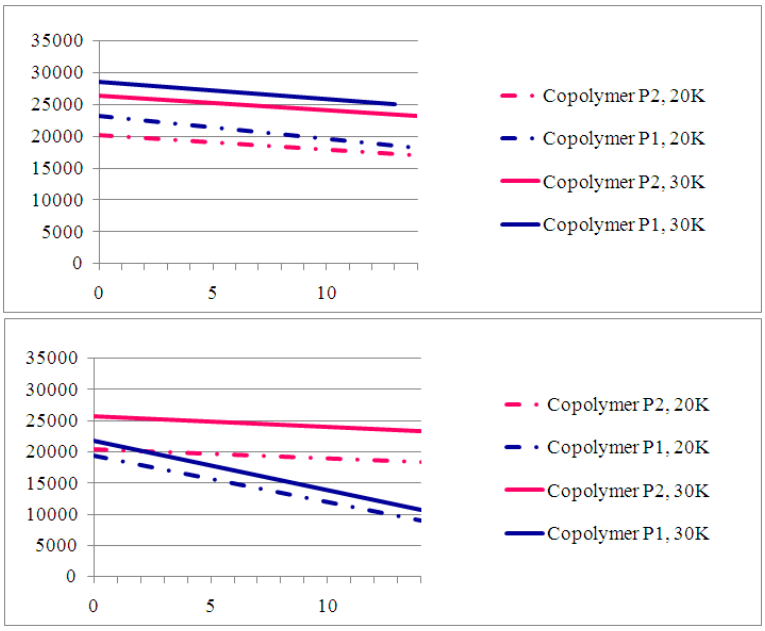

Figure 3.11. Molecular weight change comparison of Copolymer P1 vs. Copolymer P2 a) pH 5.5, b) pH 7.4

Furthermore, biodegradation behaviors of Copolymer P1 and Copolymer P2 are investigated at distinct pH values. A noticeable difference is observed between acidic and neutral media for Copolymer P1, 20K and 30K average molecular weight, whereas there is no significant difference for Copolymer P2 (Figure 3.12). Copolymer P1 degrades much slower at pH 7.4 while Copolymer P2 degradation rates are approximately the same both in acidic and neutral media.

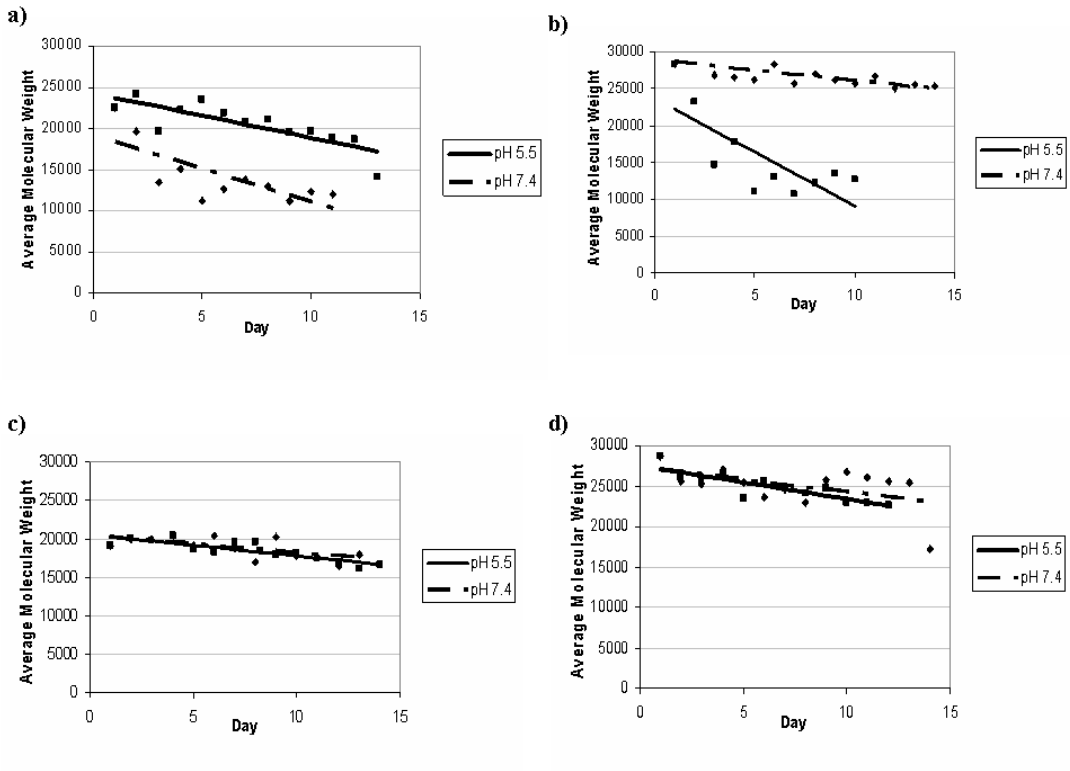

Figure 3.12. Average molecular weight changes of NHS and azide polymers
a) Copolymer P1, 20K, b) Copolymer P1, 30K, c) Copolymer P2, 20K, d) Copolymer P2, 30K

3.2. Reactive Polymers for Nanofibrous Scaffolds

Second part of this study includes synthesis of various random copolymers bearing different reactive groups and preparation of electrospun nanofibers via electrospinning technique (Figure 3.13). The reactive copolymers can be grouped into 3 according to their composition: PEGMA based, MMA based or both, since hydrophilicity and biocompatibility properties are influenced due to the composition.

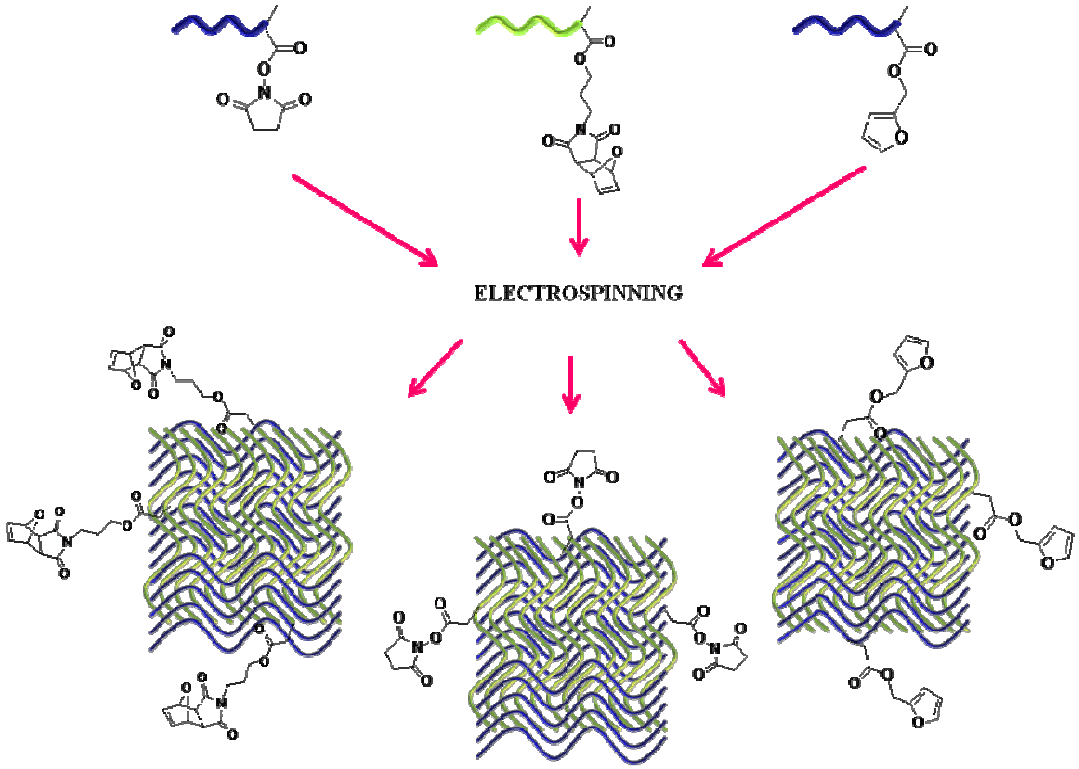

Figure 3.13. General scheme for obtaining reactive nanofibers

3.2.1. Synthesis and Activation of the Furan Protected Maleimide Copolymers

Furan protected maleimide copolymers are synthesized via ATRP (e.g., Copolymer P3) to be electrospun, since furan protected maleimide monomer (Compound 8) enables further thiol functionalization following the activation of maleimide reactive group.

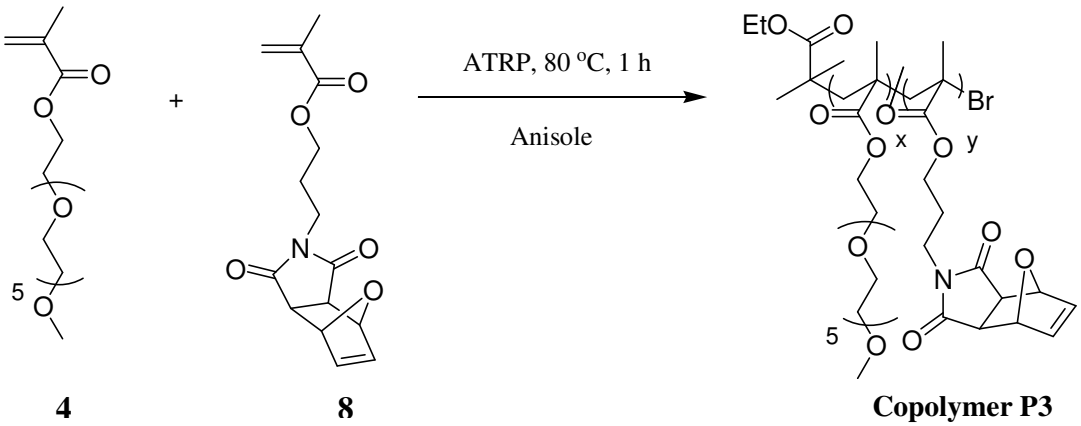

Figure 3.14. Synthesis of Copolymer P3

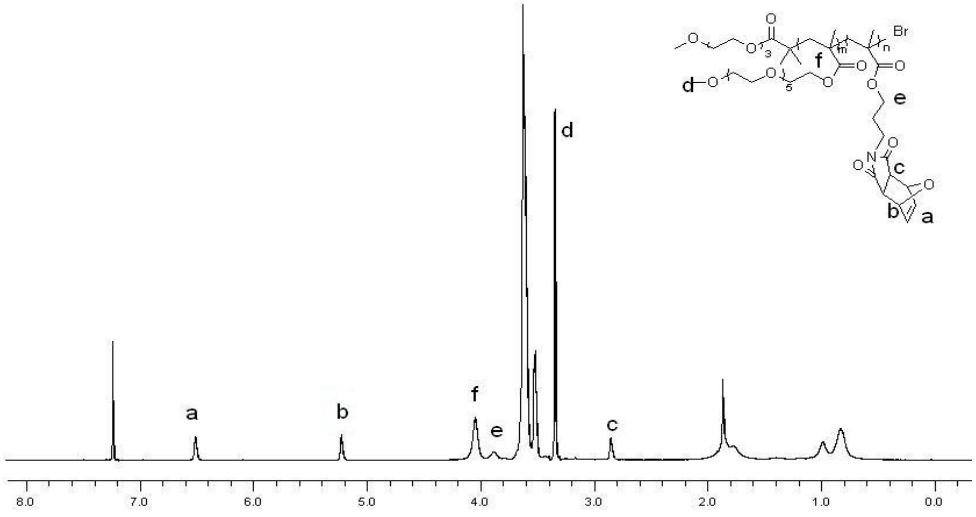

Figure 3.15. ^{1}H NMR of Copolymer P3

These furan protected maleimide copolymers were converted to their reactive form using the retro-Diels-Alder reaction (Figure 3.16). The polymers were heated for 12 h at 110 ^{o}C using toluene as the solvent. This resulted in complete cycloreversion of the furan-maleimide adducts (Figure 3.14) to afford thiol reactive polymers bearing maleimide groups in the side chain (Figure 3.17). ^{1}H NMR analysis proved that the cycloreversion was almost quantitative (Figure 3.18). Appearance of a new peak at 6.75 ppm (peak a, Figure 3.18), accompanied by disappearance of peaks at 5.25 and 6.51 ppm (Figure 3.16, peaks b & a, respectively) corresponding to the oxabicyclic moiety shows successful cycloreversion. GPC analysis proved that there was no detrimental effect on the polymer as confirmed by presence of a monomodal peak with low polydispersity.

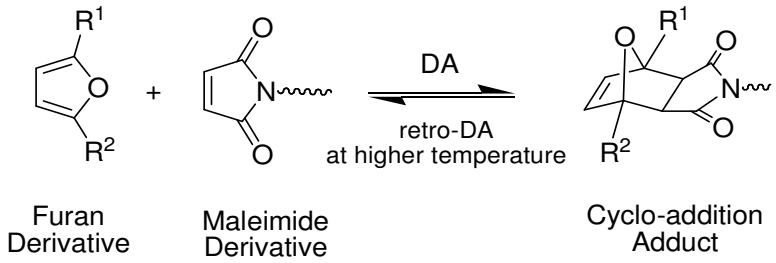

Figure 3.16. Representation of the DA and rDA reactions [51]

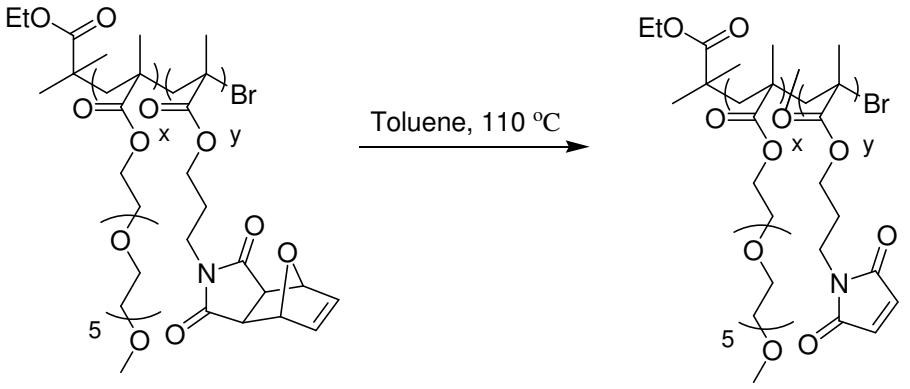

Copolymer P3 **Copolymer P4**

Figure 3.17. Activation of Copolymer P3 yielding Copolymer P4

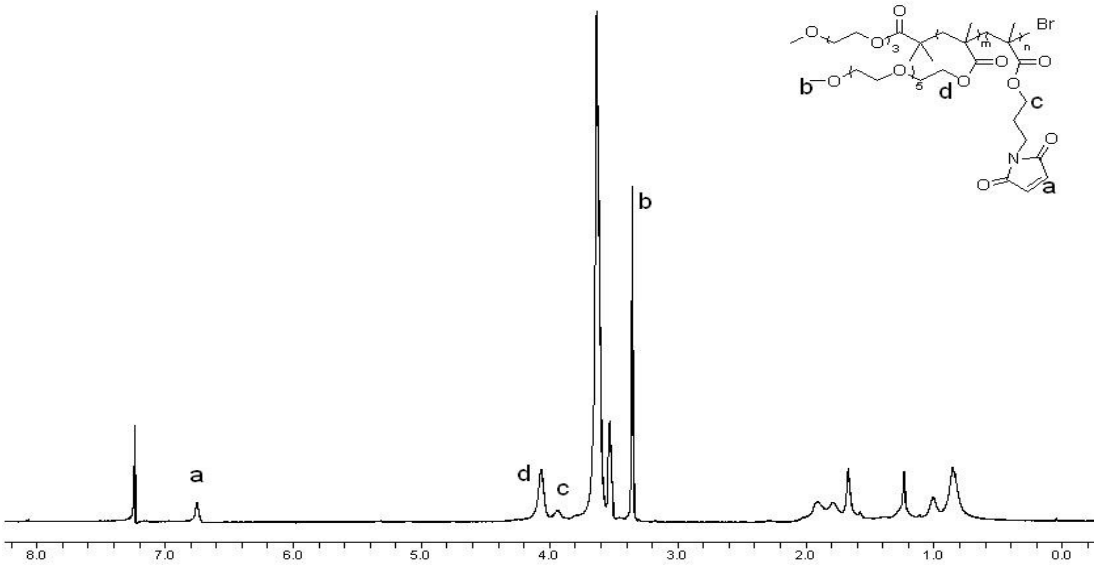

Figure 3.18. ^{1}H NMR of activated Copolymer P4

3.2.2. Electrospun Reactive Nanofibers

Electrospinning technique is used to generate electrospun reactive nanofibers. Several parameters, such as concentration, solvent, flow rate, distance to collector, applied voltage, average molecular weight of the polymers, are arranged and optimized. As the solvent 50:50, THF: DMF mixture was chosen and used for all experiments. Distance to collector was 10 cm and applied voltage varied between 8-12 kV.

Following the synthesis of methacrylate based polymer (Figure 3.19, Mn: 15038, PDI: 1,85) bearing succinimide reactive group (namely Copolymer P5, MMA: NHSMA, 8:1, Figure A.2), which enables amine functionalization, fine hydrophobic reactive nanofibers (Figure 3.20) are obtained by electrospinning 25 % per weight concentrated polymer solution.

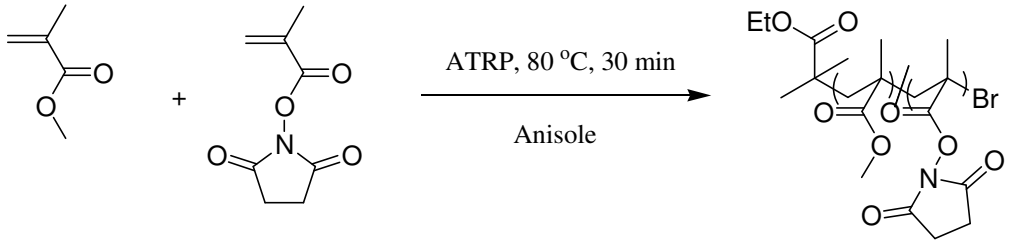

9 **3** **Copolymer P5**

Figure 3.19. Synthesis of Copolymer P5

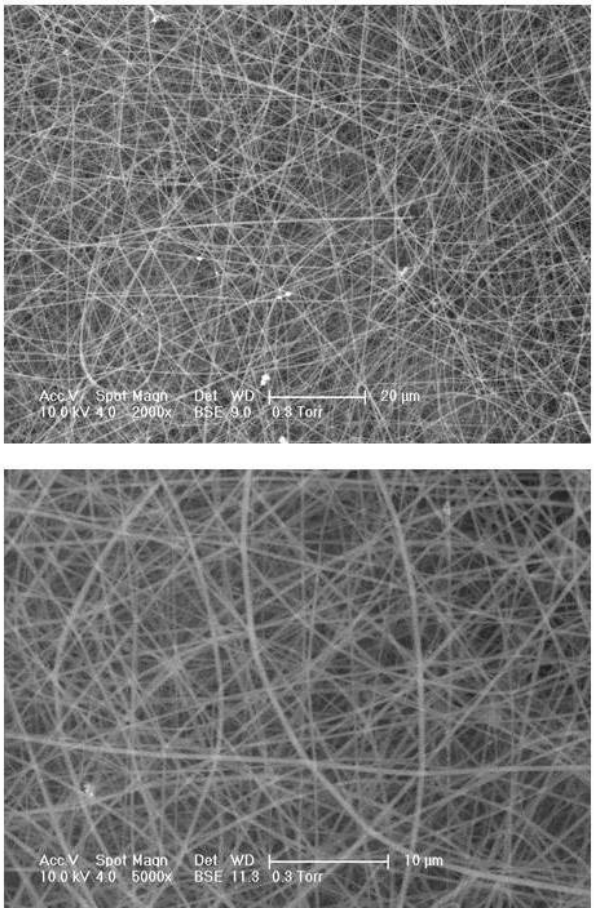

Figure 3.20. Nanofibrous scaffolds of Copolymer P5

Besides, a PEG based hydrophilic copolymer (Figure 3.21, Mn: 11133, PDI: 1,28) containing maleimide reactive group (namely Copolymer P3, PEGMEMA: FuM-MA, 4:1) is synthesized, in order to obtain biocompatible nanostructures due to favorable properties of PEG, and electrospun. However, beaded nanofibers are obtained (Figure 3.22) which is most probably a result of low molecular weight of the polymer.

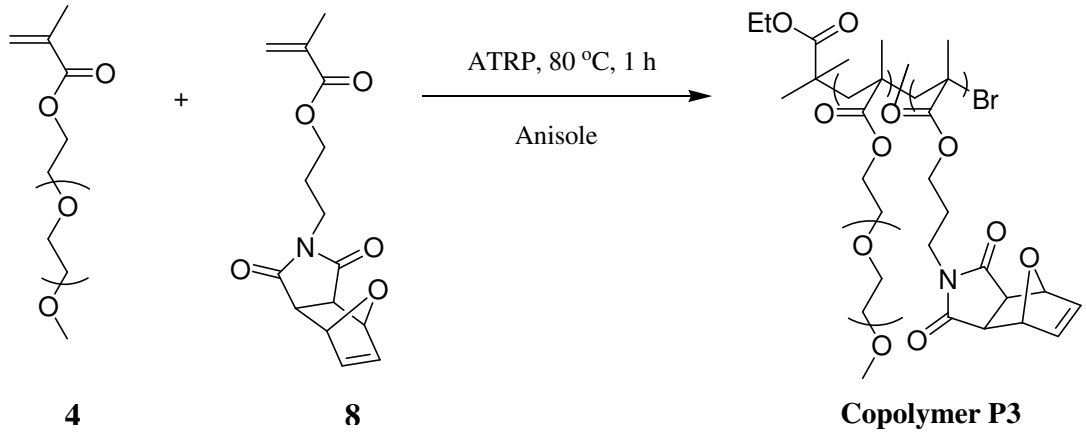

Figure 3.21. Synthesis of Copolymer P3

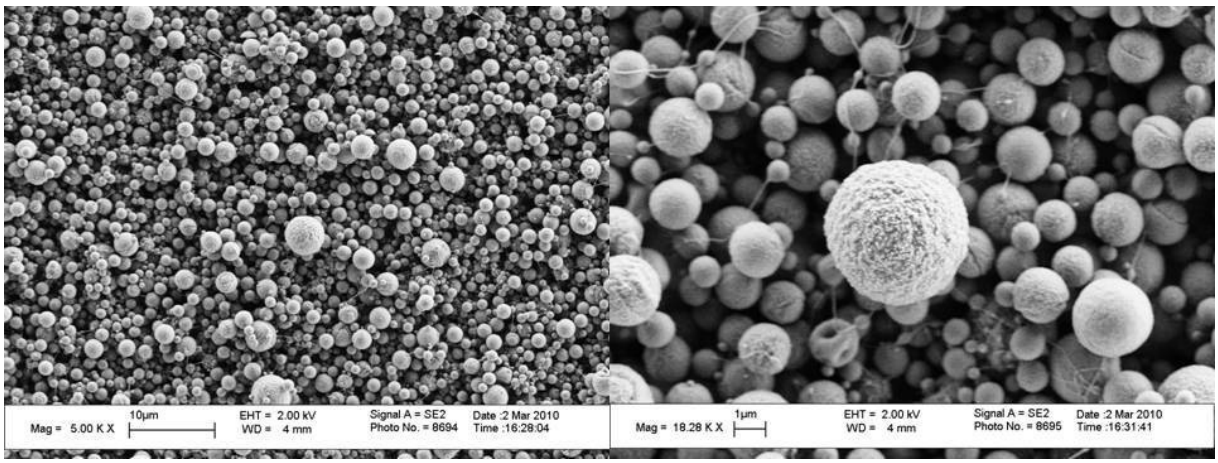

Figure 3.22. Beaded nanofibers of Copolymer P3

Subsequently, another PEG based maleimide containing copolymer (Figure 3.23, Mn: 9646, PDI: 1,30) is synthesized (Figure A.3), yet with participation of FMA (namely Copolymer P6, PEGMEMA: FuM-MA: FMA, 7:2:1, respectively) and electrospun, to obtain crosslinkable nanofibers, eventuating in elegant nanofibers (Figure 3.24). The aim is to crosslink the nanofibers after electrospinning via UV shine with the incorporation of

FMA and maleimide groups, regarding Diels Alder cycloaddition reaction leading to biocompatible and stable reactive fibrous scaffolds. Unfortunately, after UV curing stable nanofibrous structure could not be obtained (Figure 3.25).

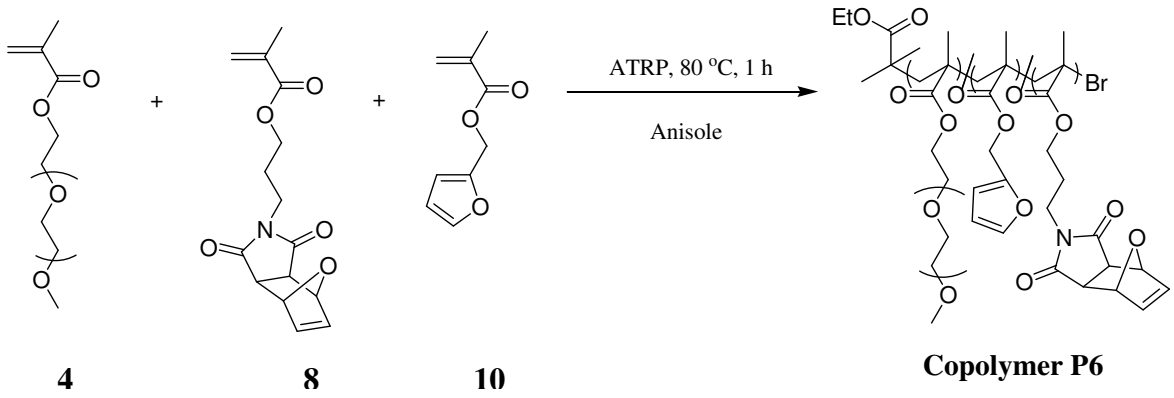

Figure 3.23. Synthesis of Copolymer P6

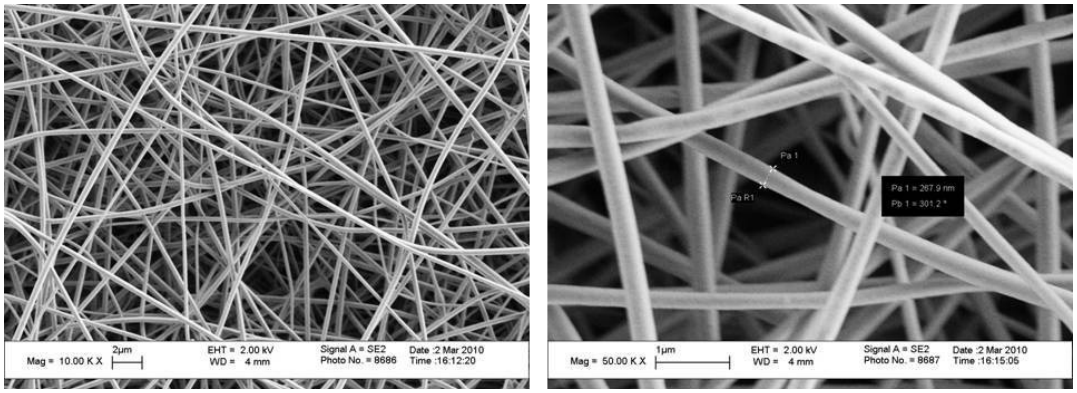

Figure 3.24. Biocompatible reactive nanofibers of Copolymer P6

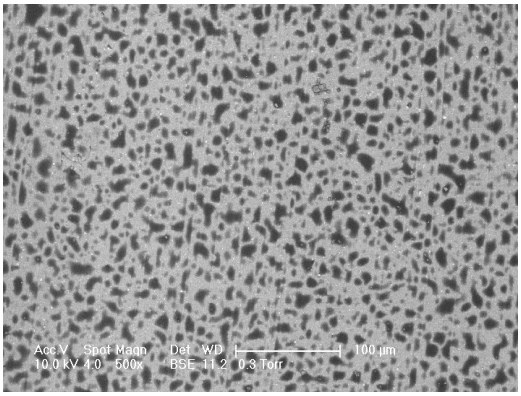

Figure 3.25. Structure after UV curing

Regarding an assumption of the positive effect of furan groups on fiber formation, PEGMEMA is copolymerized (Figure 3.26, Mn: 16021, PDI: 1,89) with protected maleimide and hydrogenated maleimide groups (namely Copolymer P7, PEGMEMA: FuM-MA: HFuM-MA, 60:20:20, Figure A.9) and electrospun (Figure 3.27) in order to obtain both reactive and furan containing polymer since during the activation step with high temperature protective furan groups leave the structure to form a reactive group whereas hydrogenated furan groups keep their structure. However, this experiment shows that the assumption was wrong as unreasonable results are acquired and it is understood that furan groups do not influence nanofiber formation.

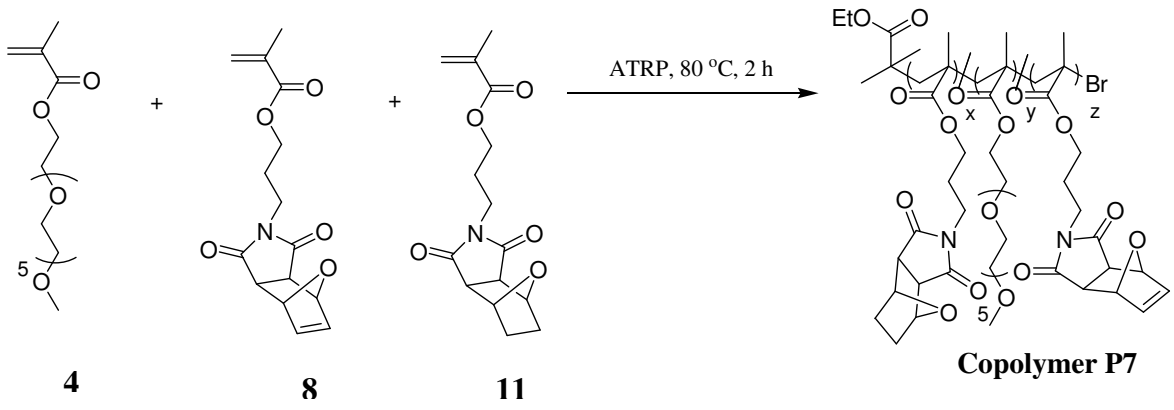

Figure 3.26. Synthesis of Copolymer P7

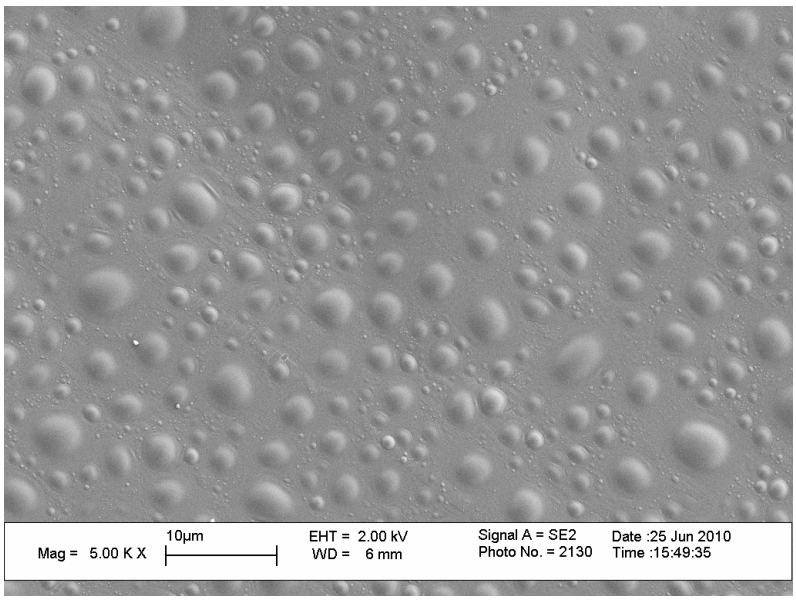

Figure 3.27. Electrosprayed surface of Copolymer P7

Ulterior strategy is to synthesize MMA – FMA copolymer (Figure 3.28, Mn: 31266, PDI: 1,25), electrospin and then introduce a 4 armed crosslinker in order to achieve stable structure. The copolymer is synthesized (namely Copolymer P8, MMA: FMA, 3:2, Figure A.4), electrospun and bring forth beaded nanofibrous structure (Figure 3.29). However, after increasing the concentration and introducing the crosslinker an agreeable structure is obtained (Figure 3.30).

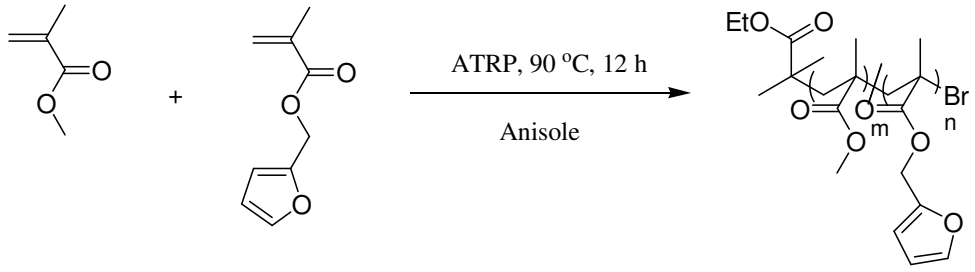

9 **10** **Copolymer P8**

Figure 3.28. Synthesis of P8

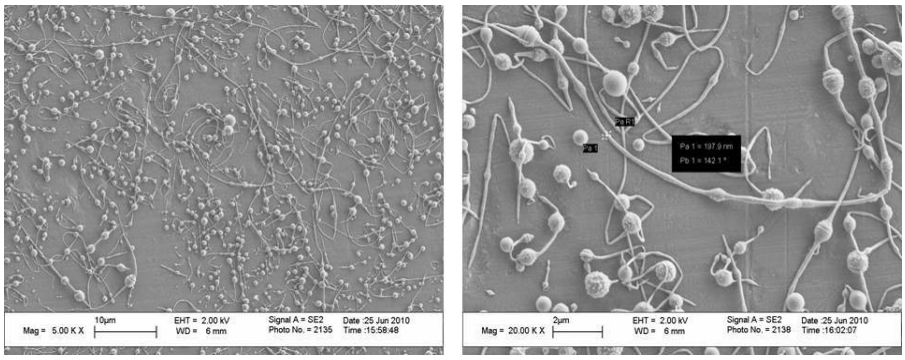

Figure 3.29. Beaded nanofibrous structure of Copolymer P8

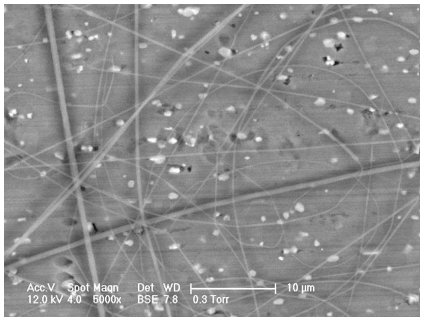

Figure 3.30. Nanofibrous stable structure of Copolymer P8

Lastly, another PEG based thiol functionalizable copolymer containing silane groups (Figure 3.31, Mn: 19230, PDI: 1,45) instead of succinimide (Copolymer P9, PEGMEMA:FuM-MA: Silane, 55:40:5) is utilized. Silane groups enable reagent free crosslinking and this is a considerable property for a biocompatible reactive nanofibrous scaffold. Following the synthesis step reactive copolymer is electrospun and leads up to beaded nanofibers even though various trials with different electrospinning parameters (Figure 3.32).

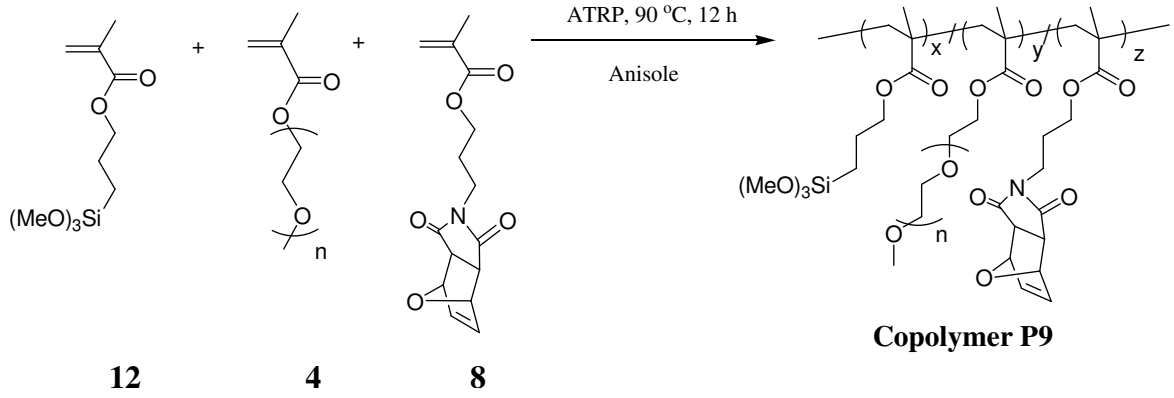

Figure 3.31. Sythesis of Copolymer P9

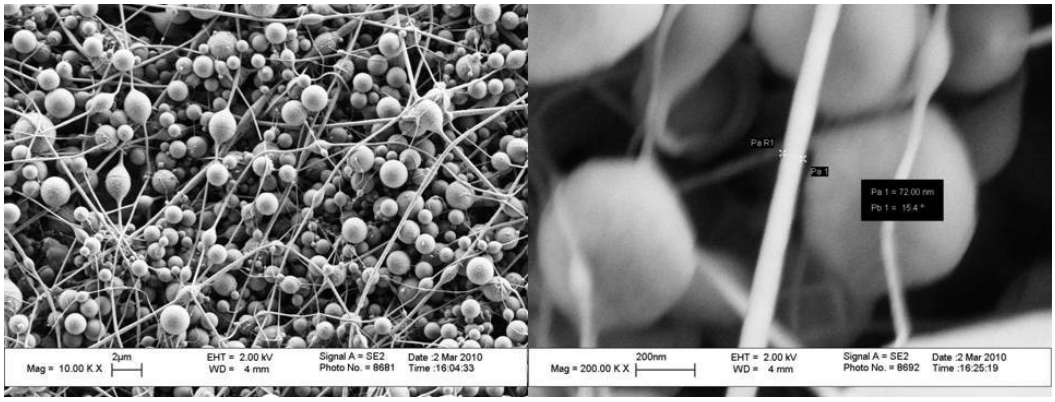

Figure 3.32. Beaded nanofibers electrospun from Copolymer P9

3.2.3. Reactive Nanoparticles

Concerning instability of PEG based nanofibers, an amphiphilic thiol reactive polymer (Figure 3.33, Mn: 19401, PDI: 1,14) with the composition of PEGMEMA: MMA: FuM-MA, 1:2:2 is synthesized (namely Copolymer P10, Figure A.5) and electrospun in

order to obtain biocompatible, stable and reactive nanostructures. Followingly, activated polymer is also electrospun. Fine nanoparticles with narrow size distribution are produced, having even more homogeneous size distribution after activation procedure (Figure 3.34).

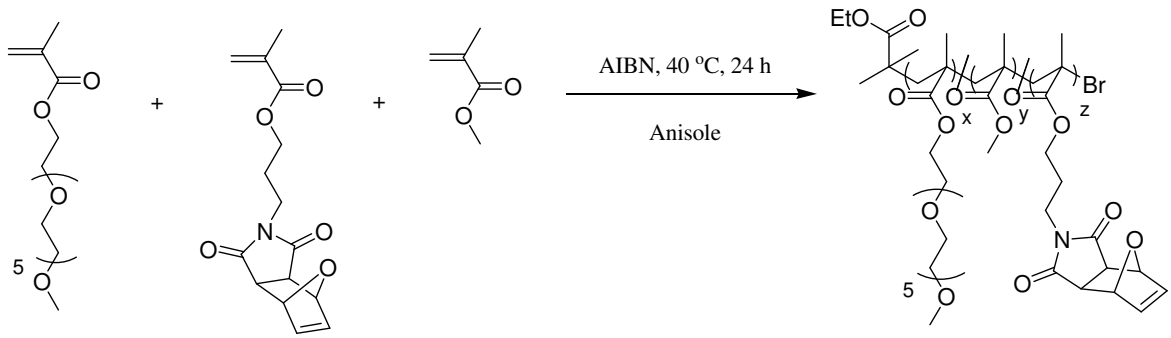

Figure 3.33. Synthesis of Copolymer P10

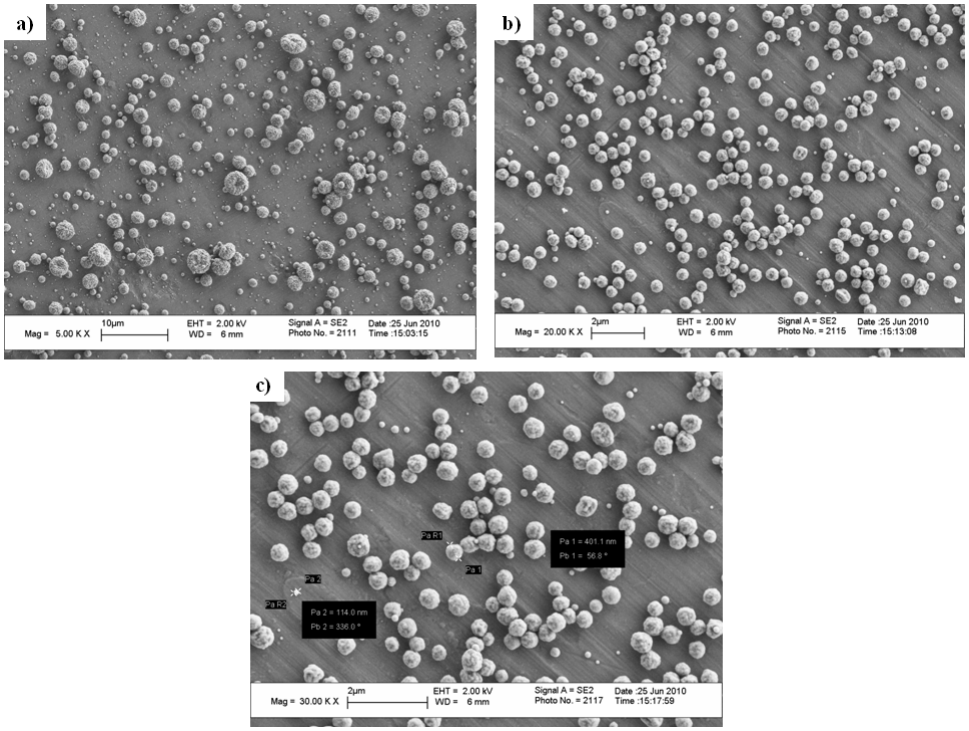

Figure 3.34. Electrospun amphiphilic nanoparticles a) Copolymer P10, b) Activated Copolymer P10, c) Size information of thiol reactive nanoparticles

Furthermore, another methacrylate based copolymer (Figure 3.35, Mn: 8033, PDI: 1,37), yet bearing both succinimide and protected maleimide reactive groups (namely

Copolymer P11, MMA: NHSMA: FuM-MA, 70:20:10, Figure A.6) is synthesized and electrospun resulting in agreeable nanoparticles having narrow range of size distribution (Figure 3.36). The same process is repeated after activation of the protected maleimide reactive group (Figure A.7) and the same results are noted.

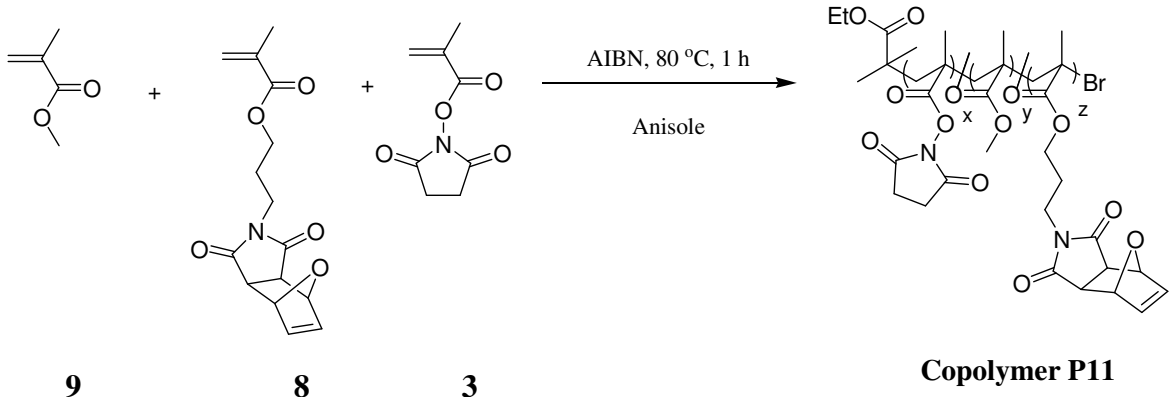

9 **8** **3** **Copolymer P11**

Figure 3.35. Synthesis of Copolymer P11

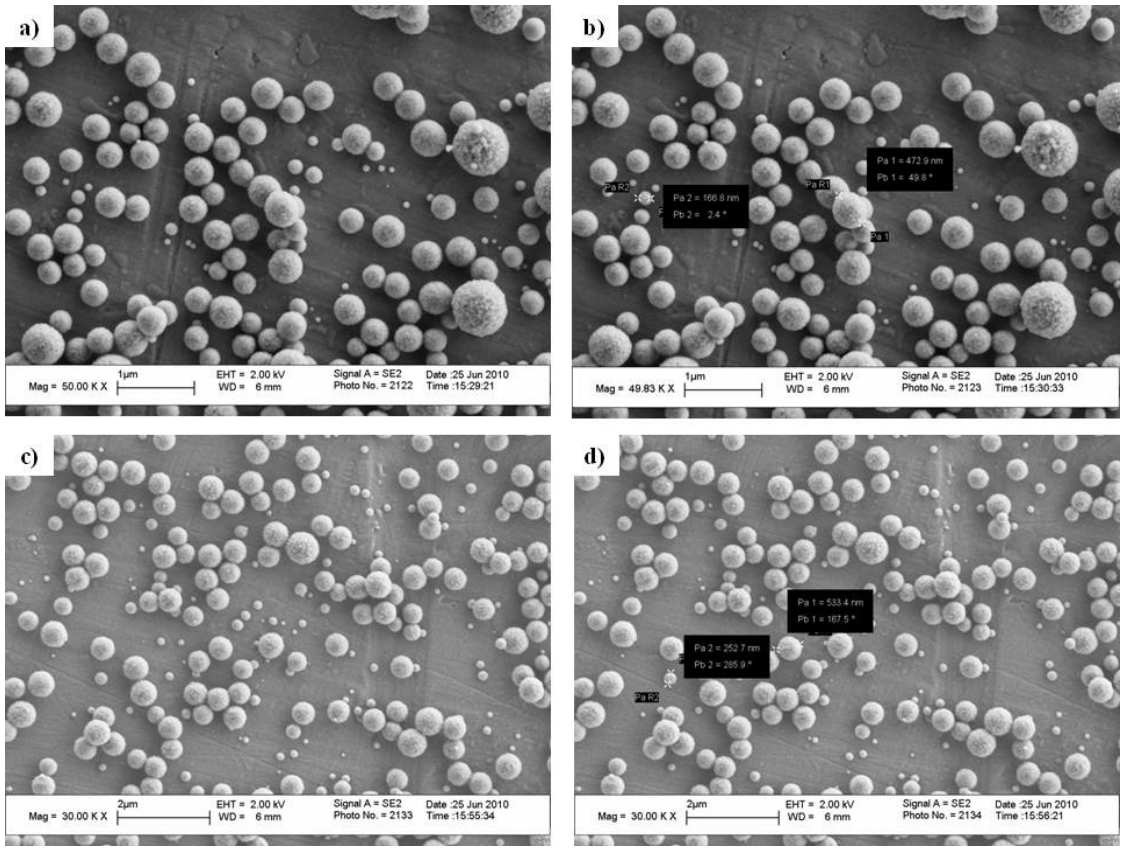

Figure 3.36. Nanoparticles of Copolymer P11 a) Copolymer P11, b) Size information of a, c) Activated Copolymer P11, d) Size information of c

Finally, PEG based biocompatible polymer in which both succinimide and maleimide reactive groups exist (Figure 3.37, Mn: 19353, PDI: 1,49), is synthesized (namely Copolymer P12, PEGMEMA: NHSMA: FuM-MA, 40:20:40, Figure A.8) and electrospun. Over again reactive nanostructures are formed, however no reasonable size distribution is observed (Figure 3.38).

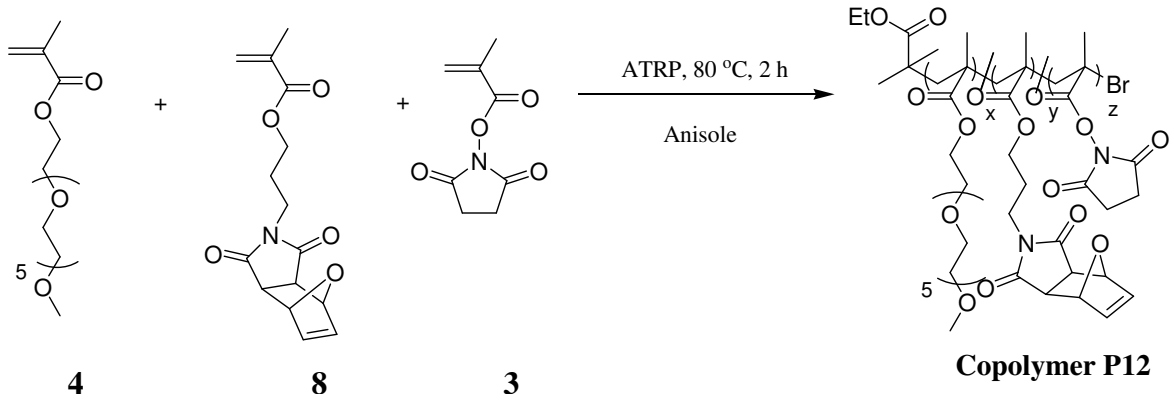

Figure 3.37. Synthesis of Copolymer P12

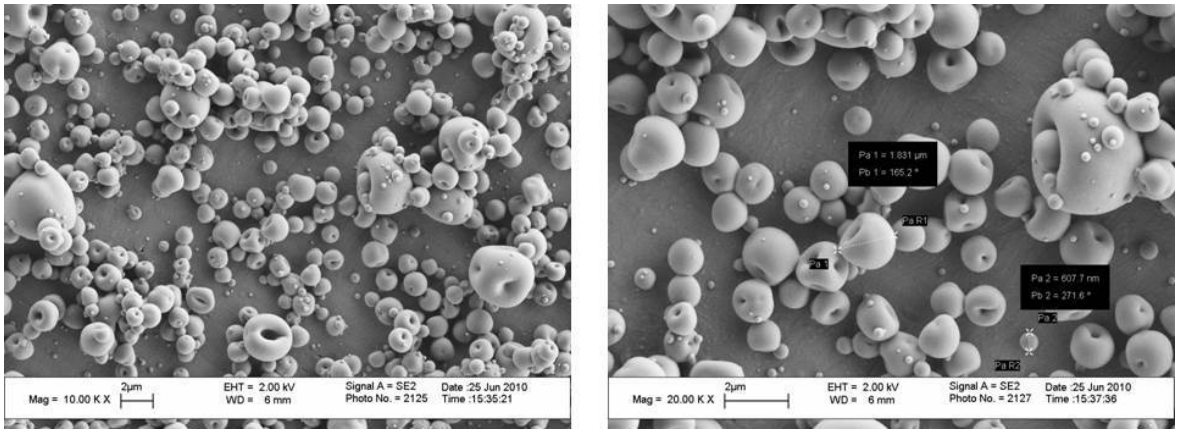

Figure 3.38. PEG based nanoparticles of Copolymer P12

4. EXPERIMENTAL

4.1. Materials and Methods

All chemicals were used as received from manufacturer (Merck, Aldrich, and Alfa Aesar). Dry solvents (CH_2Cl_2, THF, and toluene) were obtained from ScimatCo Purification System, other dry solvents were dried over molecular sieves. Column chromatography was performed using silica gel-60 (43-60 nm). Thin layer chromatography was performed using silica gel plates (Kiesel gel 60 F254, 0.2 mm, Merck). Plates were viewed under 254 nm UV lamp otherwise plates were developed either by $KMnO_4$ stain. Infrared spectroscopy was carried out on Thermo Scientific Nicolet 380 FT-IR spectrophotometer. ^1H NMR (operating at 400 MHz) was recorded on Varian Mercury-MX in $CDCl_3$ as solvent at the Advanced Technologies Research and Development Center at Boğaziçi University. The molecular weights were estimated by gel permeation chromatography (GPC) with polystyrene as a standard and with refractive index detector, and the sample was eluted with THF. The pH values of the PBS solutions for biodegradation studies were observed with an InoLab Multi Level 1 pH meter. The surface characterization of the nanowebs was done with an ESEM-FEG/EDAX Philips XL-30.

4.2. Water Soluble Reactive Polymeric Supports for Drug Delivery Applications

4.2.1. Synthesis of Amine Reactive Monomer

To a solution of N-Hydroxysuccinimide (2.54 g, 20.11 mmol) and triethylamine (3.37 mL, 24.17 mmol) in dry dichloromethane (150 mL) at 0 ˚C, was added methacryloyl chloride (2 mL, 20.66 mmol) in 0.1 mL portions over 30 min (Figure 4.1). The clear solution was stirred for 3 h at 0 ˚C. After the reaction mixture was washed with H_2O (2 x 30 mL), the combined organic layers were dried over anhydrous Na_2SO_4 and concentrated to give a yellowish white residue that was recrystallized from EtOAc/hexane (100 mL, 1:1) mixture affording 3.4 g (83% yield) monomer as a white crystalline solid. The final product was dried under vacuum for 15 min. Purity was determined by TLC (EtOAc:

Hexane, 75:25). ^{1}H NMR ($CDCl_3$, ppm): 6.4 (s, H, CH_2=C), 5.9 (s, H, CH_2=C), 2.83 (s, 4H, CH_2-CH_2), 2.04 (s, 3H, CH_3) corresponding to the literature values [19].

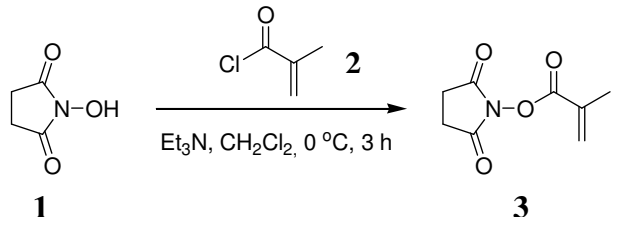

Figure 4.1. Synthesis of methacryloxysuccinimide

4.2.2. Synthesis of Amine Reactive Polymer

In a typical polymerization, N-methacryloxysuccinimide (179.5 mg, 0.98 mmol) and copper (I) bromide (CuBr) (2.5 mg, 0.018 mmol) were weighed into a dry 10 mL round bottom flask equipped with a stir-bar. The flask was sealed and purged with dry nitrogen gas. Then, degassed N,N,N′,N″,N″-Pentamethyldiethylenetriamine (PMDETA) (7.3 μL, 0.035 mmol), PEGMEMA (1.72 mL, 6.02 mmol) and anhydrous anisole (2 mL) were added to the RBF via syringe and the reaction mixture was stirred for 20 min at room temperature to allow catalyst formation, indicated by a color change to blue (Figure 4.2). To the stirring mixture was added ethyl 2-bromoisobutyrate (EBIB) (2.57 μL, 0.0175 mmol) via syringe then the reaction mixture was placed in an 80 ˚C oil bath for 30 min. The reaction ratio was [PEGMEMA]:[NHSMA]:[PMDETA]:[CuBr]:[EBIB], 86:14:0.5:0.25:0.25. After terminating the polymerization the crude mixture was purified by precipitation into cold diethyl ether and passed through aluminum oxide to remove cupper catalyst. The final filtered product was dried under vacuum.

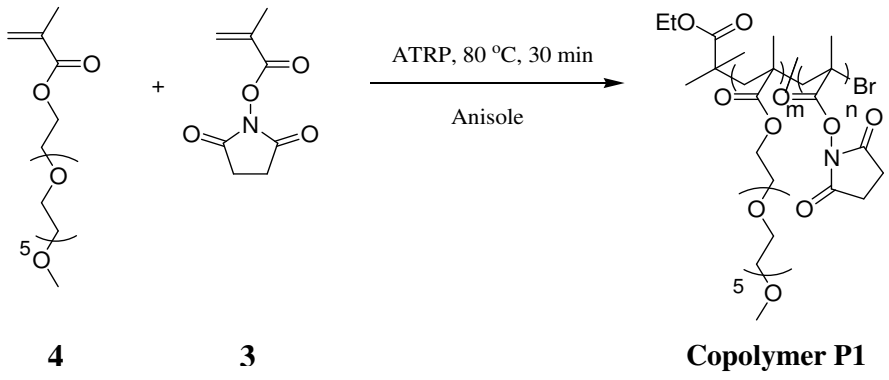

Figure 4.2. Synthesis of Copolymer P1

Table 4.1. Synthesis and characterization of Copolymer P1

Polymers	Monomer ratio (PEGMEMA:NHSMA)	Catalyst system (PMDETA:CuBr:EBIB)	Conversion	Mn	Mw/Mn
P1.1	86:14	0.5:0.25:0.25	41%	28389	1.22
P1.2	86:14	1:1:1	52%	22559	1.39

4.2.3. Functionalization with Benzylamine

P1 (50 mg, 0.003 mmol) was weighed and replaced into a conical tube equipped with a stir-bar. Benzyl amine (6.4 μL, 0.057 mmol) is added and the tube is sealed then purged with dry nitrogen gas. Dry THF (0.3 mL) was injected into the tube and the reaction mixture was stirred until it became homogeneous. TEA (6.12 μL, 0.044 mmol) was added under dry nitrogen gas and the tube was heated at 60 ˚C for 12 h (Figure 4.3). After the reaction was terminated the crude mixture was concentrated at 40 ˚C to afford benzyl amine functionalized polymer. Then, the product was dissolved in minimum amount of CH_2Cl_2 and the polymeric product was isolated by precipitation in cold diethyl ether. The final polymeric product was dried under vacuum.

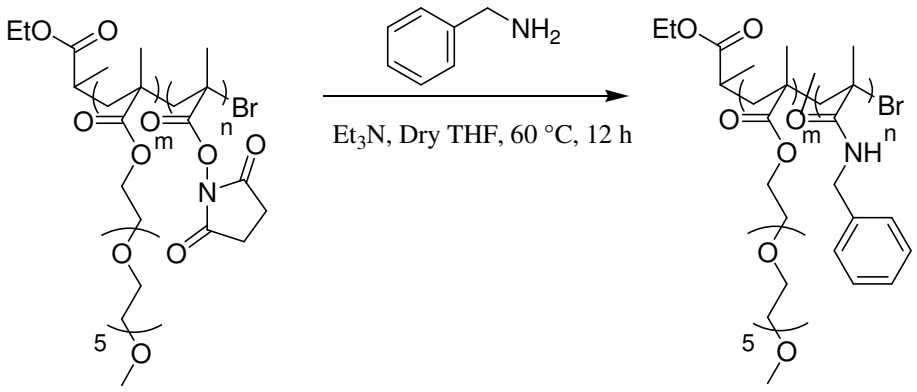

Figure 4.3. Functionalization of amine reactive polymer with benzyl amine

4.2.4. Synthesis of Alkyne Reactive Polymer

In a typical polymerization, AHMA (170 mg, 0.81 mmol) and copper (I) bromide (CuBr) (5.71 mg, 0.04 mmol) were weighed into a dry 10 mL round bottom flask equipped

with a stir-bar. The flask was sealed and purged with dry nitrogen gas. Then, degassed N,N,N′,N″,N″-Pentamethyldiethylenetriamine (PMDETA) (14.67 µL, 0.08 mmol), PEGMEMA (1.84 mL, 6.44 mmol) and anhydrous anisole (1.5 mL) were added to the RBF via syringe and the reaction mixture was stirred for 20 min at room temperature to allow catalyst formation, indicated by a color change to blue (Figure 4.4). To the stirring mixture was added ethyl 2-bromoisobutyrate (EBIB) (5.83 µL, 0.04 mmol) via syringe then the reaction mixture was placed in an 80˚C oil bath for 30 min. The reaction ratio was [PEGMEMA]: [AHMA]:[PMDETA]:[CuBr]:[EBIB], 80:10:1:0.5:0.5. After terminating the polymerization the crude mixture was purified by precipitation into diethyl ether and passed through aluminum oxide to remove cupper catalyst. The final filtered product was dried under vacuum.

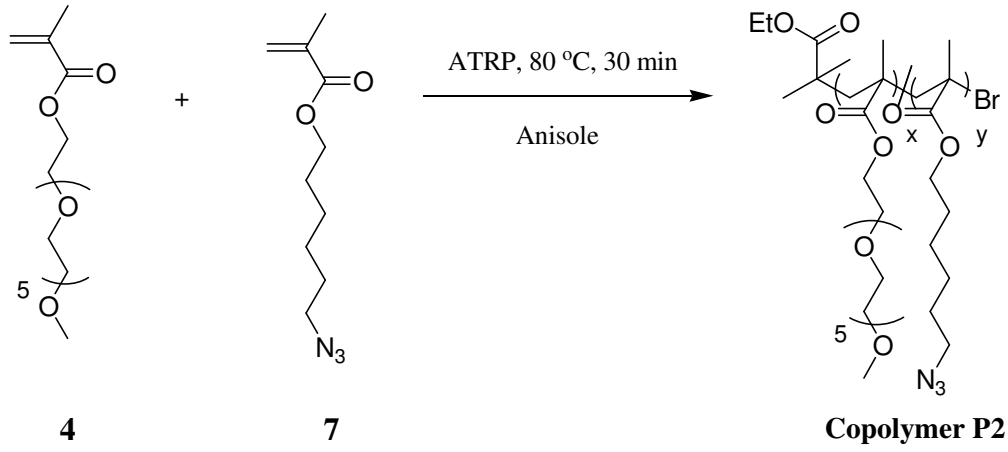

Figure 4.4. Synthesis of Copolymer P2

Table 4.2. Synthesis and characterization of Copolymer P2

Polymers	Monomer ratio (PEGMEMA:AHMA)	Catalyst system (PMDETA:CuBr:EBIB)	Conversion	Mn	Mw/Mn
P2.1	80:10	1:0.5:0.5	72%	28654	1.69
P2.2	60:10	1:0.5:0.5	52%	19087	1.24

4.2.5. In Vitro Biodegradation Behaviors of Polymers

P1.1, P1.2, P2.1 and P2.2 bearing two different molecular weights per each (3mg/mL) were incubated at 37˚C in phosphate buffered saline (PBS) at pH 7.4 and 5.5, separately. The pH of the solutions was determined by using an InoLab Multi Level 1 pH meter. Every day, up to 14 days, aliquots were removed and the molecular weight changes were determined by gel permeation chromatography (GPC).

4.3. Reactive Fibrous Scaffolds

4.3.1. Synthesis of Latent Reactive Monomer

The furan protected maleimide monomer was prepared as reported below. To a solution of the alcohol (2.00 g, 8.86 mmol) and triethylamine (1.05 mL, 10.63 mmol) in dichloromethane (120 mL) at 0˚C, was added methacryloyl chloride (0.91 mL, 9.39 mmol) in 0.1 mL portions over 30 min. The clear solution was stirred for 2 h at 0˚C (Figure 4.5). To the reaction mixture was added dichloromethane (40 mL) and the mixture was washed with $NaHCO_3$ (2 x 40 mL) and H_2O (2 x 40 mL). The combined organic layers were dried over anhydrous Na_2SO_4 and concentrated to give a yellow residue that was purified by flash chromatography on SiO2 (CH2Cl2: EtOAc: Hexane, 1:4:15) affording 2.50 g (96% yield) monomer as a white waxy solid. Purity has been determined by HPLC (98.4%). ^{1}H NMR ($CDCl_3$), 6.49 (s, 2H, CH=CH), 6.11 (s, 1H, CH_2=C), 5.55 (m, 1H, CH_2=C), 5.24 (s, 2H, CH bridgehead protons), 4.09 (t, 2H, J = 6.2 Hz, OCH_2), 3.59 (t, 2H, J = 7.0 Hz, NCH_2), 2.82 (s, 2H, CH-CH, bridge protons), 1.98-1.91 (m, 5H, $CH_2CH_2CH_2$ and CH_3); ^{13}C NMR ($CDCl_3$) 176.0, 167.1, 136.4, 136.1, 125.4, 80.8, 61.4, 47.3, 35.7, 26.6, 18.2; IR (KBr): υ = 1705.8 cm^{-1}.

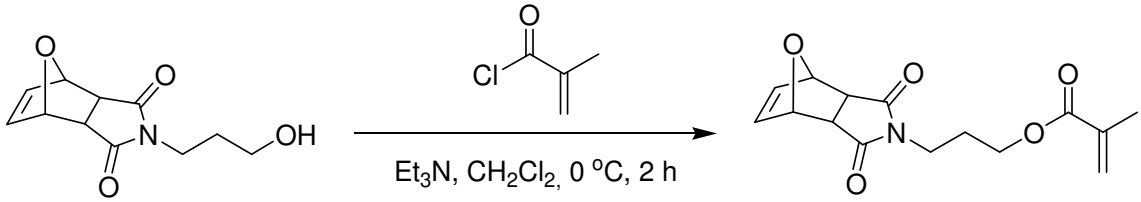

Figure 4.5. Latent reactive monomer synthesis

4.3.2. Synthesis of Furan Protected Maleimide-PEGMEMA Copolymer

In a typical polymerization, furan protected maleimide monomer (203.77 mg, 0.7 mmol) and copper (I) bromide (CuBr) (5 mg, 0.035 mmol) were weighed into a dry 10 mL round bottom flask equipped with a stir-bar. The flask was sealed and purged with dry nitrogen gas. Then, degassed N,N,N′,N″,N″-Pentamethyldiethylenetriamine (PMDETA) (14.1 μL, 0.07 mmol), PEGMEMA (0.8 mL, 2.8 mmol) and anhydrous anisole (1.5 mL) were added to the RBF via syringe and the reaction mixture was stirred for 20 min at room temperature to allow catalyst formation, indicated by a color change to blue (Figure 4.6). To the stirring mixture was added ethyl 2-bromoisobutyrate (EBIB) (5.1 μL, 0.035 mmol) via syringe then the reaction mixture was placed in an 80 ˚C oil bath for 1 h. The reaction ratio was [PEGMEMA]:[FuM – MA]:[PMDETA]:[CuBr]:[EBIB], 80:20:2:1:1. After terminating the polymerization the crude mixture was purified by precipitation into cold diethyl ether and passed through aluminum oxide to remove cupper catalyst. The final filtered product was dried under vacuum.

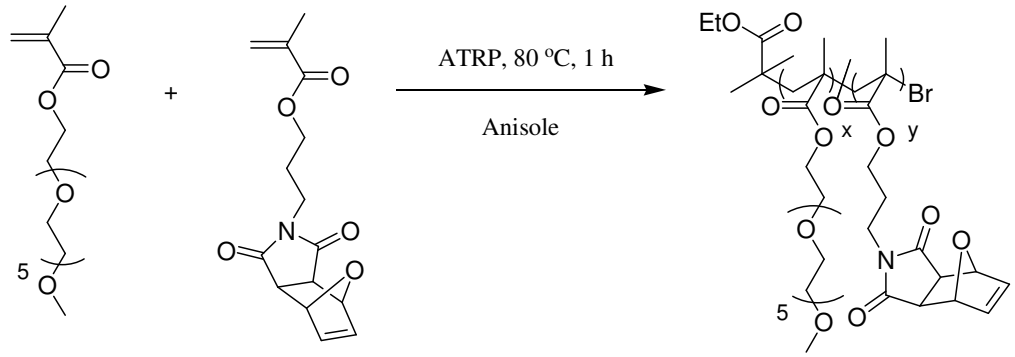

4 **8** **Copolymer P3**

Figure 4.6. Synthesis of Copolymer P3

4.3.3. Activation of Furan Protected Maleimide Group

Polymer (200.0 mg) was dissolved in dry toluene and heated at 110 °C for 4 hours. NMR analysis proved quantitative conversion of the oxabicyclic moiety to the maleimide functional group (Figure 4.7). NMR for polymer: ^{1}H NMR ($CDCl_3$, ppm) 6.71 (s, 2H, CH=CH, 4.06(s, OCH_2 of PEGMEMA), 3.93 (br s, 2H, OCH_2), 3.57 (br s, 5H, OCH3 and

NCH_2), 3.35 (s,OCH_3), 2.85 (s, 2H, CH-CH, bridge protons), 1.92–0.84 (m, 7H, $NCH_2CH_2CH_2O$, CH_2 and CH_3 along polymer backbone); IR (KBr): v = 1707.1 cm^{-1}.

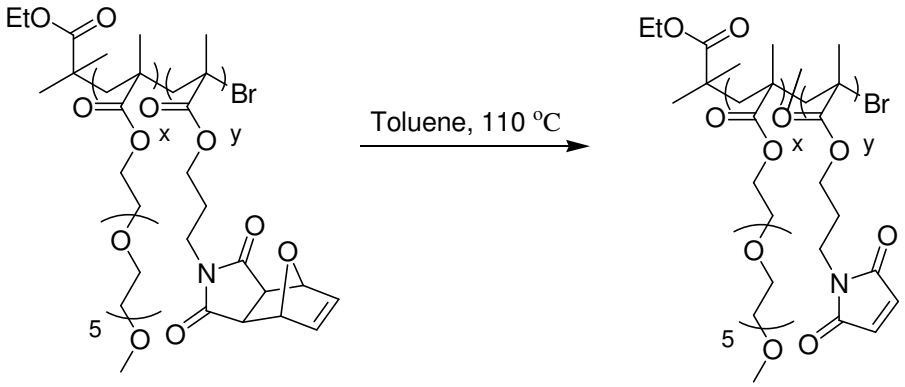

Copolymer P3 **Copolymer P4**

Figure 4.7. Activation of maleimide groups

4.3.4. Synthesis of Poly [MMA-co-(NHSMA)]

In a typical polymerization, N-methacryloxysuccinimide (916 mg, 5.00 mmol) and copper (I) bromide (CuBr) (3.6 mg, 0.025 mmol) were weighed into a dry 10 mL round bottom flask equipped with a stir-bar. The flask was sealed and purged with dry nitrogen gas. Then, degassed N,N,N′,N″,N″-Pentamethyldiethylenetriamine (PMDETA) (10.5 μL, 0.05 mmol), MMA (4.3 mL, 40.37 mmol) and anhydrous anisole (2 mL) were added to the RBF via syringe and the reaction mixture was stirred for 20 min at room temperature to allow catalyst formation, indicated by a color change to blue (Figure 4.8). To the stirring mixture was added ethyl 2-bromoisobutyrate (EBIB) (3.65 μL, 0.025 mmol) via syringe then the reaction mixture was placed in an 80 ˚C oil bath for 30 min. The reaction ratio was [MMA]:[NHSMA]:[PMDETA]:[CuBr]:[EBIB], 80:10:0.1:0.05:0.05. After terminating the polymerization the crude mixture was purified by precipitation into cold MeOH and passed through aluminum oxide to remove cupper catalyst. The final filtered product was dried under vacuum.

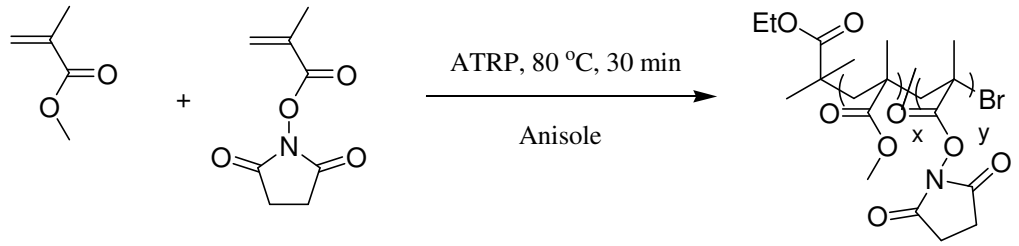

9 **3** **Copolymer P5**

Figure 4.8. Synthesis of Copolymer P5

4.3.5. Synthesis of Maleimide-FMA-PEGMEMA Copolymer

In a typical polymerization, furan protected maleimide monomer (203.77 mg, 0.7 mmol) and copper(I) bromide (CuBr) (5 mg, 0.035 mmol) were weighed into a dry 10 mL round bottom flask equipped with a stir-bar. The flask was sealed and purged with dry nitrogen gas. Then, degassed N,N,N′,N″,N″-Pentamethyldiethylenetriamine (PMDETA) (14.1 μL, 0.07 mmol), PEGMEMA (0.7 mL, 2.45 mmol), FMA (53.96 μL, 0.35 mmol) and anhydrous anisole (1.5 mL) were added to the RBF via syringe and the reaction mixture was stirred for 20 min at room temperature to allow catalyst formation, indicated by a color change to blue (Figure 4.9). To the stirring mixture was added ethyl 2-bromoisobutyrate (EBIB) (5.1, 0.035 mmol) via syringe then the reaction mixture was placed in an 80 ˚C oil bath for 1 h. The reaction ratio was [PEGMEMA]:[FuM – MA]:[FMA]:[PMDETA]:[CuBr]:[EBIB], 70:20:10:2:1:1. After terminating the polymerization the crude mixture was purified by precipitation into cold diethyl ether and passed through aluminum oxide to remove cupper catalyst. The final filtered product was dried under vacuum.

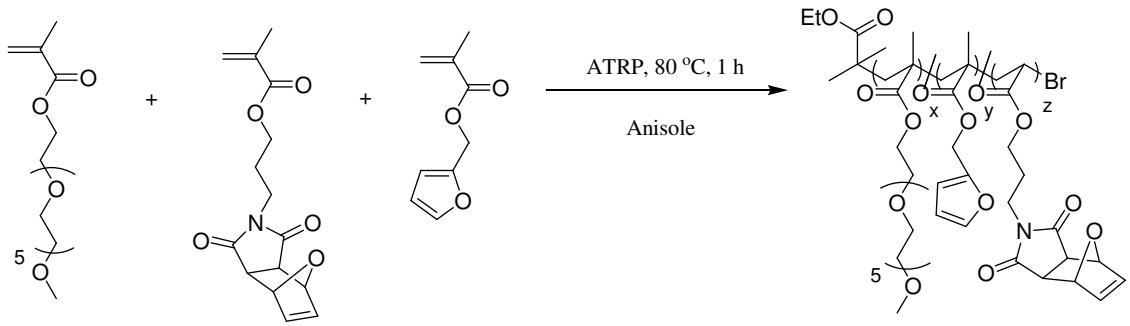

4 **8** **10** **Copolymer P6**

Figure 4.9. Synthesis of Copolymer P6

4.3.6. Synthesis of Hydrogenated Maleimide Monomer

4.3.6.1. Hydrogenation of the Cyclo Adduct: To a solution of the alcohol (0.5 g, 2.24 mmol) was added Pd on C (0.05 g, 10 % by weight). The mixture was dissolved in a mixture of EtOH:EtOAc (3 mL:7 mL) and purged with hydrogen gas using hydrogen gas balloons. The mixture was reacted 18 h. After the reaction the mixture was filtered to remove Pd on C and concentrated under vacuum to obtain hydrogenated alcohol.

4.3.6.2. Synthesis of the Hydrogenated Monomer: To a solution of the hydrogenated alcohol (0.20 g, 0.89 mmol) and triethylamine (0.15 mL, 1.08 mmol) in dichloromethane (60 mL) at 0 ˚C, was added methacryloyl chloride (0.09 mL, 0.93 mmol) over 30 min. The clear solution was stirred for 2 h at 0 ˚C (Figure 4.10). To the reaction mixture was added dichloromethane (40 mL) and the mixture was washed with saturated $NaHCO_3$ (2 x 40 mL) and H_2O (2 x 40 mL). The combined organic layers were dried over anhydrous Na_2SO_4 and concentrated to give a yellow residue that was purified by flash chromatography on SiO_2 (EtOAc: CH2Cl2, 1:1) affording 2.50 g (96% yield) monomer as white waxy solid. ^1H NMR ($CDCl_3$), 6.11 (s, 1H, CH_2=C), 5.55 (m, 1H, CH_2=C), 4.84 (s, 2H, CH bridgehead protons), 4.08 (t, 2H, J = 5.9 Hz, OCH_2), 3.56 (t, 2H, J = 6.4 Hz, NCH_2), 2.84 (s, 2H, CH-CH, bridge protons), 1.93-1.57 (m, 5H, $CH_2CH_2CH_2$, CH_3 and CH_2CH_2).

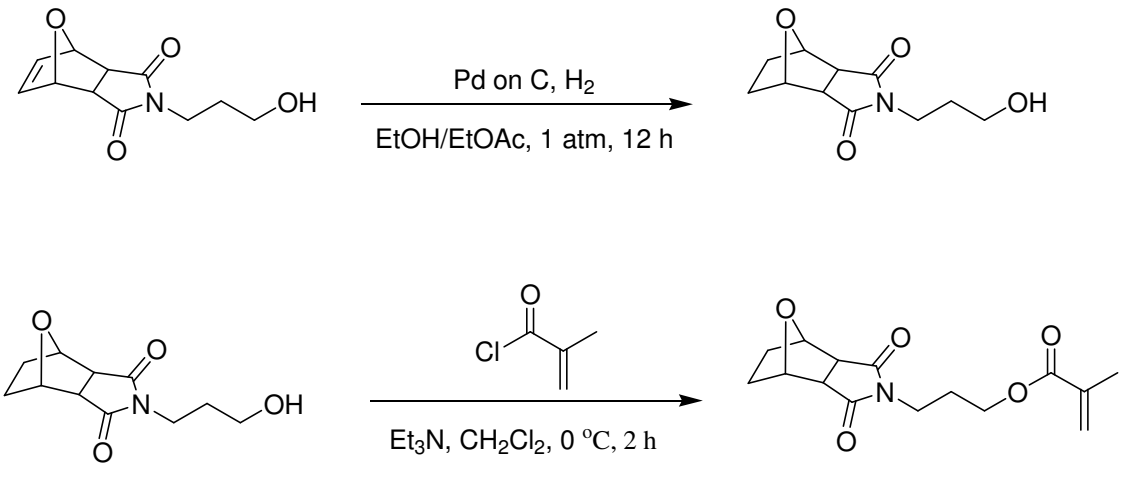

11

Figure 4.10. Synthesis of hydrogenated monomer

4.3.7. Synthesis of Hydrogenated Maleimide Containing Polymer

In a typical polymerization, furan protected maleimide monomer (204 mg, 0.7 mmol), hydrogenated furan protected maleimide monomer (205.19 mg, 0.7 mmol) and copper (I) bromide (CuBr) (5 mg, 0.035 mmol) were weighed into a dry 10 mL round bottom flask equipped with a stir-bar. The flask was sealed and purged with dry nitrogen gas. Then, degassed N,N,N′,N″,N″-Pentamethyldiethylenetriamine (PMDETA) (14.1 μL, 0.07 mmol), PEGMEMA (0.8 mL, 2.8 mmol) and anhydrous anisole (1 mL) were added to the RBF via syringe and the reaction mixture was stirred for 20 min at room temperature to allow catalyst formation, indicated by a color change to blue (Figure 4.11). To the stirring mixture was added ethyl 2-bromoisobutyrate (EBIB) (5.1 μL, 0.035 mmol) via syringe then the reaction mixture was placed in an 80 ˚C oil bath for 2 h. The reaction ratio was [PEGMEMA]: [FuM – MA]:[HFuM – MA]:[PMDETA]:[CuBr]:[EBIB], 60:20:20:2:1: 1. After terminating the polymerization the crude mixture was purified by precipitation into cold diethyl ether and passed through aluminum oxide to remove cupper catalyst. The final filtered product was dried under vacuum.

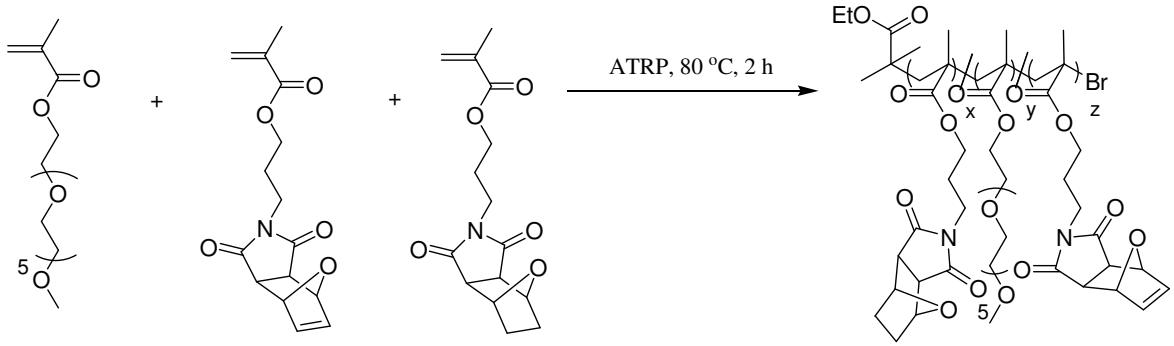

4 **8** **11** **Copolymer P7**

Figure 4.11. Synthesis of Copolymer P7

4.3.8. Synthesis of Poly [MMA-co-(furfuryl methacrylate)]

In a typical polymerization, copper (I) bromide (CuBr) (28.7 mg, 0.2 mmol) was weighed into a dry 10 mL round bottom flask equipped with a stir-bar. The flask was sealed and purged with dry nitrogen gas. Then, degassed N,N,N′,N″,N″-Pentamethyldiethylenetriamine (PMDETA) (42 μL, 0.2 mmol), MMA (1.28 mL, 12

mmol), FMA (1.23 mL, 8 mmol) and anhydrous toluene (6 mL) were added to the RBF via syringe and the reaction mixture was stirred for 20 min at room temperature to allow catalyst formation, indicated by a color change to blue (Figure 4.12). To the stirring mixture was added ethyl 2-bromoisobutyrate (EBIB) (29.4 μL, 0.2 mmol) via syringe then the reaction mixture was placed in a 90 ˚C oil bath for 12 h. The reaction ratio was [MMA]:[FMA]:[PMDETA]:[CuBr]:[EBIB], 60:40:1:1:1. After terminating the polymerization the crude mixture was purified by precipitation into cold MeOH and passed through aluminum oxide to remove cupper catalyst. The final filtered product was dried under vacuum.

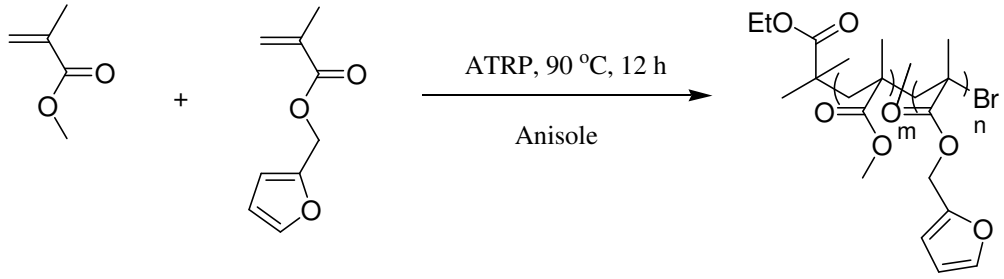

9 **10** **Copolymer P8**

Figure 4.12. Synthesis of Copolymer P8

4.3.9. Synthesis of Maleimide-MMA-PEGMEMA Copolymer

In a typical polymerization, furan protected maleimide monomer (100 mg, 0.34 mmol) and AIBN (1.6 mg, 0.01 mmol) were weighed into a dry 10 mL round bottom flask equipped with a stir-bar and the flask was sealed. Then, PEGMEMA (48.57 μL, 0.17 mmol), MMA (37.23 μL, 0.34 mmol) and THF (5 mL) were added to the RBF via syringe and the reaction mixture was placed in a 40 ˚C oil bath for 24 h (Figure 4.13). The reaction ratio was [PEGMEMA]:[MMA]: [FuM – MA]:[AIBN], 36:36:18:1. After terminating the polymerization the crude mixture was purified by precipitation into cold diethyl ether. The final product was dried under vacuum.

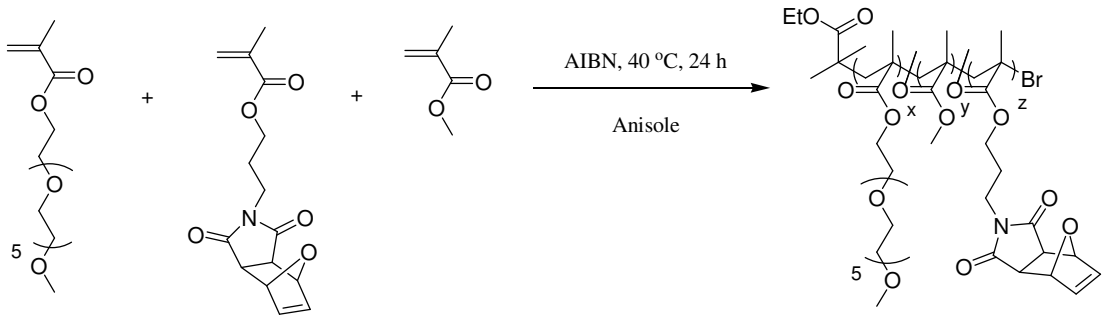

4 **8** **9** **Copolymer P10**

Figure 4.13. Synthesis of Copolymer P10

4.3.10. Synthesis of Maleimide-NHSMA-MMA Copolymer

In a typical polymerization, N-methacryloxysuccinimide (128.24 mg, 0.7 mmol), furan protected maleimide monomer (102 mg, 0.35 mmol) and copper (I) bromide (CuBr) (5 mg, 0.035 mmol) were weighed into a dry 10 mL round bottom flask equipped with a stir-bar. The flask was sealed and purged with dry nitrogen gas. Then, degassed N,N,N′,N″,N″-Pentamethyldiethylenetriamine (PMDETA) (14.1 μL, 0.07 mmol), MMA (29.8 μL, 2.8 mmol) and anhydrous anisole (1 mL) were added to the RBF via syringe and the reaction mixture was stirred for 20 min at room temperature to allow catalyst formation, indicated by a color change to blue (Figure 4.14). To the stirring mixture was added ethyl 2-bromoisobutyrate (EBIB) (5.1 μL, 0.035 mmol) via syringe then the reaction mixture was placed in an 80 ˚C oil bath for 1 h. The reaction ratio was [MMA]: [NHSMA]:[FuM – MA]:[PMDETA]: [CuBr]:[EBIB], 80:20:10:2:1:1. After terminating the polymerization the crude mixture was purified by precipitation into cold diethyl ether and passed through aluminum oxide to remove cupper catalyst. The final filtered product was dried under vacuum.

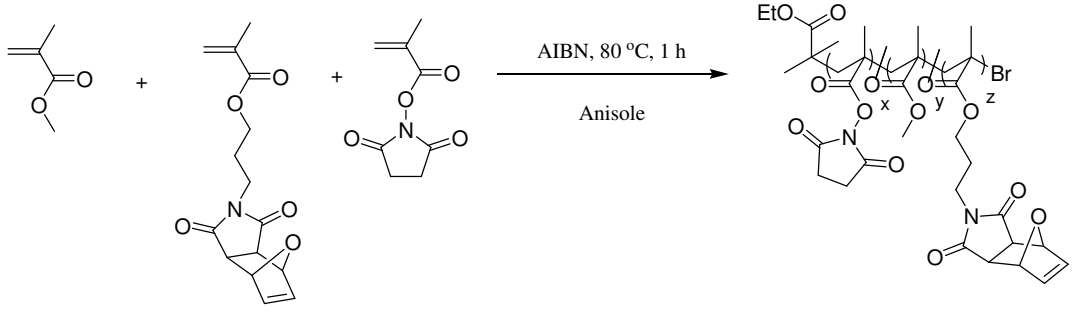

9 **8** **3** **Copolymer P11**

Figure 4.14. Synthesis of Copolymer P11

4.3.11. Synthesis of Maleimide-NHSMA-PEGMEMA Copolymer

In a typical polymerization, N-methacryloxysuccinimide (128.2 mg, 0.7 mmol), furan protected maleimide monomer (408 mg, 1.4 mmol) and copper (I) bromide (CuBr) (2.5 mg, 0.0175 mmol) were weighed into a dry 10 mL round bottom flask equipped with a stir-bar. The flask was sealed and purged with dry nitrogen gas. Then, degassed N,N,N′,N″,N″-Pentamethyldiethylenetriamine (PMDETA) (7.3 μL, 0.035 mmol), PEGMEMA (0.4 mL, 1.4 mmol) and anhydrous anisole (1 mL) were added to the RBF via syringe and the reaction mixture was stirred for 20 min at room temperature to allow catalyst formation, indicated by a color change to blue (Figure 4.15). To the stirring mixture was added ethyl 2-bromoisobutyrate (EBIB) (2.6 μL, 0.0175 mmol) via syringe then the reaction mixture was placed in an 80 ˚C oil bath for 2 h. The reaction ratio was [PEGMEMA]:[NHSMA]: [FuM – MA]:[PMDETA]:[CuBr]:[EBIB], 40:20:40:1:0.5:0.5. After terminating the polymerization the crude mixture was purified by precipitation into cold diethyl ether and passed through aluminum oxide to remove cupper catalyst. The final filtered product was dried under vacuum.

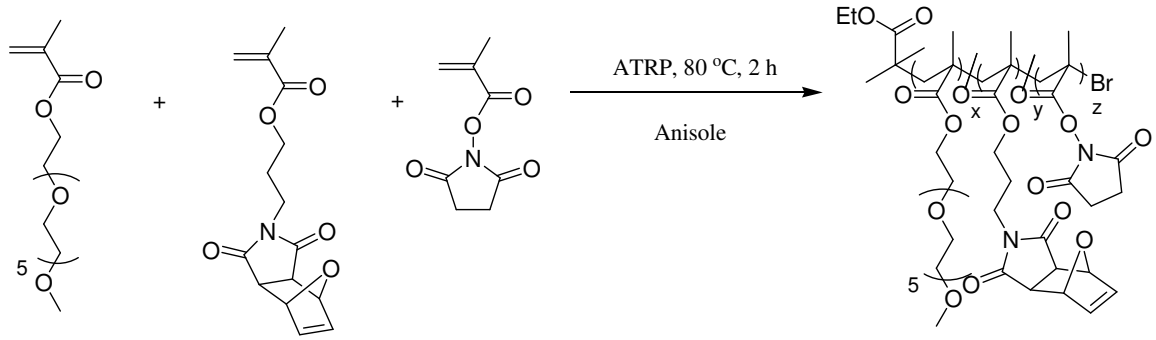

Figure 4.15. Synthesis of Copolymer P12

4.3.12. Constitution of Nanowebs

The nanofibers were fabricated by electrospinning. Solvent mixtures were prepared by mixing THF: DMF (50:50) with constant stir for 5 min at the room temperature. The spinning solutions were consisted of mixtures of different weight concentrations (i.e. 20%, 25% and 30%) of polymers in solvent mixtures. The mixtures were stirred under ambient

conditions for 30 min to attain the homogeneity required for electrospinning. Then, the solutions were loaded into a syringe connected to a stainless steel needle and a direct-current (dc) electric field was applied between the needle and collector plate using a high voltage supply that generated a dc voltage up to 30 kV depending on the experimental design. The feed rate of the precursor solutions were controlled using a syringe pump located at varying distances (10-15 cm) from the collector plate. The samples were collected on 10 x 10 cm aluminum foils and kept in a dry environment.

4.3.13. Scanning Electron Microscopy

Scanning electron microscopy is used to characterize the morphology of the nanowebs. Small pieces of the nanowebs that are coated on aluminum foil are cut and images are taken using ESEM-FEG/EDAX Philips XL-30 (Philips Eindhoven, The Netherlands) instrument using an accelerating voltage of 10 kV.

5. CONCLUSIONS

Novel variant polymers bearing FuM-MA, NHSMA, AHMA and furan copolymers are synthesized for polymer – drug conjugation and electrospinning approaches, independently.

Throughout the first part of this study, water soluble, biocompatible, biodegradable, N-Hydroxy succinimide and furan protected maleimide copolymers are synthesized with desirable molecular weight and PDI via atom transfer radical polymerization. To show that these polymers could be functionalized, using an amine containing compound, benzyl amine is reacted with succinimide polymer and regarding ^{1}H NMR results it is concluded that functionalization completed successfully. As an extension of this work, in vitro biodegradation behaviors of these polymers (20K and 30K) in acidic and neutral medias are investigated, concluding that polymers with higher initial molecular weights degrade slower while biodegradation behavior of reactive copolymers differ due to the composition and acidity.

In the second part, reactive nanofibrous scaffolds and nanoparticles are produced by use of various electrospinning parameters and compositions resulting in hydrophilic, hydrophobic and amphiphilic nanofibers and nanoparticles with narrow size distribution, which can be used in different approaches such as tissue engineering, drug delivery, yet especially wound dressing regarding excellent biocompatible property of PEG based reactive copolymers. An outstanding conclusion is that electrospinning may be a practical and an alternative method for nanoparticle production. In addition, obtained nanostructures enable further functionalization of wide range of molecules for several application fields due to the reactivity towards amine and thiol groups.

APPENDIX

^{1}H NMR data of the newly synthesized compounds are included.

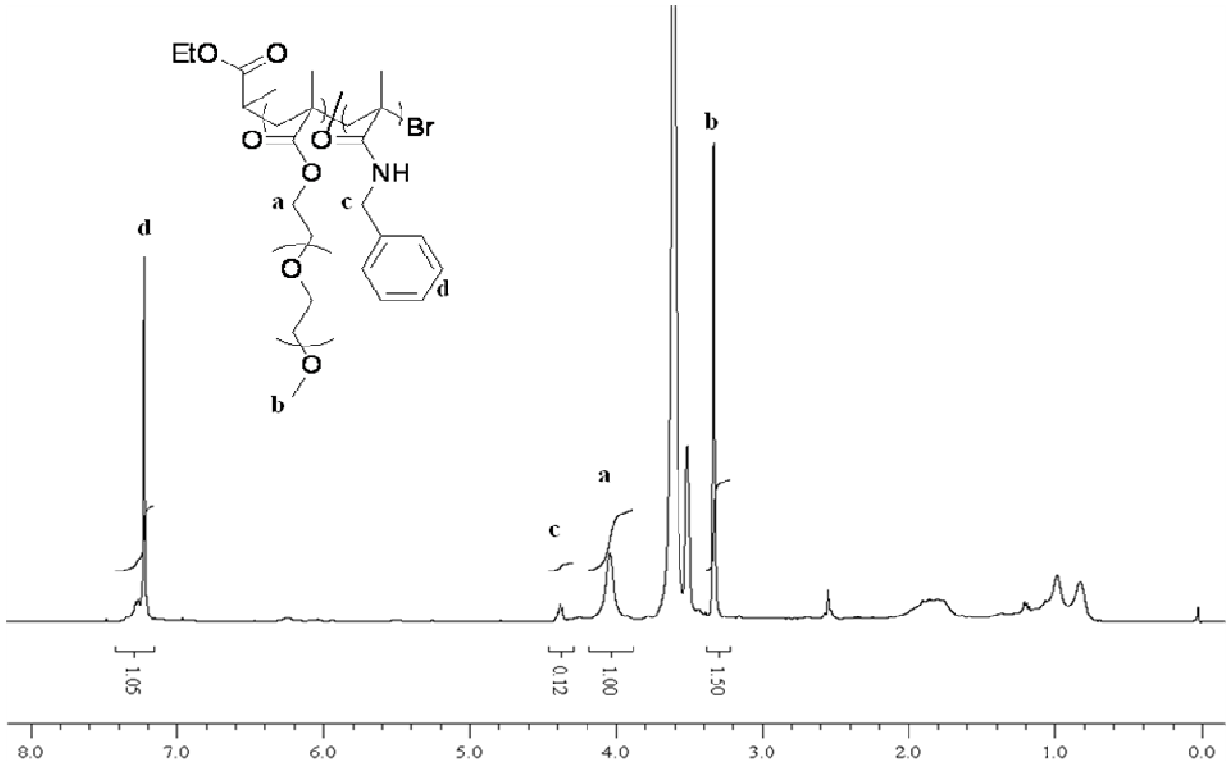

Figure A.1. ^{1}H NMR spectrum of functionalized Copolymer P1 with benzyl amine

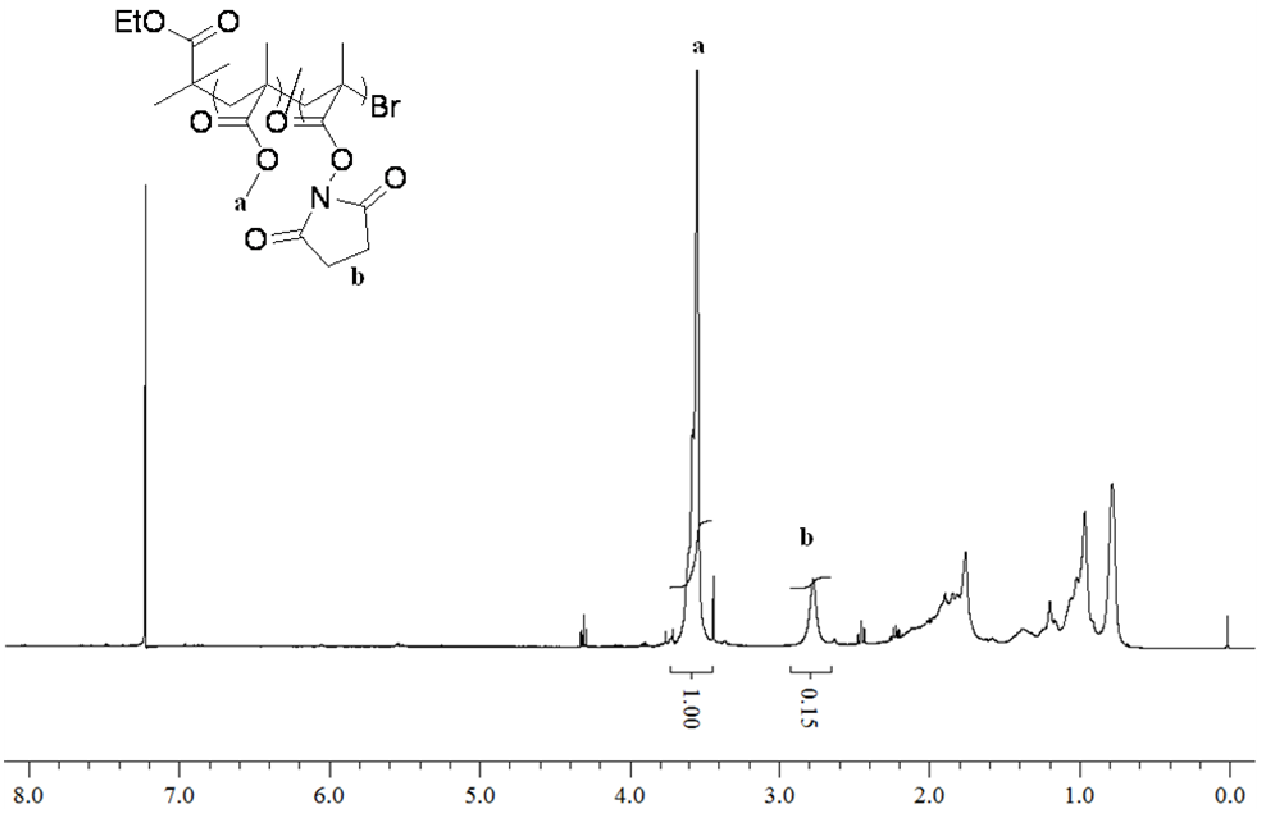

Figure A.2. ^{1}H NMR spectrum of Copolymer P3

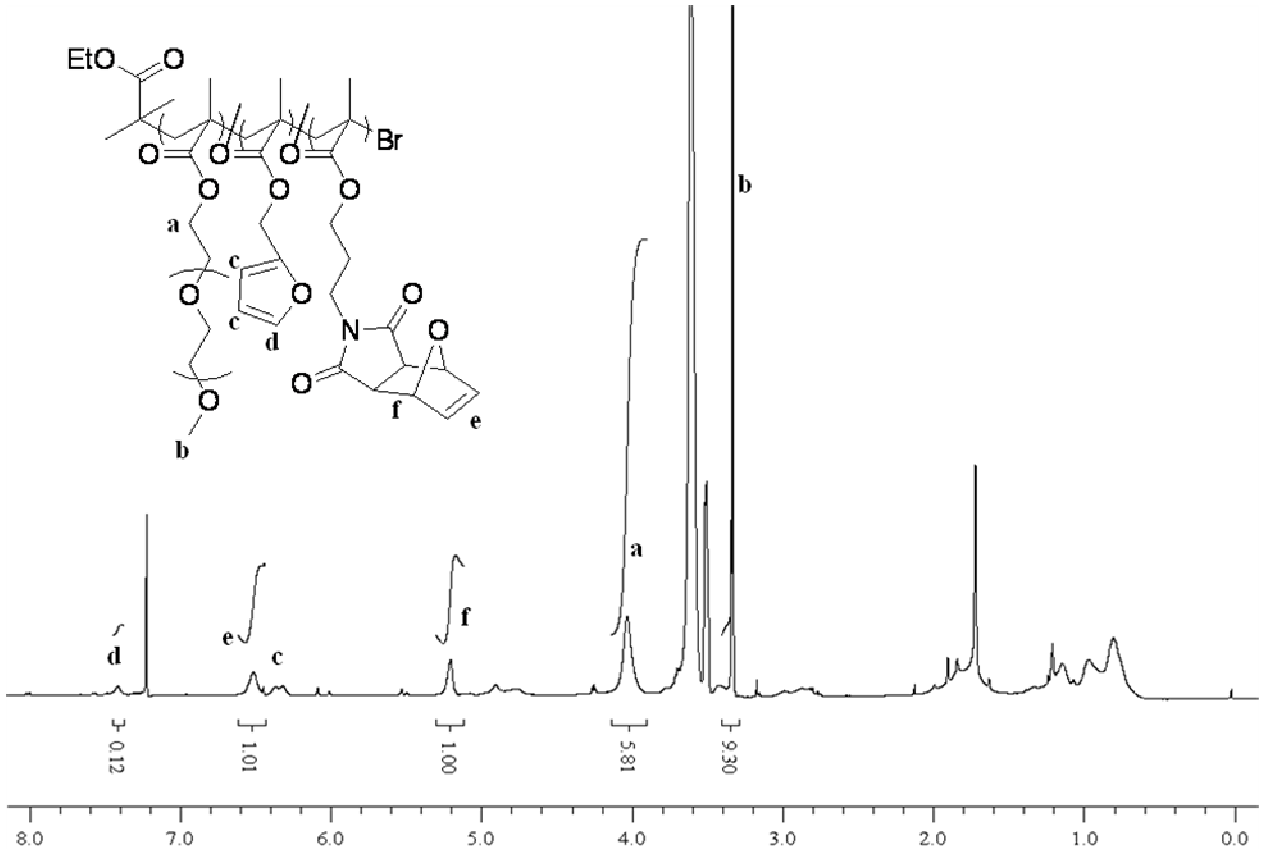

Figure A.3. ^{1}H NMR spectrum of Copolymer P6

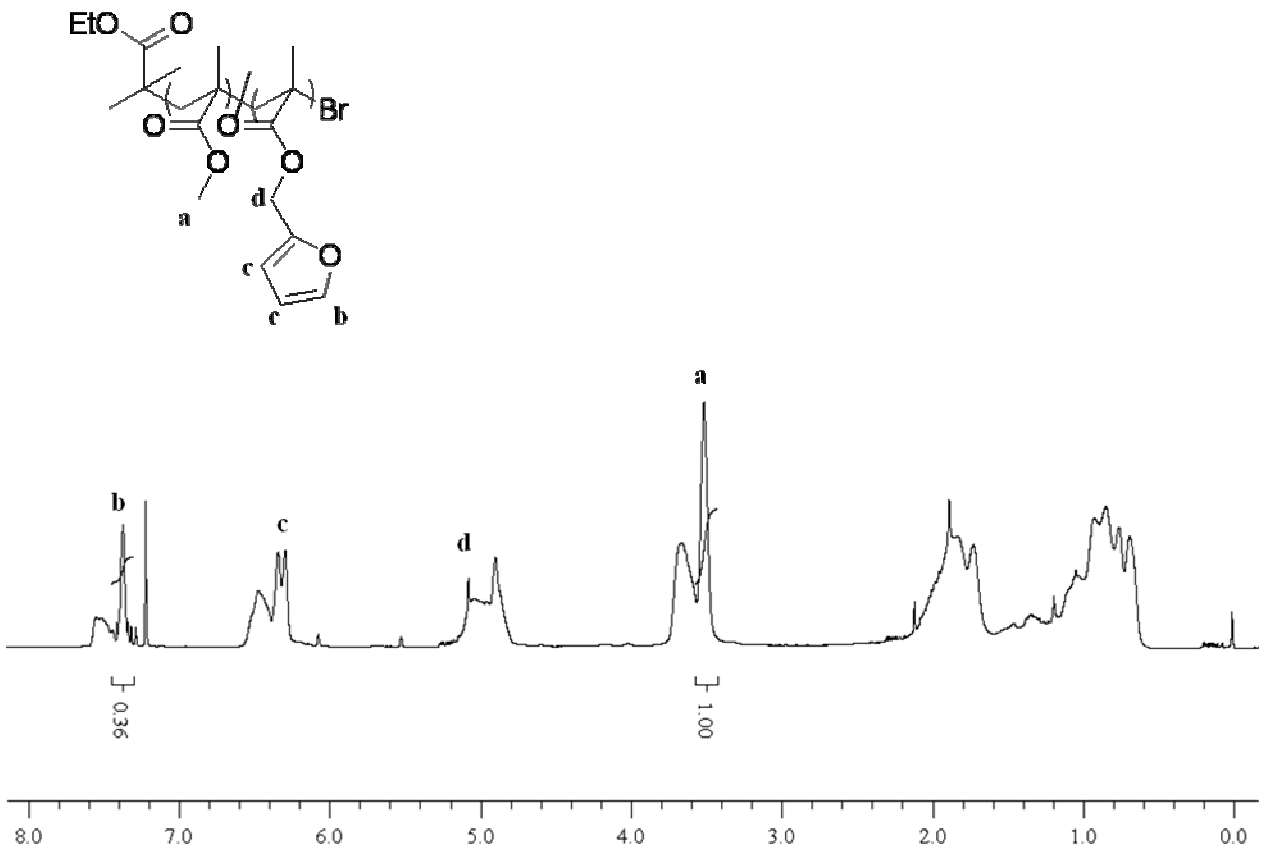

Figure A.4. ^{1}H NMR spectrum of Copolymer P8

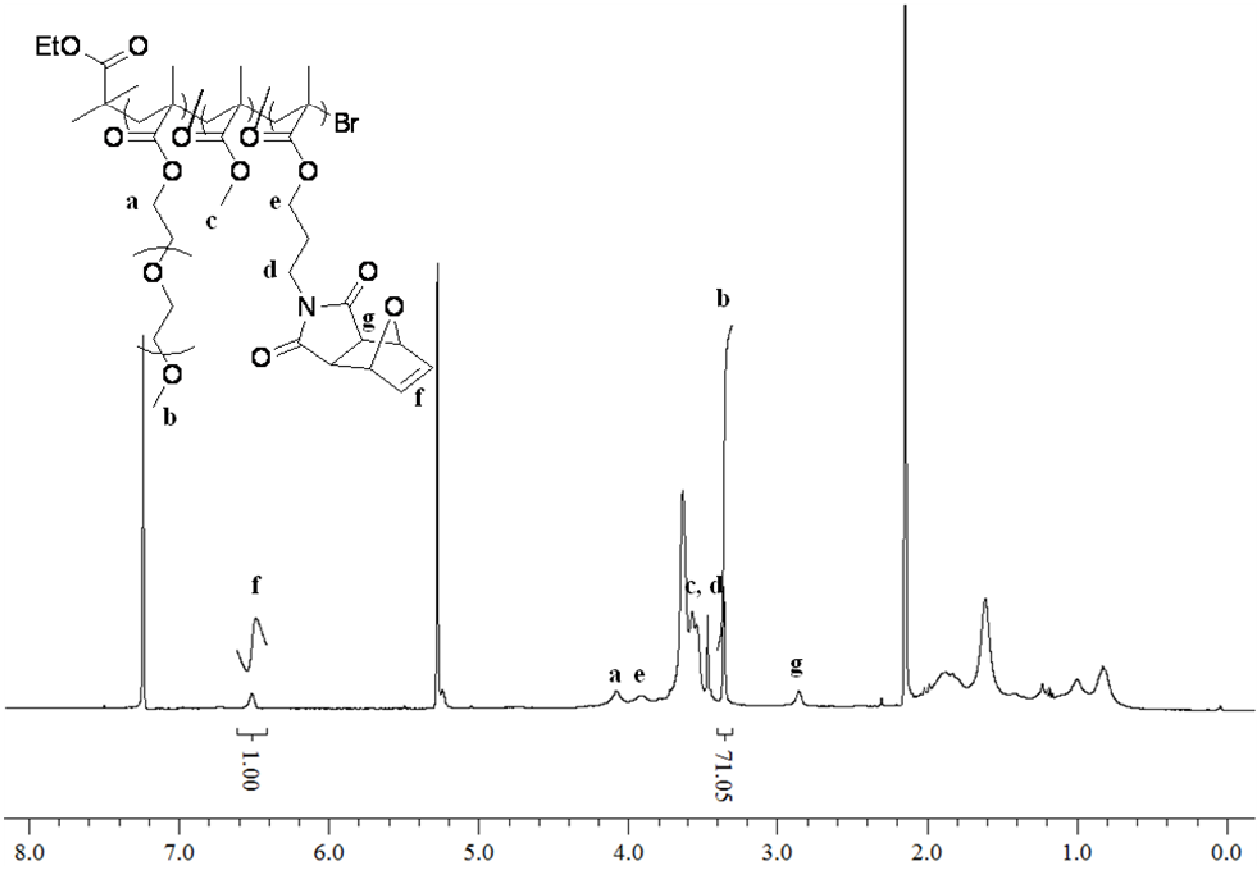

Figure A.5. ^{1}H NMR spectrum of Copolymer P10

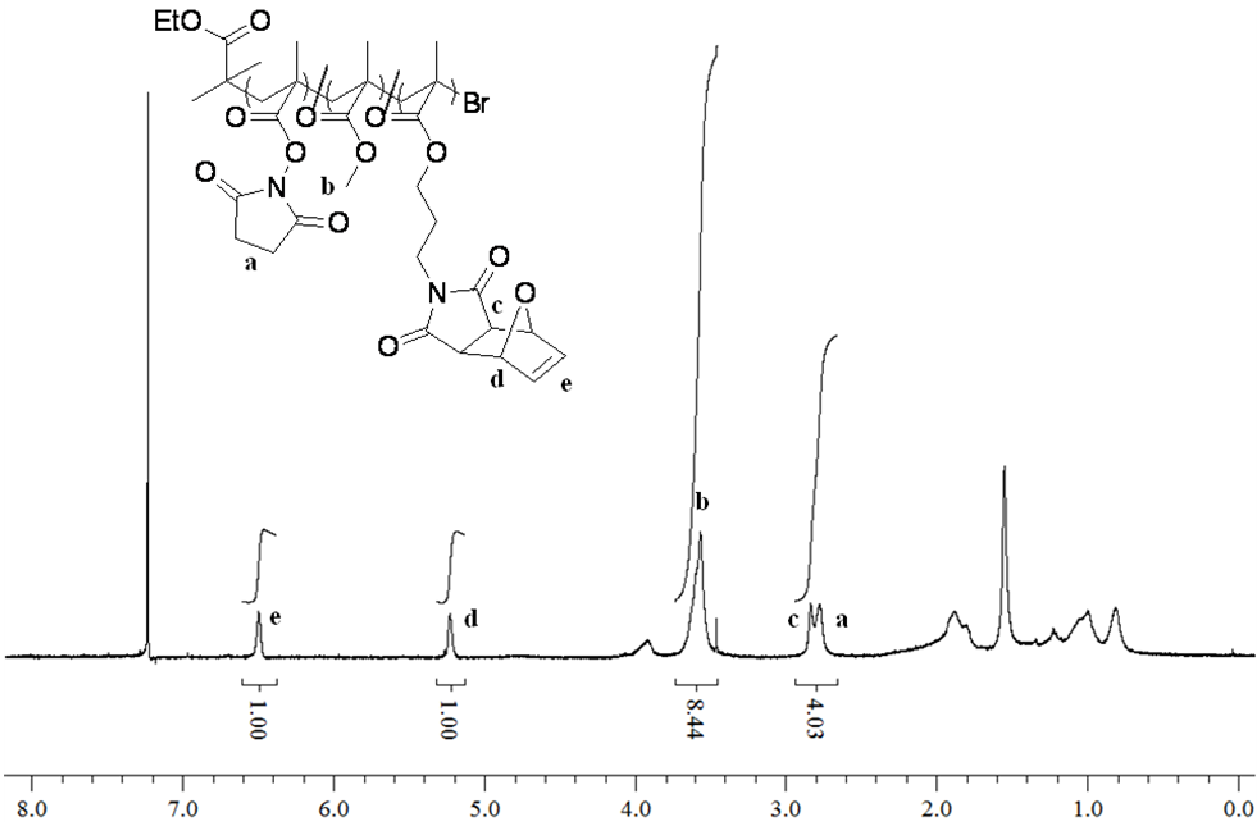

Figure A.6. ^{1}H NMR spectrum of Copolymer P11

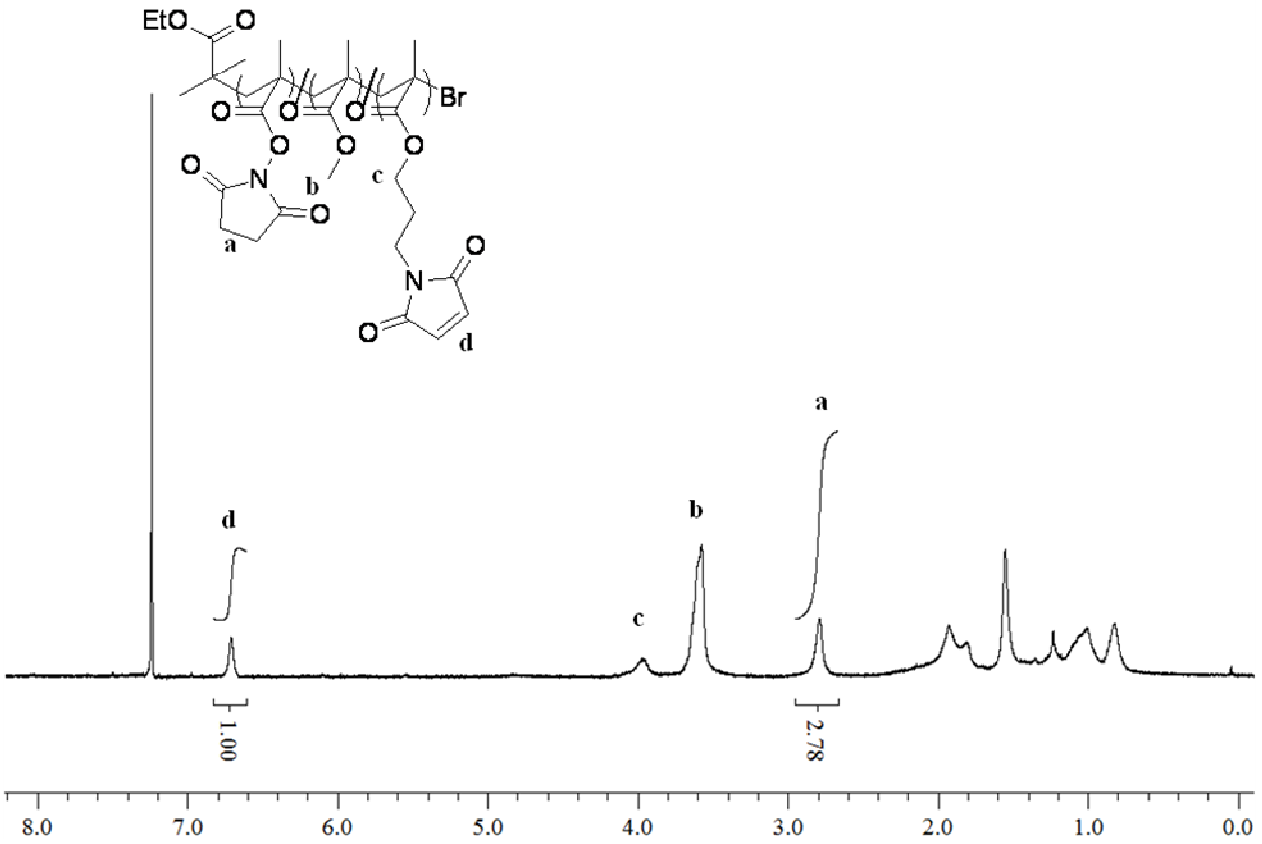

Figure A.7. ^{1}H NMR spectrum of activated form of Copolymer P11

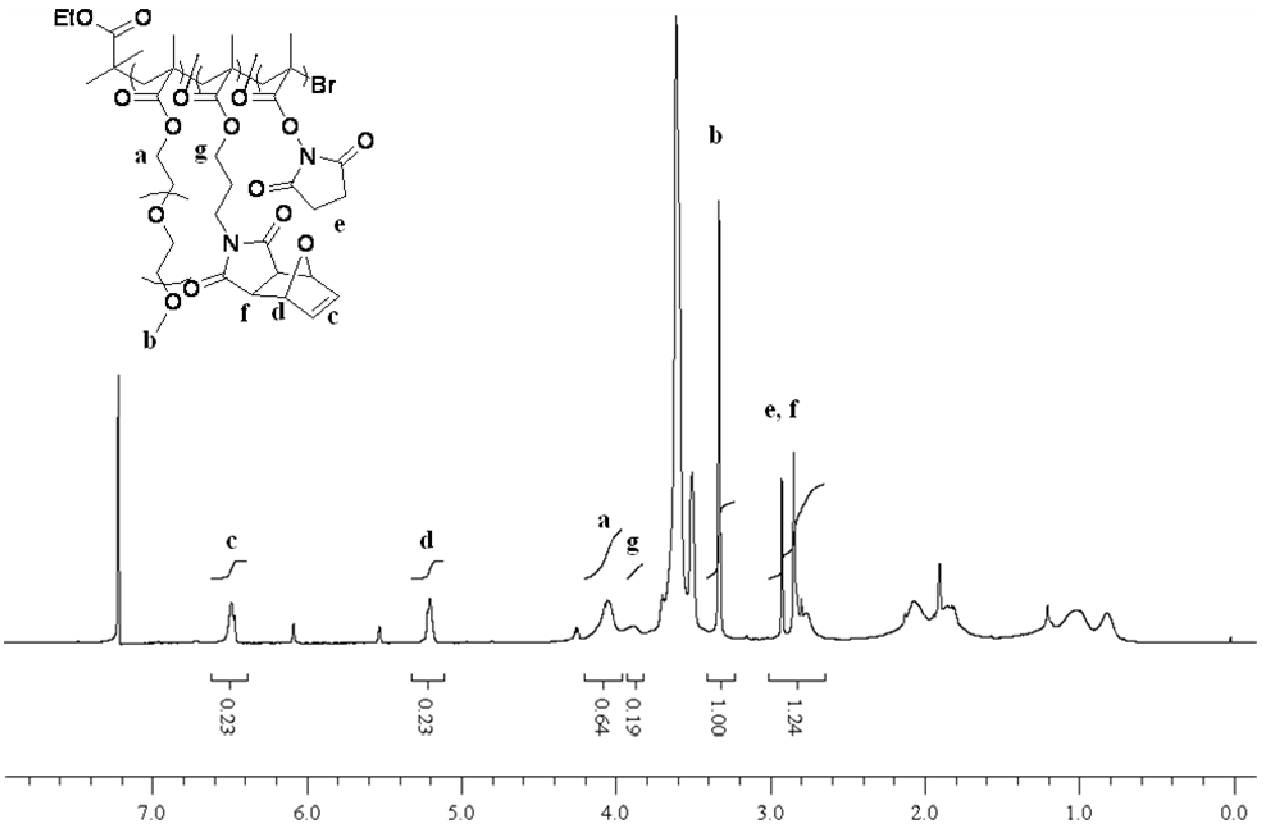

Figure A.8. ^{1}H NMR spectrum of Copolymer P12

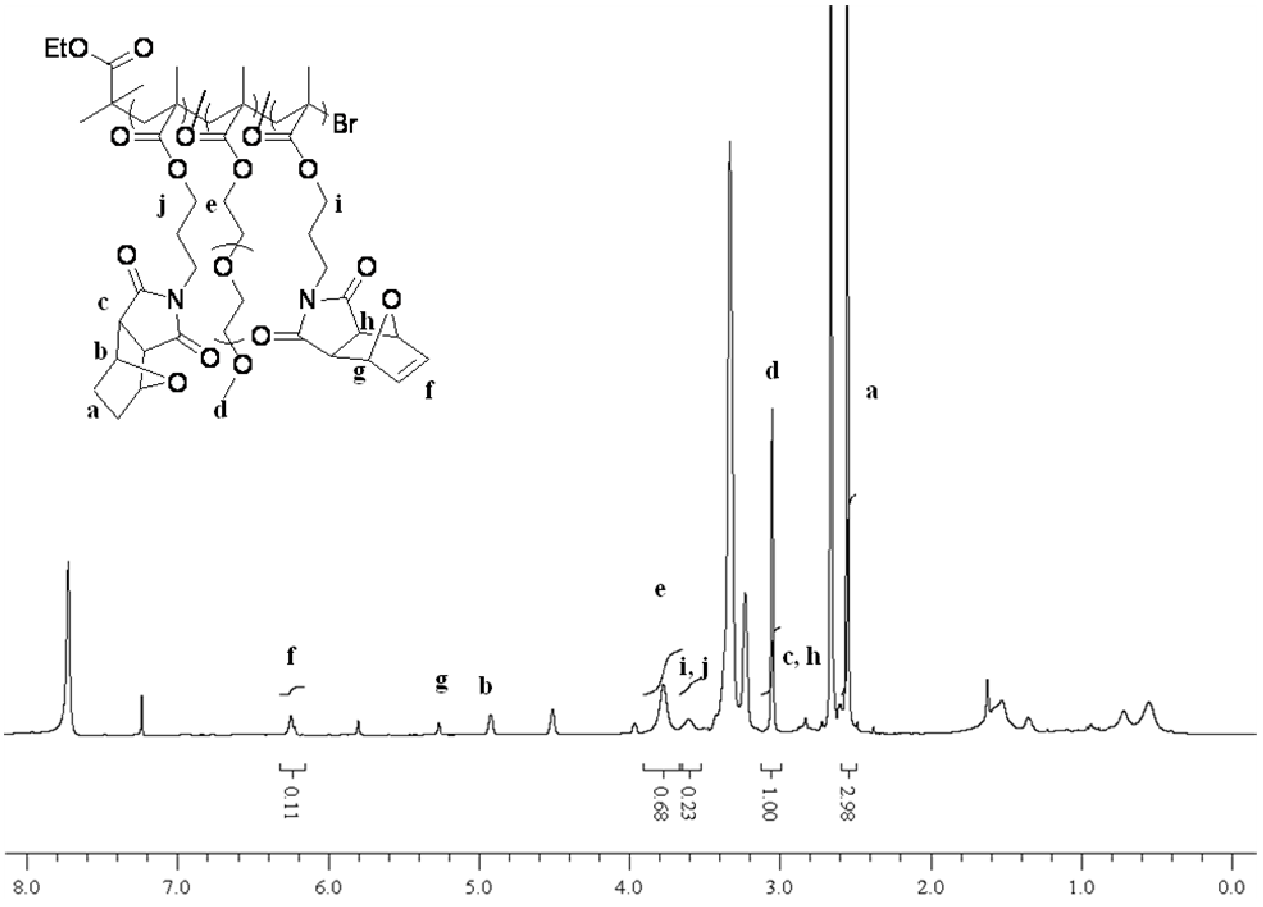

Figure A.9. ^{1}H NMR spectrum of Copolymer P7

REFERENCES

1. Charman, W. N., H. K. Chan and B. C. Finnin, "Drug delivery: a key factor in realising the full therapeutic potential of drugs", *Drug Dev. Res.*, Vol. 46, 316–327, 1999.

2. Je´roˆme, C., K. Van Butsele and R. Je´roˆme, "Functional amphiphilic and biodegradable copolymers for intravenous vectorisation", *Polymer*, Vol. 48, 7431–7443, 2007.

3. Goh, P. P., D. M. Sze and B. D. Roufogalis, "Molecular and cellular regulators of cancer angiogenesis" , *Curr Cancer Drug Targets*, Vol. 7, pp. 743–758, 2007.

4. Iyer, A. K., G. Khaled, J. Fang and H. Maeda, *Drug Discovery Today*, Vol. 11 (17–18), pp. 812–8, 2006.

5. Takakura, Y. and M. Hashida, *Critical Reviews in Oncology/Hematology*, Vol. 18 (3), pp. 207–31, 1995.

6. Maeda, H., L. W. Seymour and Y. Miyamot, *Bioconjugate Chemistry*, Vol. 3 (5), pp. 351–62, 1992.

7. Maeda, H., J. Wu, T. Sawa, Y. Matsumura and K. Hori, *Journal of Controlled Release*, 65 (1-2), pp. 271–84, 2000.

8. Pasut, G. and F. M. Veronese, *Advanced Drug Delivery Reviews*, Vol. 61, pp. 1177–1188, 2009.

9. Pasut, G. and F. M. Veronese, "Polymer-drug conjugation, recent achievements and general strategies", *Prog. Polym. Sci.*, Vol. 32, pp. 933–961, 2007.

10. Veronese, F. M. and J. M. Harris, Theme issue on "Peptide and Protein Pegylation I", *Adv. Drug Deliv. Rev.*, Vol. 54, 453–606, 2002.

11. Mutter, M., E. Bayer, E. Gross and J. Meienhofer, *Academic Press: New York*, Vol. 2, pp. 285–332, 1979.

12. Pang, S. N. and J. J. Amer, *Coll. Toxicol.*, Vol. 12, pp. 429–456, 1993.

13. Dreborg, S. and E. B. Akerblom, *Crit. Rev. Ther. Drug Carrier Syst.*, Vol. 6, pp. 315–365, 1990.

14. Yamaoka, T., Y. Tabata and Y. J. Ikada, *Pharm. Sci.*, Vol. 83, pp. 601–606, 1994.

15. Zalipsky, S., *Adv. Drug Delivery Rev.*, Vol. 16, pp. 157–182, 1995.

16. Delgado, C., G. E. Francis and D. Fisher, *Crit. Rev. Therap. Drug Carrier Syst*., Vol. 9, pp. 249–304, 1992.

17. Zalipsky, S., C. Lee and J. M. Harris (editor), *Plenum Press: New York*, pp. 347–370, 1992.

18. Katre, N. V., *Adv. Drug Delivery Rev.*, Vol. 10, pp. 91–1, 1993.

19. Shunmugam R. and Tew G. N., "Efficient Route to Well-Characterized Homo, Block, and Statistical Polymers Containing Terpyridine in the Side Chain", *Journal of Polymer Science: Part A: Polymer Chemistry*, Vol. 43, pp. 5831–5843, 2005.

20. Harris, J. M. and R.B. Chess RB, "Effect of pegylation on pharmaceuticals", *Nat. Rev. Drug Discov.*, Vol. 2, pp. 214–221, 2003.

21. Yamaoka, T., Y. Tabata and Y. Ikada, "Distribution and tissue uptake of poly(ethylene glycol) with different molecular weights after intravenous administration to mice", *J. Pharm. Sci.*, Vol. 83, pp. 601–606, 1994.

22. Yamaoka, T., Y. Tabata, Y. Ikada, "Comparison of body distribution of poly(vinyl alcohol) with other water-soluble polymers after intravenous administration", *J. Pharm. Pharmacol.*, Vol. 47, pp. 479–486, 1995.

23. Dosia, F., Silvia Arpicco, Paola Brusa, Barbara Stella, Luigi Cattel, "Poly(ethylene glycol)–human serum albumin–paclitaxel conjugates: preparation, characterization and pharmacokinetics", *Journal of Controlled Release*, Vol. 76, pp. 107–117, 2001.

24. Monge, S., and D. Haddleton, "Synthesis of precursors of poly(acryl amides) by copper mediated living radical polymerization in DMSO", *Eur. Polym. J.*, Vol. 40, pp. 37–45, 2004.

25. Pedone, E., X. Li, N. Koseva, O. Alpar and S. Brocchini, "An information rich biomedical polymer library", *J. Mater. Chem.*, Vol. 13, pp. 2825–2837, 2003.

26. Godwin, A., M. Hartenstein, A. Muller and S. Brocchini, "Narrow molecular weight distribution precursors for polymer-drug conjugates", *Angew. Chem.*, Vol. 113, pp. 614–617, 2001.

27. Rickerby, J., R. Prabhakar, A. Patel, J. Knowles and S. Brocchini, "Water-soluble polyacetals derived from diphenols", *J. Controlled Release*, Vol. 101, pp. 21-34, 2005.

28. Lynn, D., D. Anderson, D. Putnam and R. Langer, "Accelerated discovery of synthetic transfection vectors: parallel synthesis and screening of a degradable polymer library", *J. Am. Chem. Soc.,* Vol. 123, pp. 8155–8156, 2001.

29. Anderson, D., S. Levenberg and R. Langer, "Nanoliterscale synthesis of arrayed biomaterials and application to human embryonic stem cells", *Nat. Biotechnol.,* Vol. 22, pp. 863–866, 2004.

30. Anderson, D., W. Peng, A. Akinc, N. Hossain, A. Kohn, R. Padera, R. Langer and J. Sawicki, "A polymer library approach to suicide gene therapy for cancer", *Proc. Natl. Acad. Sci. U.S.A.,* Vol. 101, pp. 16028–16033, 2004.

31. Hermanson, G., *Bioconjugate Techniques*, Academic Press, New York, 1996.

32. Benicewicz, B. C. and Y. Li, "Functionalization of Silica Nanoparticles via the Combination of Surface-Initiated RAFT Polymerization and Click Reactions", *Macromolecules*, Vol.41, pp. 7986–7992, 2008.

33. Ratner, B. D., A.S. Hoffman and F.J. Schoen, J.E. Lemons (Eds.), "An Introduction to Materials in Medicine", *Biomaterials Science*, Academic Press, San Diego, CA, 1996.

34. Tamada, J. A. and R. Langer, "Erosion kinetics of hydrolytically degradable polymers", *Proc. Natl. Acad. Sci. USA*, Vol. 90, pp. 552–556, 1993.

35. Nucci, M. L., D. Shorr and A. Abuchowski, *Adv. Drug Delivery Rev*., Vol. 6, pp. 133–151, 1991.

36. Greenwald, R. B., C. D. Conover and Y. H. Choe, *CRC Crit. Rev. Ther. Drug Carrier Sys.*, Vol. 17, pp. 101–161, 2000.

37. Pan, J., Mingmei Zhao, Ying Liu, Bin Wang, Li Mi and Li Yang, "Development of a new poly(ethylene glycol)-graftpoly(D,L-lactic acid) as potential drug carriers", *Journal of Biomedical Materials Research Part A*, Vol. 89A, Issue 1, pp. 160–167, 2009.

38. Huang, Z. M., Y.-Z. Zhang, M. Kotaki and S. Ramakrishna, "A review on polymer nanofibers by electrospinning and their applications in nanocomposites", *Composites Science and Technology*, Vol. 63, pp. 2223–2253, 2003.

39. Greiner, A., and Joachim H. Wendorff, "Electrospinning: A Fascinating Method for the Preparation of Ultrathin Fibers", *Angew. Chem. Int. Ed.*, Vol. 46, pp. 5670 – 5703, 2007.

40. Agarwal, S., Joachim H. Wendorff and Andreas Greiner, "Use of electrospinning technique for biomedical applications", *Polymer*, Vol. 49, pp. 5603–5621, 2008.

41. GeunHyung, K.,SuA Park, Koeun Park, Hyeon Yoon, JoonGon Son and Teijin Min, "Apparatus for preparing electrospun nanofibers: designing an electrospinning process for nanofiber fabrication", *Polym. Int.*,Vol. 56, pp. 1361–1366, 2007.

42. Recum, H. A. and Travis J. Sill, "Electrospinning: Applications in drug delivery and tissue engineering", *Biomaterials*, Vol. 29, pp. 1989–2006, 2008.

43. Deitzel, J. M., J. Kleinmeyer, D. Harris, N. C. B. Tan, "The effect of processing variables on the morphology of electrospun nanofibers and textiles", *Polymer*, Vol. 42(1), pp. 261–72, 2001.

44. Taylor, G., "Electrically driven jets", *Proc. Natl. Acad. Sci.*, Part A, Vol. 313, Issue 1515, pp. 453–75, 1969.

45. Megelski, S., J. S. Stephens, D. B. Chase and J. F. Rabolt, "Micro- and nanostructured surface morphology on electrospun polymer fibers", *Macromolecules*, Vol. 22, 35(22), pp. 8456–66, 2002.

46. Doshi, J. and D. H. Reneker, "Electrospinning process and applications of electrospun fibers", *J. Electrostatics*, Vol. 35(2–3), pp. 151–60, 1995.

47. Baumgarten, P., "Electrostatic spinning of acrylic microfibers", *J. Colloid Interface Sci.*, Vol. 36(1), pp. 71–9, 1971.

48. Hayati, I., A. I. Bailey and T. F. Tadros, "Investigations into the mechanisms of electrohydrodynamic spraying of liquids. 1. Effect of electric-field and the environment on pendant drops and factors affecting the formation of stable jets and atomization", *J. Colloid Interface Sci.*, Vol. 117(1), pp. 205-21, 1987.

49. Fu, G. D., L. Q. Xu, F. Yao, K. Zhang, X. F. Wang, M. F. Zhu and S. Z. Nie, “Smart Nanofibers from Combined Living Radical Polymerization, “Click Chemistry”, and Electrospinning”, *Applied Materials and Interfaces*, Vol. 1, No 2, pp. 239–243, 2009.

50. Fu, G. D., L. Q. Xu, F. Yao, G. L. Li and E. T. Kang, “Smart Nanofibers with a Photoresponsive Surface for Controlled Release”, *Applied Materials and Interfaces*, Vol. 1, No 11, pp. 2424–2427, 2009.

51. Gandini, A. *Polimeros: Cicia e Tecnologia,* Vol. 15, pp. 95–101, 2005.

52. Kenji Yasugi, Yukio Nagasaki, Masao Kato, Kazunori Kataoka, “Preparation and characterization of polymer micelles from poly(ethylene glycol)-poly(D,L-lactide) block copolymers as potential drug carrier”, *Journal of Controlled Release,* Vol. 62, pp. 89–100, 1999.